NEAR-ROAD TRAFFIC-RELATED AIR POLLUTION: MONITORING, MODELING, AND DATA ANALYSIS

A Dissertation

by

MOHAMMAD HASHEM ASKARIYEH

Submitted to the Office of Graduate and Professional Studies of
Texas A&M University
in partial fulfillment of the requirements for the degree of

DOCTOR OF PHILOSOPHY

Chair of Committee,	Robin L. Autenrieth
Co-Chair of Committee,	Josias Zietsman
Committee Members,	Richard W. Baldauf
	Sergio Capareda
	Qi Ying
	Yunlong Zhang
Head of Department,	Robin L. Autenrieth

May 2020

Major Subject: Civil Engineering

ABSTRACT

Long-term exposure to air pollution has been shown to be associated to many different adverse health outcomes. Vehicles considerably contribute to pollutant emissions in urban areas. Air quality modeling is being widely used for research and regulatory studies to predict future traffic-related air pollution or in cases where air quality monitoring data are not available. In this study, near-road traffic-related particulate matter (PM) data were investigated. The application of dispersion modeling for research and regulatory analysis was explored. In addition, the effect of influential variables on traffic-related dispersion modeling was investigated, followed by a comprehensive evaluation of AERMOD, developed by the United States Environmental Protection Agency for regulatory air dispersion modeling.

Traffic contribution to a 24-hour $PM_{2.5}$ increment in the near-road environment was estimated to be about 27% of background concentration. A multiple linear regression model can explain 85% of the variability of 24-hour $PM_{2.5}$ concentrations in the near-road environment and shows improvement in near-road concentration predictions when accounting for wind speed and wind direction.

In this study, dispersion modeling was used to perform a worst-case particulate matter hot-spot scenario analysis specific to El Paso, Texas. In addition, a novel application of dispersion modeling was developed to assess traffic-related air pollution exposure by integrating mobility patterns tracked by Global Positioning System (GPS) devices. The results exhibit a significant variation of traffic-related air pollution exposure across different time periods and spatial locations that cannot be captured by simpler

metrics such as traffic density and near-road distance or even modeling air pollution without accounting for mobility.

The sensitivity of traffic-related air pollution dispersion modeling to a variety of input sets was investigated. Results show a significant effect of meteorological variables on near-road traffic-related air pollution. As such, annual average pollutant concentrations dispersed during nighttime conditions were shown to be higher by 100% to 120% compared to daytime periods for identical emission rates. This relative difference increased to 150% to 200% for rural land-use conditions. Emission and dispersion modeling based on regulatory guidelines was conducted to evaluate the effect of emission rate variation (due to the inclusion of resuspended dust in traffic-related $PM_{2.5}$ emissions) on near-road traffic-related air pollution. Results show a nonlinearity between emission rates and concentrations due to the effect of meteorological variables and the geometry of the network, which emphasizes the importance of dispersion modeling for traffic-related air quality analysis. Results show the increase in $PM_{2.5}$ emission rates due to resuspended dust inclusion on arterials range between 39% and 108% and between 16% and 19% on highways. This increase in emission rates is associated with an overall increase in near-road traffic-related $PM_{2.5}$ concentrations by between 49% and 74%, an important percentage range from an exposure and health point of view. Sensitivity analysis of dispersion modeling to source and dispersion parameters shows the importance of parametrization when assessing near-road traffic-related exposure.

A comprehensive evaluation of AERMOD shows the necessity of using volume representation of vehicular emission sources. Results show general weaknesses of area

representation of emission sources in predicting concentrations at upwind locations, at higher elevations, and in cases of low wind speed.

CONTRIBUTORS AND FUNDING SOURCES

Part 1, faculty committee recognition

This work was supervised by a dissertation committee consisting of Professor Robin Autenrieth [advisor] of the Zachry Department of Civil Engineering and Doctor Josias Zietsman [co-advisor] of the Texas A&M Transportation Institute, Doctor Richard Balduaf of the United States Environmental Protection Agency, Professors Qi Ying and Yunlong Zhang of the Zachry Department of Civil Engineering, and Professor Sergio Capareda of the Department of Biological and Agricultural Engineering.

Part 2, student/collaborator contributions

The traffic and maternal mobility datasets used in Chapter 3 were obtained from Texas A&M Transportation Institute (TTI) and both projects in this chapter were supervised by Dr. Suriya Vallamsundar of the Texas A&M Transportation Institute (TTI). The Tracer Study dataset used in Chapter 4 and Chapter 5, which was originally generated during General Motors study (1978), was obtained from Professor Qi Ying of the Zachry Department of Civil Engineering. All work for the dissertation was completed by the student, in collaboration with, Dr. Suriya Vallamsundar, Dr. Andrew Birt, Dr. Reza Farzaneh, Mr. Madhusudan Venugopal, Mr. Chaoyi Gu, Dr. Eun Sug Park, and Dr. Haneen Khreis of the Texas A&M Transportation Institute (TTI).

Funding Sources

Graduate study was supported by two fellowships during Spring and Fall 2018 from College of Engineering at Texas A&M University. This work was made possible in part by Texas Department of Transportation (TxDOT) and the US Department of

Transportation (USDOT) under TTI account numbers: 409201-0015, 409276-00004, 468645-00001, 468646-00001, 468647-00001, 469438-00001, 469439-00001, 608101-00707. Its contents are solely the responsibility of the authors and do not necessarily represent the official views of the TxDOT and USDOT.

TABLE OF CONTENTS

Page

LIST OF FIGURES

Page

LIST OF TABLES

Page

1. INTRODUCTION [1]

Adverse health effects from exposure to fine particulate matter (particulate matter that have a diameter of less than 2.5 micrometers: $PM_{2.5}$) have been investigated in a growing number of studies *(1-3)*. Exposure to an increased level of $PM_{2.5}$ concentrations has been shown to be associated with many adverse health effects including but not limited to increased blood pressure and hypertension, increased rates of ischemic stroke, and narrow arterial diameter *(4-7)*. Recent studies also reveal strong evidence of the relationship between long-term exposure to $PM_{2.5}$ and common neurodegenerative diseases *(8)*. Further studies also show a significant association between an increase in traffic-related $PM_{2.5}$ exposure and diseases like cardiac anomalies *(9)*. The increment of traffic-related $PM_{2.5}$ in the near-road environment can potentially yield a series of adverse health effects for a large number of people who reside near roadways *(10)*. Rowangould reported that more than 19% of the United States (US) population lives within 100 m of a high-volume roadway *(11)*. According to the 2013 national household survey, 16.88 million households live within half a block of a major transportation facility in 2011, resulting in the exposure of more than 40 million people to an elevated level of $PM_{2.5}$ *(12)*. Many people throughout the world also live near major roadways, so the worldwide population exposed to an elevated level of traffic-related air pollutants including $PM_{2.5}$ is much larger.

---

[1] *Reproduced with permission from:* Askariyeh, M.H., Kota, S., Vallamsundar, S., Zietsman, J. and Ying, Q., Transportation Research Part D, Vol. 57, pp 392-402. Copyright 2017, Elsevier. and Askariyeh, M.H., Zietsman, J. and Autenrieth, R., Atmospheric Environment, https://doi.org/10.1016/j.atmosenv.2019.117113, Copyright 2017, Elsevier.

Characterization of near-road traffic-related air pollutants has been performed in a variety of studies including tracer studies *(13-16)*, short-term field studies *(16-20)*, intensive field studies *(21-23)*, and modeling *(24-28)*. These studies show that traffic-related air pollution depends on wind speed and direction, peaks at the nearest points to the roadway, decreases exponentially with distance from the road, and reaches the background concentration over a distance of a few hundred meters. A synthesis of previously collected real-world data show a 22% increment of $PM_{2.5}$ in the near-road area compared with background $PM_{2.5}$ concentration *(29)*, while other studies estimate this value to be 13% to 20% *(23)* and 10% to 15% *(30-32)*.

The US Environmental Protection Agency (EPA) added a number of near-road monitors to its network and mandated inclusion of near-road monitoring data in the Air Quality Index (AQI) to reflect the potential for an elevated level of near-road $PM_{2.5}$ concentration to which millions of people in major urban areas may be exposed on a daily basis *(33)*. One of the key objectives of this program was to collect National Ambient Air Quality Standards (NAAQS)–comparable datasets in the near-road environment in order to support studies on adverse health effects of long-term exposure to $PM_{2.5}$. However, air quality monitoring datasets have considerable temporal and spatial limitations. Having a better understanding of the temporal and spatial distribution of near-roadway air pollutants plays an instrumental role in assessing exposure to transportation-related air pollutants. Air dispersion models are being used generally to estimate the temporal and spatial variation of transportation-related air pollutants under near-roadway conditions for research and regulatory purposes *(34)*. Several air dispersion models have been developed to predict

temporal and spatial dispersion of air pollutants *(35-38)*. The American Meteorological Society – US EPA Regulatory Model (AERMOD) is the current regulatory dispersion model supplied by the EPA for estimating the temporal and spatial distribution of pollutants in stable and convective boundary layers for both simple and complex terrains *(39-41)*.

The capability of dispersion models like AERMOD needs to be evaluated so that predictions can be used with confidence in analyses of exposure and health effects, as well as regulatory analysis. Heist et al. (2013) *(26)* conducted a model inter-comparison study to assess the abilities of different near-road dispersion models, including CALINE3 *(42)*, CALINE4 *(15)*, ADMS *(43, 44)*, RLINE *(45)*, and AERMOD, using surface-level onsite data from the Caltrans Highway 99 tracer experiment and the Idaho Falls tracer study. The study found all models to have similar overall performance statistics except CALINE3, which produces a larger degree of scattering in concentration estimates. AERMOD appeared to have the best performance among all the dispersion models, especially for the highest concentrations. AERMOD results using volume sources also were found to be slightly better than the ones using area sources. Based in part on the findings of that study, the US EPA proposed replacing CALINE3 with AERMOD for all future transportation-related air quality analyses *(46)*. However, some other model validation studies show that AERMOD might not perform as well as expected. For example, Chen et al. (2009) *(47)* found CALINE4 and CAL3QHC predictions of airborne particulate matter (PM) to match well with observations, and they found AERMOD to lead to underpredictions at a near-road site. Claggett and Bai (2012) *(48)* found both CAL3QHCR and AERMOD to

underpredict the observed $PM_{2.5}$ concentration at a signalized intersection, but they found CAL3QHCR to have more data points within a factor of 2 of observations than AERMOD. The performance of AERMOD might be sensitive to the representation of vehicle emissions (i.e., volume vs. a resource). Claggett and Bai (2012) *(48)* and Claggett (2014) *(49)* found higher concentrations of PM to be predicted by AERMOD when emission sources were characterized as area sources as opposed to volume sources. In contrast, Schewe (2011) *(50)* reported 1.8 to 3.8 times higher concentration predictions from AERMOD for highways configured as volume sources compared with those configured as area sources. It is obvious that more studies are needed to evaluate further the performance of AERMOD for near-road predictions using different model configurations.

Air quality dispersion modeling using Gaussian models like AERMOD requires inputs to represent emission rates, meteorological conditions, and emission source characteristics. Numerous studies have investigated the effects of these three main input sets on near-roadway traffic-related air pollution dispersion modeling. Comprehensive studies of influential factors on near-roadway air pollutants show the significant role of wind direction in dispersion modeling using the Gaussian distribution equation *(16)*, which is shown in field studies *(18)*. Evaluation of AERMOD particularly has shown the determinant effects of wind direction *(28)* and speed on model performance and has revealed overprediction of concentrations under low-wind conditions *(51, 52)*. Limitation of surface layer similarity theory in explaining dispersion mechanism in low-wind speed *(34, 53)*, and a lack of reasonable vehicles induced turbulence (VIT) *(54-59)* can be the

main reasons for this inaccuracy in dispersion modeling. VIT has proved to play a determinant role in the dispersion mechanism under low-wind conditions *(56, 59, 60)*.

Different dispersion mechanisms and turbulences including VIT usually are considered in air dispersion models using parameterized forms *(61)*. In particular, AERMOD estimates a meander component, vertical and horizontal wind velocity fluctuation due to turbulence (σ_w and σ_v [m/s]), and standard deviations of the vertical and lateral concentration distributions (σ_z and σ_y) *(62)*. It also uses release height, the initial vertical dispersion coefficient (σ_{zo}), and the initial lateral dispersion coefficient (σ_{yo}) while modeling transportation-related emission sources as volume sources *(62)*. The effects of the parametrization on dispersion modeling have been investigated using limited tracer study results, but there remains a lack of holistic studies of different dispersion factors using a comprehensive tracer study result set with a focus on traffic-related air pollution.

Following a comprehensive literature review on near-roadway traffic-related air pollution, several gaps have been identified. Numerous studies show a variety of magnitudes for near-road traffic-related air pollution increment. Because near-roadway monitoring data are not always available and because of the need to predict future traffic-related air pollution, dispersion modeling is being used widely for research and regulatory purposes. However, various aspects of research and regulatory dispersion modeling with a focus on vehicular emission sources need more work. For example, there have been few recent studies with focus on improving the process of PM hot-spot analyses, while the model setup and input data preparation for this purpose involve a considerable amount of time and effort to deal with technical details for the PM hot-spot analysis process. From a

research point of view, applying dispersion modeling for exposure assessment considering spatial variation of population location using a real-time Global Positioning System (GPS) dataset is a novel aspect of dispersion modeling applications. As previously explained, air pollution dispersion modeling requires three sets of main inputs: emission rates, meteorological inputs, and emission source characteristics (dispersion parameters). Although numerous studies have been conducted on dispersion modeling, a holistic sensitivity analysis of traffic-related dispersion modeling to its main input sets can supply a better understanding of how this process can be improved. One of the main reasons for these gaps in the literature (lack of a holistic sensitivity analysis and a comprehensive evaluation of traffic-related air pollution dispersion modeling) is the lack of accurate and comprehensive monitoring data. The availability of results from a General Motors tracer study conducted in the 1970s, as well as access to novel datasets, remove this obstacle and made possible this current research.

This research has four objectives. The first objective is to quantify near-roadway traffic-related air pollution. The main purpose is to understand near-roadway traffic-related air pollution. As such, all $PM_{2.5}$ concentrations monitored by NAAQS stations in Houston including the near-road ones were used to quantify the $PM_{2.5}$ increment due to traffic in the near-roadway environment based on EPA guidelines.

The second objective of this research is to investigate the application of dispersion modeling in both research and regulatory traffic-related air quality analysis. The main purpose is to use dispersion modeling as a widely accepted procedure in predicting future traffic-related air pollutant concentration or when monitoring data are not available. As

such, guidance was provided (with a focus on regulatory guidelines) on performing a worst-case PM hot-spot analysis specific to El Paso, the only PM nonattainment area in Texas. In addition, dispersion modeling was used to assess exposure of a vulnerable community, pregnant women, to traffic-related air pollution. This study is one of the first to use real-time locations and dispersion modeling for exposure assessment.

The third objective of this research is to evaluate the sensitivity of dispersion models to input sets. As such, the effect of variation in each of the three sets of inputs (meteorological variables, emission rates, and dispersion parameters) was investigated. The main purpose is to understand the individual effect of these different input sets on traffic-related dispersion modeling results and exposure assessment.

The fourth objective of this research is to perform a comprehensive evaluation of traffic-related dispersion modeling. The main purpose is to evaluate the accuracy of dispersion modeling results given maximum control on traffic-related emission rates and monitoring. To this end, the General Motors tracer study results were used to evaluate dispersion model outputs at different heights and distances from the edge of the road.

In conclusion, monitoring data and dispersion modeling were used in this study to understand traffic-related air pollution. Application of dispersion modeling in regulatory analysis and in exposure assessment was investigated. Additionally, the effect of utilizing different input sets to model air pollutant concentrations dispersed from vehicular emission sources was evaluated. Finally, strengths and weaknesses of dispersion modeling in an ideal situation (comprehensive tracer study results) were explored. Overall, the

results from this study will aid model developers, practitioners, and decision makers in having a better understanding of traffic-related air pollution.

2. TRAFFIC CONTRIBUTION TO THE NEAR-ROAD AIR POLLUTION[2]

2.1. The $PM_{2.5}$ Increment Traffic Contributes in the Near-Road Environment

A growing number of studies have reported the adverse health effects of long-term exposure to air pollutants, especially fine particulate matter ($PM_{2.5}$). Vehicular emission sources have been shown to contribute to elevated air pollution concentrations in the near-road environment, including $PM_{2.5}$, based on monitoring data collected mainly during short-term campaigns. The United States Environmental Protection Agency (EPA) added near-road monitors to its national network to collect long-term National Ambient Air Quality Standard (NAAQS)–comparable data in the near-road environment. The EPA also mandated inclusion of near-road monitoring data in the Air Quality Index to reflect the elevated level of near-road $PM_{2.5}$ concentrations to which millions of people in major urban areas are exposed to on a daily basis. For the first time, $PM_{2.5}$ data collected at one of these near-road monitors were compared with those of other NAAQS monitors during 2016 in Houston, Texas. One of these NAAQS monitors was selected based on EPA guidance for quantitative hotspot analyses of particulate matter to represent background concentrations. The near-road $PM_{2.5}$ increment was statistically significant. The traffic contribution to 24-hour $PM_{2.5}$ increment in the near-road environment was estimated to be about 23% of background concentration, which is close to estimates given by previous studies (22%) and is greater than a recent estimate based on a national-scale data analysis

[2] *Reproduced with permission from:* Askariyeh, M.H., Zietsman, J., and Autenrieth, R., Atmospheric Environment, https://doi.org/10.1016/j.atmosenv.2019.117113, Copyright 2019, Elsevier.

(17%), emphasizing the importance of background monitor selection criteria. Wind speed and direction were shown to have a considerable effect on $PM_{2.5}$ increment in the near-road environment. A multiple linear regression model was developed to predict 24-hour near-road $PM_{2.5}$ concentrations using background $PM_{2.5}$ concentration, wind speed, and wind direction. This model explained 83% of the variability of 24-hour $PM_{2.5}$ concentrations in the near-road environment and showed improvement in near-road concentration predictions when accounting for wind speed and wind direction.

2.1.1. Introduction

Adverse health effects of exposure to fine particulate matter ($PM_{2.5}$) have been investigated in a growing number of studies *(1-3)*. Exposure to an increased level of $PM_{2.5}$ concentrations has been associated with adverse health effects such as increased blood pressure and hypertension, increased rates of ischemic stroke, and narrower arterial diameter *(4-7)*. Recent studies have also revealed strong evidence of the relationship between long-term exposure to $PM_{2.5}$ and common neurodegenerative diseases *(8)*. Further studies also have shown a significant association between an increase in traffic-related $PM_{2.5}$ and diseases like cardiac anomalies *(9)*. The increment of traffic-related $PM_{2.5}$ in the near-road environment can potentially yield a series of adverse health effects for a large number of people who reside near roadways *(10)*. Rowangold *(11)* reported that more than 19% of the United States (US) population lives within 100 m of a high-volume roadway. According to the 2013 national household survey, 16.88 million households lived within half a block of a major transportation facility in 2011, yielding

exposure of more than 40 million people to an elevated level of $PM_{2.5}$ *(12)*. Many people throughout the world also live near major roadways, so the worldwide population exposed to an elevated level of traffic-related air pollutants including $PM_{2.5}$ is potentially much larger.

The US Environmental Protection Agency (EPA) added a number of near-road monitors to its network and mandated inclusion of near-road monitoring data in the Air Quality Index (AQI) to reflect the potential for an elevated level of near-road $PM_{2.5}$ concentration to which millions of people may be exposed on a daily basis in a considerable portion of major urban areas *(33)*. One of the key objectives of this program was to collect National Ambient Air Quality Standards (NAAQS)–comparable datasets from the near-road environment as input to studies on adverse health effects of long-term exposure to $PM_{2.5}$. The appropriate monitoring methods for this purpose are the Federal Reference Method (FRM), Federal Equivalent Method (FEM), and Approved Regional Method (ARM), despite some limitations of these methods *(33, 63)*. EPA guidance *(64)* requires a probe for near-road monitoring to be located as close as possible to and not farther than 50 m from the outside nearest edge of the road and between 2 and 7 m in height from the road elevation. It also requires $PM_{2.5}$ state and local air monitoring stations "to operate on at least a 1-day-in-3 sampling schedule" to be able to characterize elevated $PM_{2.5}$ concentration near heavily traveled roads *(33)*.

Characterization of near-road traffic-related air pollutants has been performed in a variety of studies including tracer studies *(13-16)*, short-term field studies *(16-20)*, intensive field studies *(7, 21-23)*, and modeling *(24-28, 65)*. These studies have reported

that traffic-related air pollution depends on: wind speed and direction; peaks at the nearest points to the roadway; decreases exponentially with distance from the road; and, reaches the background concentration over a distance of a few hundred meters. A synthesis of previously collected real-world data showed a 22% increment of $PM_{2.5}$ in the near-road area compared with background $PM_{2.5}$ concentration *(29)*, while other studies have estimated this value to be 13% to 20% *(23)*, and 10% to 17% *(30-32)*. It should be noted that a recent national-scale review of near-road concentrations provided the average near-road $PM_{2.5}$ increment in the US and did not investigate the Houston monitor because the methodology completeness criteria were not met for background monitor selection *(30)*.

A key factor in understanding the traffic contribution to the near-road increment of air pollution is the background concentration estimate when speciation monitor analysis *(23, 66)* is not available. EPA guidance *(67)* for quantitative hotspot analyses of particulate matter describes how to determine background concentrations from sources other than the study target. It describes how to use the data of a single monitor with similar characteristics, that is close in proximity, and that is located upwind of a target area to be as representative as possible for the background concentration. This guidance also explains how to use a wind rose to identify upwind sources and how to use inverse distance weighting to interpolate among several monitors if no single monitor represents the background concentration *(67)*. Researchers have used concentrations observed at a distance of a few hundred meters from the target roadway and the first percentile of hourly near-road monitoring *(19)*, as well as concentrations monitored at a location not affected by any close emission sources and a high correlation with target monitor *(30)*, to determine

background concentrations and estimate traffic-related $PM_{2.5}$ increment in the near-road environment. Considering different methods and datasets, mainly obtained from short-term campaigns due to the rare availability of long-term near-road monitoring, range of values have been reported to quantify the traffic contribution to $PM_{2.5}$ increment in the near-road environment.

The main objective of this study was to quantify $PM_{2.5}$ increment due to traffic contributions in a near-road environment at different wind speeds and wind directions using NAAQS-comparable near-road monitoring data. To accomplish this objective, the 24-hour $PM_{2.5}$ concentrations monitored at a near-road location, collected as part of the EPA near-road monitoring network *(33)*, as well as data from all other NAAQS monitoring stations during 2016 in Houston, were compared and analyzed. The monitor representing background $PM_{2.5}$ concentrations was selected to estimate the $PM_{2.5}$ increment due to traffic in a near-road environment. The $PM_{2.5}$ increment due to traffic was evaluated under different wind speeds and wind directions, and a multiple linear regression model was developed to predict the near-road 24-hour $PM_{2.5}$ concentration. To the knowledge of the authors, this is the first time that near-road $PM_{2.5}$ concentrations observed by a NAAQS monitor in Houston were investigated to quantify the traffic contribution to near-road $PM_{2.5}$ increment. The results of this study will give researchers a better understanding of the effect of transportation sectors on near-road $PM_{2.5}$ concentrations based on long-term observations that can be used for exposure assessments.

2.1.2. Materials and Methods

2.1.2.1. Monitoring Data

Selected for near-road monitoring was the north section of Interstate 610 in Houston, Texas (also called the North Loop), which is a heavily traveled road with a significant presence of heavy-duty diesel vehicles that is surrounded by a residential area. Continuous air monitoring station (CAMS) 1052, located on the north side of the North Loop became operational in April 2015. The CAMS 1052 probe was located at a 15-m distance and 4-m height from the outside nearest edge of the road. A 1-day-in-3 sampling dataset of monitored $PM_{2.5}$ using the gravimetric FRM at CAMS 1052, including the 24-hour $PM_{2.5}$ concentrations for 107 days during 2016, was available on the Texas Commission on Environmental Quality (TCEQ) database *(68)*. The CAMS 1052 did not monitor hourly $PM_{2.5}$ concentrations. Therefore, the only near-road $PM_{2.5}$ monitoring data during 2016 in Houston is available in a 24-hour time resolution at CAMS 1052. The hourly $PM_{2.5}$ concentration dataset for 10 other NAAQS beta attenuation monitors (BAMs) around Houston is also available on the TCEQ database. Among all air quality–monitoring stations in Houston, four stations were equipped with collocated FRM-BAM monitors, which provided both FRM and BAM data in 24-hour and hourly time resolutions during 2016. Hence, there are 15 $PM_{2.5}$ monitoring datasets available for Houston from 2016 (1 near-road monitor, 10 BAMs, and 4 FRM datasets from collocated monitors).

Figure 1 shows the location of the near-road $PM_{2.5}$ monitor (CAMS 1052) and the 10 other NAAQS monitoring stations in Houston. Considering the main intention of the EPA to collect near-road $PM_{2.5}$ concentrations that are comparable with the NAAQS

monitoring dataset, $PM_{2.5}$ concentrations monitored at CAMS 1052 were compared with those of other NAAQS monitors. To this end, the 24-hour $PM_{2.5}$ concentrations were obtained from four FRM monitors (other than the near-road monitor during 2016 in Houston) and were calculated for all NAAQS BAMs to be compared with the corresponding 107 measurements of 24-hour concentrations at CAMS 1052 (near-road monitor). In addition, hourly wind speed and wind direction monitoring data at CAMS 1052 (near-road environment) were obtained from the TCEQ dataset. It should be noted that gravimetric sampling is typically used to monitor the time-weighted average concentration of $PM_{2.5}$ in different ambient situations *(69, 70)*, and comparison of its data with continuous hourly data monitoring (obtained via BAM) has some limitations including sampling artifacts and averaging time differences *(71-73)*. A comparison of $PM_{2.5}$ monitoring data showed the precisions of FRM monitors and BAMs to be different *(74)*. Although a recent comparison of FRM and BAM $PM_{2.5}$ data obtained from a collocated monitor showed a correlation of 0.92 between two datasets *(75)*, this might not be the case for Houston considering its hot and humid climate. Availability of $PM_{2.5}$ monitoring data obtained from collocated stations during 2016 in Houston gives the opportunity of performing a comparison between $PM_{2.5}$ monitoring data obtained via FRM monitors and BAMs in Houston's particular meteorological condition.

2.1.2.2. Background Concentration

Following the description on how to determine background concentrations in the EPA guidance *(67)* for hotspot analyses of particulate matter, 10 NAAQS monitoring locations in Houston were evaluated to estimate $PM_{2.5}$ background concentration in 2016.

The hourly wind speed and wind direction monitored at CAMS 1052 (near-road environment) were used to draw a wind rose (Figure 1) and define the upwind direction for this particular near-road location. Because the prevailing wind blows from the southeast, the stations not located southeast of the near-road station (CAMS 78, 699) were not considered for background concentration. Among the eight monitoring stations located upwind of the near-road environment, the three stations close to a river or bay area (CAMS 148, 45, and 1034) were not good candidates for background concentration estimation considering the different land use of the proximate area. The three stations located within a few hundred meters of a roadway or railroad (CAMS 1, 304, and 416) could not represent background concentration because they were potentially affected by a close emission source. CAMS 697 also was surrounded by unpaved roads and areas and local emission sources *(76)*. Given these exclusions, just 1 monitoring location (CAMS 35) out of 10 was upwind, was surrounded by a similar land use, and was not located within an influence radius of an emission source, making it an acceptable candidate to represent background concentration. As mentioned before, $PM_{2.5}$ concentrations were monitored via two monitoring methods, BAM and FRM, with two different time resolutions, hourly and 24-hour, at CAMS 35. Considering the location of CAMS 35 and similarity in the $PM_{2.5}$ monitoring method, $PM_{2.5}$ concentrations monitored at CAMS 35 (Deer Park Station) using FRM monitoring were considered representative of background $PM_{2.5}$ in Houston relative to the near-road site, and the difference between CAMS 1052 (near-road concentration) and CAMS 35 FRM (background) data was considered to be the $PM_{2.5}$ "increment" due to traffic in the near-road environment.

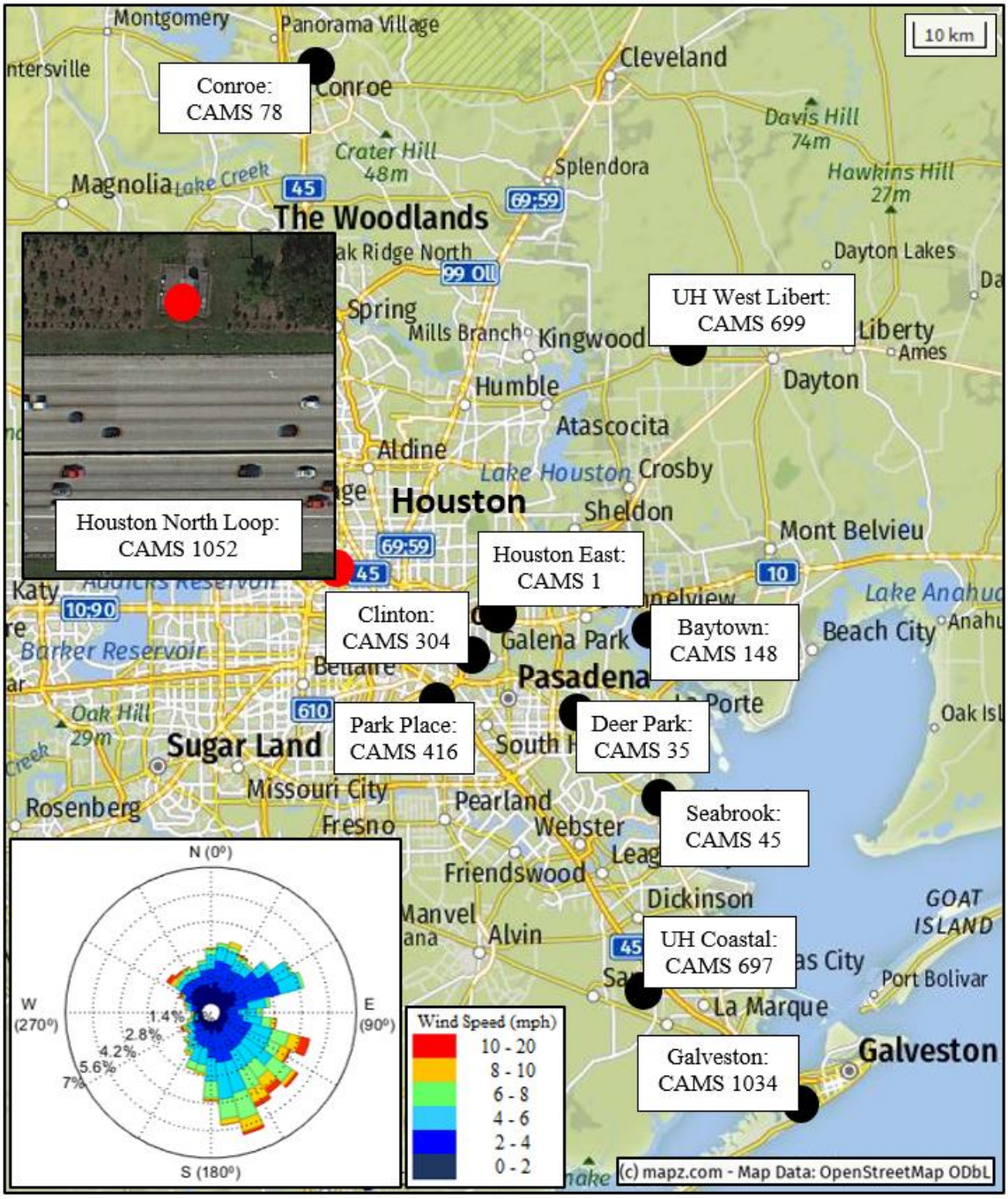

Figure 1- Locations of 10 monitoring stations, as well as the near-road monitor in Houston, 2016. (The near-road monitoring station is shown by the red mark [CAMS 1052], and other stations are shown by blue ones.) The wind rose shows prevailing winds at CAMS 1052 from the southeast.

2.1.2.3. Statistical Analysis

To investigate the $PM_{2.5}$ increment due to traffic in the near-road environment, a comparison of mean concentrations was performed between CAMS 1052 (near-road environment) and CAMS 35 FRM (background concentration) datasets. In addition, comparisons were made among all 15 sets of 24-hour concentrations to see how choosing different stations to represent background $PM_{2.5}$ concentrations lead to a different conclusion on near-road increment due to traffic. In this study, JMP Pro 13.1.0 *(77)*, a predictive analytics software, was used for statistical analysis. Figure 2 shows the relative frequency histograms of 24-hour $PM_{2.5}$ concentrations at 11 NAAQS monitoring locations (Fig. 1) including 15 datasets. Performing a Shapiro-Wilk *(78)* normality test for each set (of 24-hour concentrations) revealed enough evidence (p-value$<$ 0.05) against the normality of observation in 13 monitors other than CAMS 1052 (near-road environment) and 78. Because Figure 2 indicates that the data are log-normally distributed at most monitoring sites, a log transformation was applied to concentration data. Kolmogorov's test *(79)* did not reveal significant evidence against the log-normal distribution of any of 15 sets of 24-hour $PM_{2.5}$ concentrations (p-values$>$ 0.05).

To perform all possible pairwise comparisons of the difference of means in 15 sets of 24-hour $PM_{2.5}$ concentrations, Tukey's honestly significant difference (HSD) test was performed on log-transformed values. The main reason to perform Tukey's HSD test is that it is widely accepted to try parametric tests before moving to non-parametric test since parametric tests are generally more powerful than nonparametric tests *(80)*. To investigate the effect of using different monitoring methods (BAM and FRM) on $PM_{2.5}$ mean

concentrations observed in Houston, the Tukey's HSD test results were used to perform a pairwise comparison of two monitoring datasets obtained from each of four collocated monitors. Also, multiple linear regression models were used to investigate the relationship of near-road concentrations with background concentrations, wind speed, and wind direction.

2.1.2.4. Wind Effect on Near-Road Traffic-Related Air Pollution

The hourly wind speed and wind direction monitored at CAMS 1052 (near-road environment) were used to evaluate the effect of wind on near-road $PM_{2.5}$ increment. To this end, the average 24-hour vector of wind was calculated using 24-hourly wind vectors for each of 107 days. Plots of concentration roses (polar plots) were used to visualize wind speed and wind direction, as well as monitored concentrations all together in one figure. All concentrations and associated wind directions were classified into three wind classes of upwind, downwind, and parallel for statistical analysis to investigate if wind direction yields a statistically significant effect on near-road $PM_{2.5}$ increment. It should be noted that parallel wind class was assigned to wind directions with up to 30^0 deviation from the roadway centerline direction.

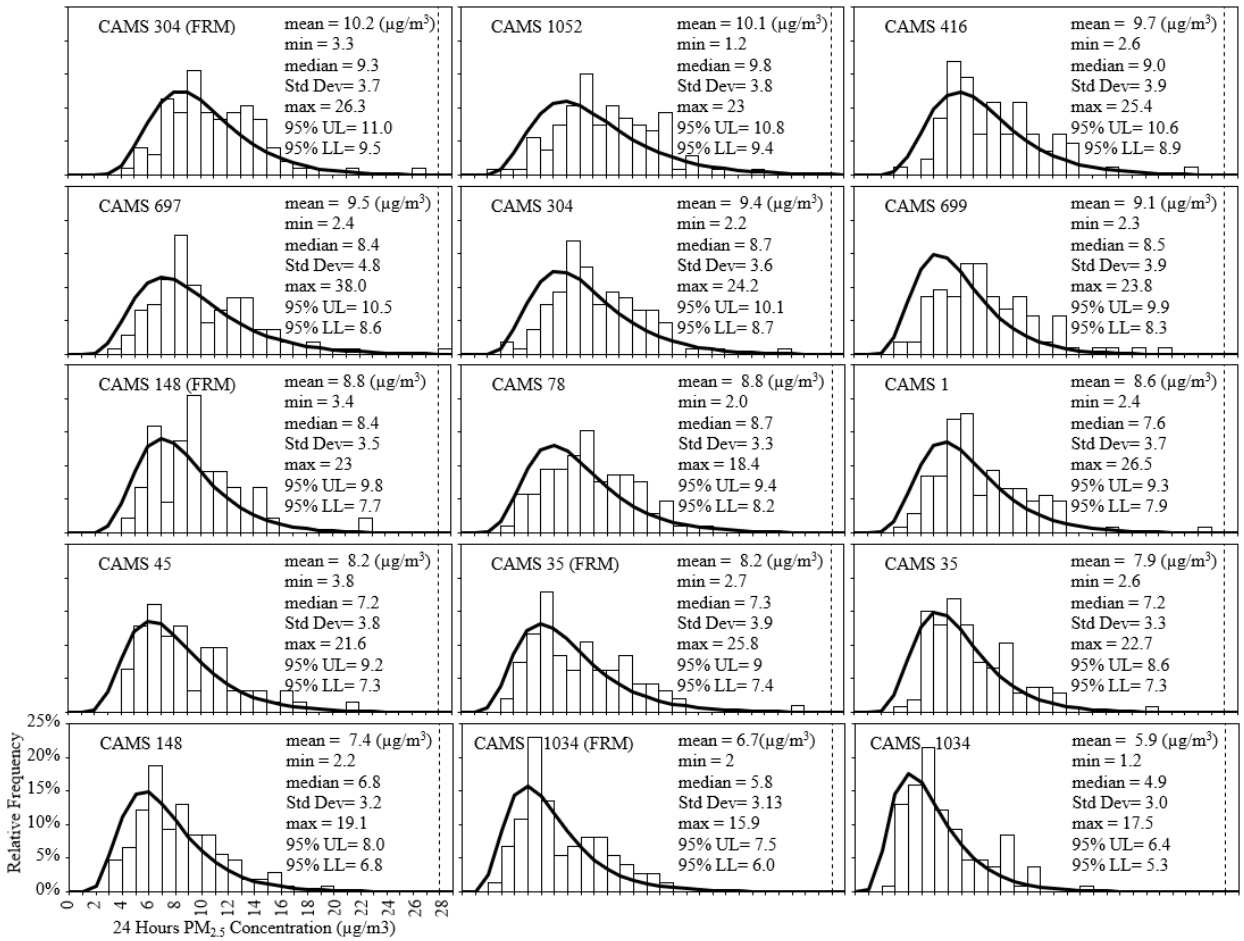

Figure 2- Relative frequency of 24-hour $PM_{2.5}$ concentrations and fitted log-normal distribution at 15 monitors in Houston, 2016. Both datasets obtained from collocated FRM-BAM monitors are included

2.1.3. Results and Discussion

2.1.3.1. Comparison of NAAQS Monitors

Tukey's HSD test was run to compare the 15 datasets based on log-transformed concentrations. Table 1 includes the results of Tukey's test, along with the mean values of 24-hour $PM_{2.5}$ (non-transformed) concentrations observed in each NAAQS monitor (calculated based on the corresponding number of available days out of 107). As can be seen, CAMS 304 (using FRM) has the highest and CAMS 1034 (BAM) has the lowest mean 24-hour $PM_{2.5}$ concentration among 15 NAAQS monitors in Houston. Tukey's test suggests that the mean concentration at CAMS 1052 is statistically significantly (p-value< 0.05) higher than that of the selected background monitor by1.92 $\mu g/m^3$ (equivalent to 23% of background $PM_{2.5}$ concentration), whereas the means of concentration monitored at CAMS 304 (FRM), 416, 697, 304, 699, 148 (FRM), 78, and 1 are not significantly different (p-value> 0.05) from the mean of CAMS 1052. Proximity to a roadway can explain the high $PM_{2.5}$ concentration monitored at CAMS 304 (FRM), 416, 304, and 1. The relatively high $PM_{2.5}$ concentration monitored at CAMS 78, 699, and 697 also can be explained by proximity to Conroe-North Houston Regional Airport (Lone Star Executive Airport), a railroad, and local emission sources, respectively. Monitored 24-hour $PM_{2.5}$ concentrations at CAMS 1034 were statistically different and lower than those of all other Houston NAAQS monitors in 2016, a fact that can be explained by the presence of no emission sources in the upwind direction. Pairwise comparisons (Table 1) show that the mean $PM_{2.5}$ concentrations provided by two monitoring methods (FRM and BAM) are not statistically significantly different in four collocated monitors (p-value> 0.05).

Comparison of mean values provided in Table 1, along with EPA guidelines provided previously in this paper, emphasize the importance of considering all selection criteria to determine a proper monitor location to represent background concentration.

Table 1- Statistics of 24-hour $PM_{2.5}$ concentrations monitored at 11 stations in Houston, 2016

Name	CAMS	Connecting Letters Report*							n	Mean ($\mu g/m^3$)
Clinton (FRM)	304	A							97	10.21
North Loop (FRM)	1052	A	B						107	10.11
Park Place	416	A	B	C					83	9.74
UH Coastal	697	A	B	C	D				107	9.54
Clinton	304	A	B	C	D				107	9.39
UH West Liberty	699	A	B	C	D				104	9.09
Baytown (FRM)	148	A	B	C	D	E			44	8.79
Conroe Relocated	78	A	B	C	D	E	F		105	8.78
Houston East	1	A	B	C	D	E	F		107	8.62
Seabrook	45		B	C	D	E	F		62	8.24
Deer Park (FRM)	35			C	D	E	F		95	8.19
Deer Park	35				D	E	F		107	7.92
Baytown	148					E	F		107	7.38
Galveston (FRM)	1034						F	G	74	6.74
Galveston	1034							G	107	5.87

* Levels not connected by the same letter are significantly different based on comparison of all pair means using Tukey's HSD test with 95% confidence (for example, the CAMS 1052's $PM_{2.5}$ concentration is statistically greater than those observed at CAMS 45, 35, 148, and 1034).

2.1.3.2. Near-Road Environment versus Background $PM_{2.5}$

Linear least squares regression was implemented to fit a model to background data in order to predict near-road concentration using a linear function of background concentration, as shown in Figure 3. A high Pearson's correlation coefficient (r= 0.87) indicates that near-road $PM_{2.5}$ concentration is highly correlated with background

concentration, as expected. The near-road measurements include background, whereas the background site is not influenced by the near-road increment explicitly, except for overall transportation contribution to the background concentration. The obtained coefficient of determination (r^2= 0.75) shows that the fitted model ($C_{Near\text{-}road}$= 0.85 $C_{Background}$ + 3.13 + ε) can explain 75% of the variability of near-road 24-hour $PM_{2.5}$ concentrations as a function of background concentration. The root mean square error (RMSE) for this model is 1.91.

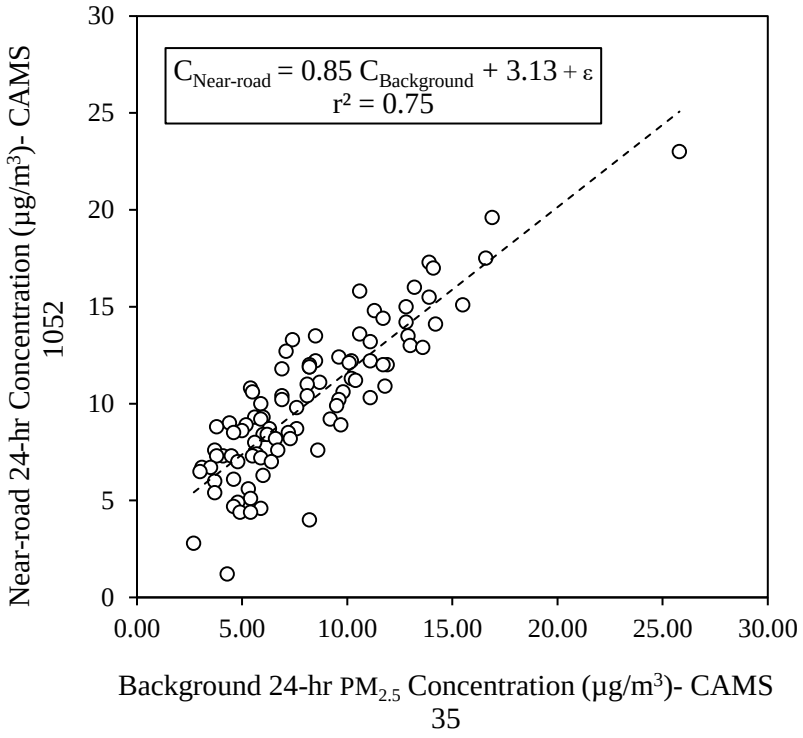

Figure 3- Near-road versus background 24-hour $PM_{2.5}$ concentration (µg/m³), linear regression (ε is the error term), and the coefficient of determination (r^2).

2.1.3.3. $PM_{2.5}$ Concentration, Wind Speed, and Wind Direction

Considering the proven influence of wind speed and wind direction on near-road traffic-related air pollutant concentrations *(16, 81)*, the effect of these two parameters also were investigated. The concentration rose plots shown in Figure 4 were used to visualize 24-hour $PM_{2.5}$ concentrations under the average wind vector for a corresponding day at background (Panel a) and near-road (Panel b) monitors. The concentration rose of the background monitor shows a more uniform distribution of concentrations in different wind directions compared with the near-road one that clearly shows higher concentrations when the wind blows predominantly from the south ($90^0 < \alpha < 270^0$), where the highway is located. The higher level of near-road concentration with wind direction varying between 90^0 and 270^0 can be explained by the fact that the near-road monitor is located downwind of the roadway in these cases and reflects the effect of traffic emissions. Both panels in Figure 4 illustrate lower concentrations for higher wind speeds, revealing a higher level of air pollutant mass transport from the emission source vicinity.

Figure 4 (Panel b) shows the near-road concentration rose with a lower level of $PM_{2.5}$ concentrations when the near-road environment is located upwind. It should be noted that this concentration rose (Figure 4, Panel b) also reflects the contribution of background concentration in each 24-hour $PM_{2.5}$ concentration. To eliminate the effects of background concentration and focus on the effect of traffic-related air pollution in the near-road environment, a concentration rose of near-road increments was plotted, as shown in Figure 5. Figure 5 clearly shows how south and southeast winds yield greater increments in the near-road environment when the near-road monitor is located downwind

of the target freeway. The negative concentrations (shown by black dots) when the wind blows from the north (near-road environment located upwind) place emphasis on the small contribution of emission sources located north of the monitoring point and the important contribution of traffic (the highway) to $PM_{2.5}$ concentrations monitored in this near-road environment. Some relatively higher concentrations also can be seen when low-speed winds blow from the north (monitor located upwind) or east (parallel), indicating elevated near-road increments with low-speed winds, as well as the effect of trapped traffic-related air pollutants on the near-road environment.

Comparisons were performed to investigate if the wind direction effect on the near-road $PM_{2.5}$ increment (Figure 5) is statistically significant in different wind classes. For this effort, all wind directions were categorized into three classes: downwind ($120^0<\alpha<240^0$), upwind ($\alpha< 60^0$ or $\alpha> 300^0$), and parallel ($60^0<\alpha<120^0$ or $240^0<\alpha<300^0$).

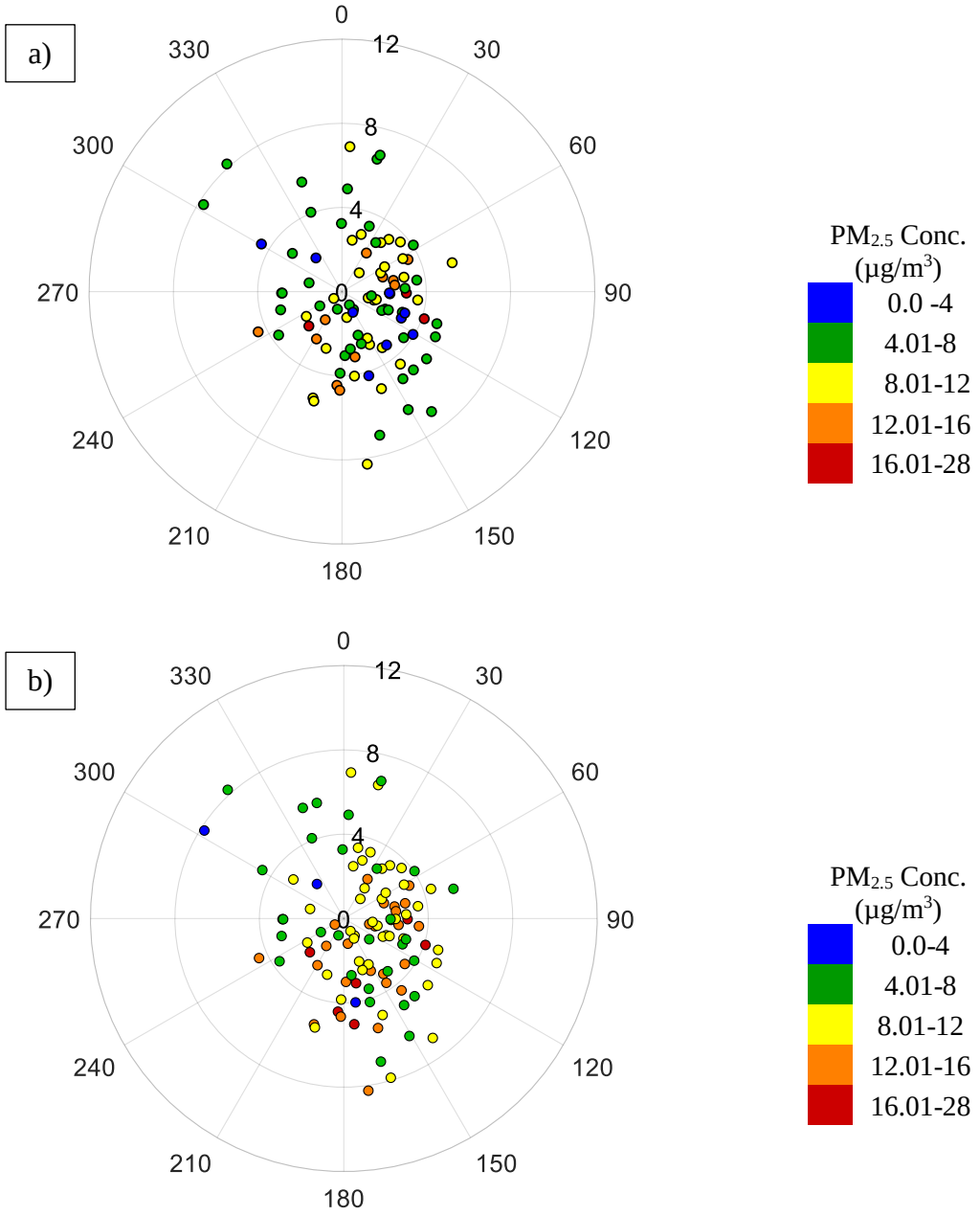

Figure 4- Comparison of 24-hour $PM_{2.5}$ concentrations (FRM) in corresponding wind speeds and wind directions at: a) background monitor (CAMS 35), and b) near-road monitor (CAMS 1052). Colors show concentration, the distance to the center shows wind speed varying between 0 and 12 mph, and the angle shows wind direction varying between 0^0 and 360^0.

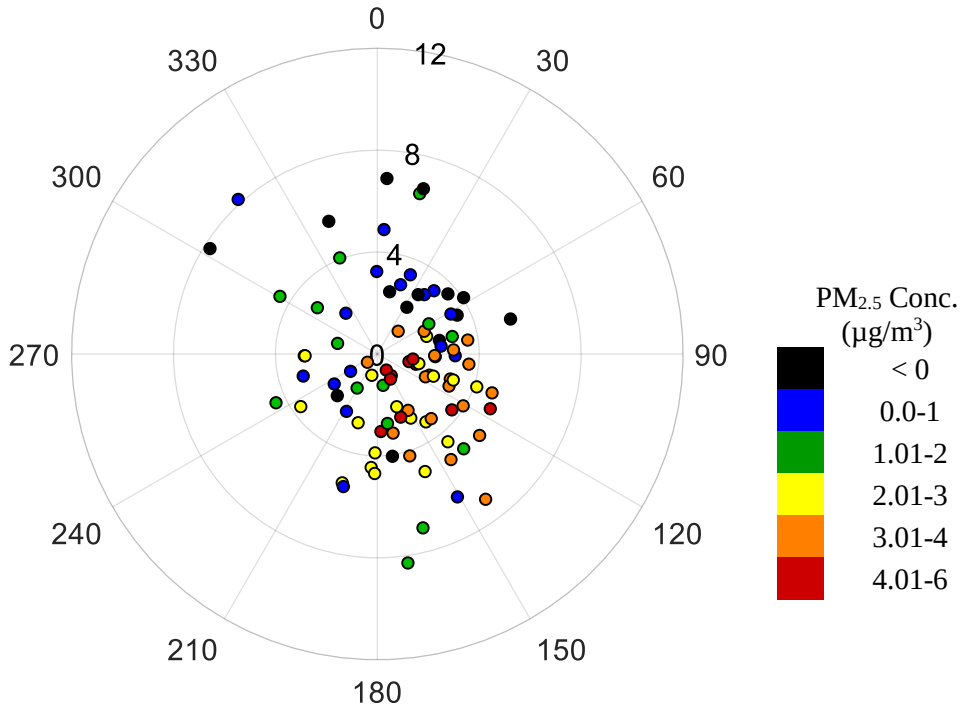

Figure 5- $PM_{2.5}$ increment in the near-road environment and corresponding wind speed and wind direction.

Table 2 shows the statistics of near-road $PM_{2.5}$ increments in different classes of wind direction. Performing a Shapiro-Wilk normality test for $PM_{2.5}$ increments in three wind classes revealed enough evidence (p-value< 0.05) against the normality of increments when the near-road is located downwind of the highway. The Kruskal-Wallis test was performed for pairwise comparison of mean near-road increments in different classes of wind direction; it revealed evidence of statistically significantly (p-value< 0.05) higher increments when the near-road monitor was located downwind or parallel compared with upwind.

Table 2- Statistics and comparison of mean near-road $PM_{2.5}$ increment in three classes of wind direction

Wind Class	Connecting Letters Report		N	Mean Increment ($\mu g/m^3$)	Std. Dev
Upwind	A		23	0.19	1.34
Downwind		B	40	2.47	2.02
Parallel		B	32	2.43	1.64

Considering the identified effects of background concentration, wind speed, and wind direction on near-road air pollutants, a multiple linear regression model was developed to predict near-road air pollutants using these three variables. It should be noted that multiple linear regression is based on specific assumptions including normality in distribution and homogeneity in variance of data, while performing the Shapiro-Wilk test revealed significant evidence (p-value< 0.05) against the normality of background concentrations (CAMS 35). Because the current analysis was performed on a relatively large dataset, the stringent requirement for normality could be waived, and the Central Limit Theorem could be assumed to be in full effect. Statistical analysis of fitting a multiple linear model to the near-road 24-hour $PM_{2.5}$ concentrations revealed a significant effect of background concentration, wind speed, and wind direction (p-values< 0.05). The multiple linear model including significant parameters and corresponding constants is:

$$C_{near-road} = 0.8\, C_{background} - 0.297\, S_w + f(D_W) + 4.349 + \varepsilon \qquad \text{Equation (1)}$$

where:

$C_{near-road}$ = Near-road 24-hour $PM_{2.5}$ concentration ($\mu g/m^3$)

$C_{background}$ = Background 24-hour $PM_{2.5}$ concentration ($\mu g/m^3$)

S_w = Wind speed (mph)

D_w = Wind direction (°)

$$f(D_W) = \begin{cases} 0.811 & \text{if } 120^0 < D_W < 240^0 \text{ (downwind)} \\ 0.672 & \text{if } 60^0 < D_W < 120^0 \text{ or } 240^0 < D_W < 300^0 \text{ (parallel)} \\ -1.483 & \text{if } D_W < 60^0 \text{ or } D_W > 300^0 \text{ (upwind)} \end{cases}$$

ε = Error term

Figure 6 shows a paired comparison of modeled to monitored near-road 24-hour $PM_{2.5}$ concentrations. The obtained adjusted coefficient of determination (r^2), and RMSE for this model are 0.91, 0.83, and 1.54, respectively. Both models' performance measures (adjusted r^2, RMSE) obtained from multiple linear regression show improvement compared with those obtained from linear regression using background concentration as the only predictor. The adjusted r^2 shows that the regression model with background concentrations, wind speed, and wind direction can explain 83% of the variability of near-road 24-hour $PM_{2.5}$ concentrations.

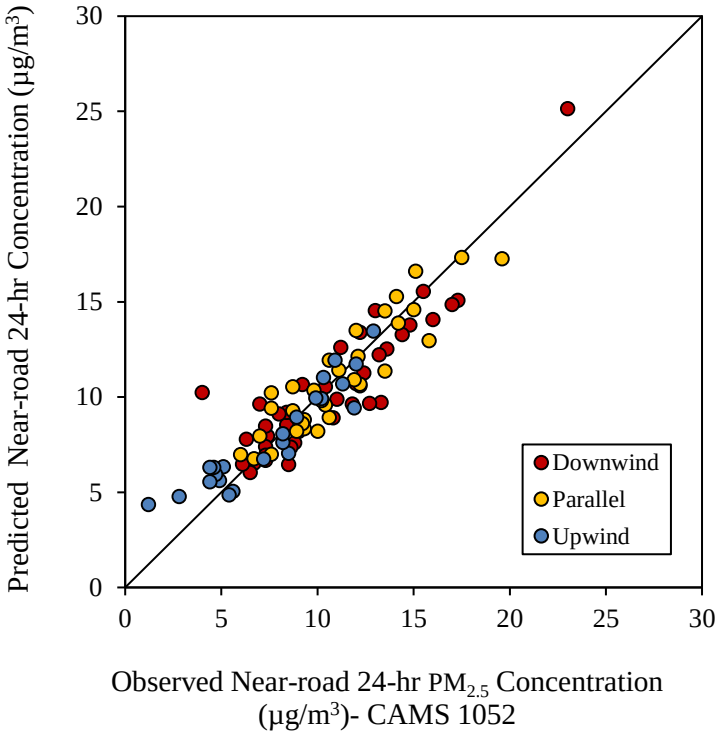

Figure 6- Multiple linear regression: paired comparison of model to monitored near-road 24-hour $PM_{2.5}$ concentrations.

2.1.4. Conclusion

For the first time, near-road $PM_{2.5}$ observations during 2016 were compared with those of other NAAQS monitors in Houston. Performing pairwise comparisons of all NAAQS $PM_{2.5}$ monitors revealed that the near-road monitor (CAMS 1052 located 15 m away from the edge of the freeway) observed $PM_{2.5}$ concentrations higher than most of the other monitors. Relatively higher $PM_{2.5}$ observations occurred for NAAQS monitoring stations located within a distance of a few hundred meters from a roadway. A NAAQS monitor (CAMS 35) was selected to represent background $PM_{2.5}$ concentrations in Houston based on EPA-provided methodology for quantitative hotspot analyses of

particulate matter. Tukey's test suggested that the mean concentration of the near-road monitor (CAMS 1052) is statistically significantly (p-value< 0.05) higher than that of the background monitor (CAMS 35). Regression analysis of near-road $PM_{2.5}$ monitoring data also showed a roughly 23% increment compared with the selected background monitoring data. This increment is close to what Karner et al. *(29)* showed (22%) and is greater than the US average near-road $PM_{2.5}$ increment (15%) that DeWinter et al. *(30)* reported. This difference might be caused by location- and traffic-specific characteristics. The difference in estimated near-road $PM_{2.5}$ increments can also be caused by selection of the background monitors using different methodologies, which emphasizes the importance of background monitor selection criteria. The near-road $PM_{2.5}$ increment was statistically lower when the near-road monitor was located upwind. Results demonstrated the effect of lower wind speeds on elevated near-road $PM_{2.5}$ concentrations, even in parallel winds, which should be taken into consideration in near-road dispersion modeling. A multiple linear regression model was developed to predict the near-road $PM_{2.5}$ concentrations using background $PM_{2.5}$ concentration, wind speed, and wind direction. Three measures (Pearson's correlation coefficient, the coefficient of determination, and RMSE) showed the multiple linear regression model performing better compared with the linear regression model using background concentration as the only predictor. The obtained adjusted r^2 for the multiple linear regression model indicates that 83% of the variability of near-road 24-hour $PM_{2.5}$ concentrations can be explained by a function of background $PM_{2.5}$ concentration, wind speed, and wind direction.

3. DISPERSION MODELING APPLICATIONS

3.1. Transportation Conformity Particulate Matter Hot-Spot Process: A Worst-Case Approach to Conduct Particulate Matter Hot-spot Analysis

The U.S Environment Protection Agency (EPA) requires project level hot-spot particulate matter (PM) transportation conformity analysis for projects in non-attainment and maintenance areas. El Paso is the only PM non-attainment area in Texas, which is in violation of the NAAQS for PM_{10}. Accordingly, PM hot-spot analysis is a requirement for projects of air quality concern (POAQC) in El Paso to ensure that the project will not contribute to localized violations of the NAAQS. The hot-spot analysis process is extensive, involving rigorous emissions and air dispersion modeling which requires state agencies to allocate considerable time and expertise. The objective of this study was to develop a worst-case scenario (WCS) analysis. WCS analysis consists of modeling with all possible combination of worst-case input parameters that would maximize PM_{10} concentrations. WCS is based on the premise that if the design value obtained is found to be less than the NAAQS, then one can logically conclude that the WCS does not cause violations of the NAAQS. The analysis is conducted for the I-10-US-54 location in El Paso near the U.S-Mexico border with a high traffic activity.

3.1.1. Introduction

Particulate matter (PM) is fine particles that are classified based on their size. Fine particles ($PM_{2.5}$) are mainly emitted from fuel combustion, and some industrial activities like processing metals *(82).* The U.S. EPA established the National Ambient Air Quality Standards (NAAQS) for PM. Transportation conformity analysis is required under the

Clean Air Act (CAA), Section 176(c) (42USC7506) *(83)* to make sure that federally supported transportation projects will not worsen existing air quality condition, or delay relevant timely plans. Hot-spot analysis is a prediction of future air pollution *(84)*, and their comparison to the NAAQS. The hot-spot analyses are a part of the CAA conformity requirements for pollutants that have localized impacts, i.e. particulate matter (PM) or carbon monoxide (CO). The U.S. EPA developed PM hot spots quantitative analysis, which includes prediction of vehicular emissions using the Motor Vehicle Emission Simulator (MOVES) model, followed by the use of dispersion modeling using CAL3QHCR or AERMOD models to assess localized concentrations *(67)*. The model set-up and input data preparation involve time-intensive and requires specific technical details.

The overall objective of this study was to provide guidance for definition of air quality projects and perform a worst-case PM hot-spot scenario (WCS) analysis specific to El Paso, TX. The study was focused on performing a "worst-case" scenario (WCS) analysis. WCS analysis consists of modeling with all possible combination of worst-case input parameters that would maximize PM_{10} concentrations. WCS is based on the premise that if the design values obtained is found to be less than the NAAQS, then one can logically conclude that the project planned will not cause violations of the NAAQS.

3.1.2. Methodology

3.1.2.1. Case Study

A WCS representative case study with high traffic volumes in El Paso is selected based on interagency consultation. The case study extent to be modeled for the WCS is consistent with the extent of the TxDOT's I-10 Connect Project (shown in Figure 7). Interstate I-10 is the main interstate within the city limits of the city of El Paso and experiences heavy traffic congestion due to new regional developments. The purpose of the I-10 project is to analyze and recommend operational improvements to the I-10 corridor. In the vicinity of the project area, I-10 and Loop 375 serve as major east-west freeway corridors while US-54 serves as a major north-south freeway corridor. The project area also includes access to the Port of Entry also known as Bridge of the Americas (BOTA).

Due to its expansive nature, the project area was divided into three sections (Figure 7) and was assessed for highest overall impact. Part 2 (Figure 7) covering a major part of I-10 interchange between La Luz Ave on the north and Rivera Ave on the south is selected for worst case analysis. Further, Part 2 is surrounded by a higher percentage of residential and commercial establishments compared to the other sections of the project area. In addition to on-road sources, the case study consists of a number of trucking and distribution facilities.

3.1.2.2. Construction of Scenarios

WCS analysis consists of modeling with all possible combination of worst-case input parameters that will maximize PM_{10} concentrations. Three sets of worst-case scenarios (WCS1, WCS2, and WCS3) were built based on different worst-case assumptions for the critical input parameters. In addition to the worst-case scenarios, an additional realistic scenario (RCS) was constructed based on realistic assumptions for the critical input parameters. The process of constructing worst-case and realistic-case scenarios consisted of a two-step process as listed below:

- Identify critical parameters that impact PM10 emissions and concentration estimates.
- Perform a sensitivity analysis for each parameters and identify the parameter value that results in worst-case and realistic-case estimates

Input parameters that have the most impact on PM10 emissions are identified based on sensitivity analyses performed as part of and relevant studies in literature (Volpe National Transportation Systems Center *(85)*, EPA Staff *(86)*, Coordinating Research Council *(87),* NCHRP Project 25-38 *(88)*. The following input parameters were utilized for constructing the scenarios:

Analysis Year

According to the EPA's PM hot-spot guidance *(89)*, hot-spot analysis must cover the year of highest expected emissions. The highest emission year typically can either be the opening year or the horizon/design year. The opening year has the highest emission factors, and the design year will have the most traffic (though lower emission factors), so

one of these years is likely to be the year of highest expected emissions. To strike a balance, the WCS is based on the year that produces the highest emission rates (ERs) and is combined with the highest traffic. Emission rates are calculated for analysis years from 2014 to 2020 at one year increment and 2020 to 2035 at five year increment. Based on the sensitivity analysis, year 2019 is identified as the worst-case year producing the highest ERs specific to El Paso.

Annual Average Daily Traffic (AADT)

The AADT is obtained from the TxDOT traffic projections from I-10 Connect Project. As part of the project, traffic demand modeling and traffic forecasting was performed. The project provided estimates of existing traffic volumes and forecasted future traffic volumes for build and no-build scenarios for calendar years 2012, 2017, 2037 and 2047. The RCS is modeled based on the build forecasts assuming a realistic case growth rate of 2%. The WCS1 is modeled based on the build forecasts assuming a worst case growth rate of 4%. In addition to TxDOT's traffic projections, new sources of data in the form of traffic counter information collected by TxDOT and real time speed data from INRIX were used to construct additional worst-case scenarios (WCS2, WCS3).

Truck Composition

Considering the determinant contribution of diesel trucks to a majority of PM emissions, Fleet mix specific to the case study is obtained for El Paso. The RCS is constructed based on the regional fleet mix (with a diesel truck fraction of 8%). The diesel truck fraction were increased to vary between 10 – 20% for different WCSs.

Seasonal Variation

Studies show that PM emission rates are higher during winter months *(86, 90)*. Since El Paso is considered to be a non-attainment area for PM10 during winter, all scenarios are modeled for January representative of the winter season.

Average speed

The effect of average speed distribution was analyzed by comparing emission rates associated with speed values ranging between 15 – 75 mph. As part of work on developing threshold values, speed values that produced the highest and lowest ERs were identified as listed in Table 3. Based on these values, and interagency consultation the average speed values for all scenarios were defined and displayed in Table 4.

(A) I-10 Connect ("BOTA") Project

(B) WCS Project Extent

Figure 7- Project extent

Table 3- Average speed from activity threshold values

	Vehicle Type	Analysis Years	Speed Bin ID (Speed in mph)
Highest ERs	Passenger Car (21)	Years 2014 – 2035	16 (75 mph)
	Passenger Truck (31)	Years 2014 – 2035	11 (50mph)
	Light Commercial Truck (32)	Years 2014 – 2035	16 (75mph)
	Combination short haul truck (61)	Years 2014 – 2035	4 (15mph)
	Combination long haul truck (62)	Years 2014 – 2035	4 (15mph)
Lowest ERs	Passenger Car (21)	Years 2014 – 2035	6 (25 mph)
	Passenger Truck (31)	Years 2014 – 2035	5 (20mph)
	Light Commercial Truck (32)	Years 2014 – 2035	5 (20mph)
	Combination short haul truck (61)	Years 2014 – 2035	16 (75mph)
	Combination long haul truck (62)	Years 2014 – 2035	16 (75mph)

The critical input parameters and their corresponding values for all scenarios are listed in Table 4. While WCS1 was developed based on sensitivity analysis of critical input parameters, WCS2 parameters were fine-tuned based on data collected in real-world (from traffic counter and INRIX) and WCS3 was solely based on a 20% increase in WCS1 traffic volume keeping all other parameters constant between WCS1 and WCS3.

Table 4- Critical input parameters for RCS, and WCS (WCS1, WCS2 and WCS3)

	RCS	WCS1	WCS2	WCS3
Analysis Period	Winter, 2019	Winter, 2019	Winter, 2019	Winter, 2019
AADT Growth rate applied on 2017 build case AADT of I-10 Project	2%	4%	4%	20% increase from WCS1
Fleet Composition	All time periods: 8% Combination trucks	All time periods: 15% Combination trucks	Morning peak, midday and evening peak: 10% Combination trucks Overnight: 20%	All time periods: 15% Combination trucks
Average Speed	Highways: (a)Off-peak: 65mph (b) Peak: 50mph	Highways: (a)Off-peak: 55mph (b) Peak: 15mph	Highways: (a)Off-peak: 55mph (overnight), 45mph (midday) (b)Peak:15mph	Highways: (a)Off-peak: 55mph (b) Peak: 15mph
	Arterials: (a)Off-peak: 40mph (b) Peak : 25mph	Arterials: (a)Off-peak: 35mph (b) Peak :10mph	Arterials: Off-peak: 25mph(overnight), 10mph (midday) Peak: 10mph	Arterials: (a)Off-peak: 35mph (b) Peak :10mph

3.1.2.3. Data Components

The overall framework to assess PM_{10} estimates for hot spot worst case analysis is shown in Figure 8. First, estimates of traffic activity were obtained from various data sources such as TxDOT traffic projections, traffic counter and emerging data source (e.g., INRIX) in varying resolution. The data was processed to have a consistent format and passed onto the emission module. The emission rates for tail pipe exhaust, brake wear, and tire wear were estimated using Motor Vehicles Emission Simulator (MOVES). The emission rates to road dust (resuspended dust) were estimated using AP-42. The emission

rates from MOVES and AP-42 were combined and processed in a format compatible for AERMOD dispersion model. AERMOD utilizes two main types of data, namely emissions data, and meteorological data. AERMOD produces concentration estimates at discrete receptor locations for different scenarios (WCSs, and RCS). Based on the modeled estimates for different scenarios and the NAAQS (150µg/m^3), the range of background concentration to achieve compliance for 24-hours PM_{10} was obtained. Descriptions about these data components is discussed in this section.

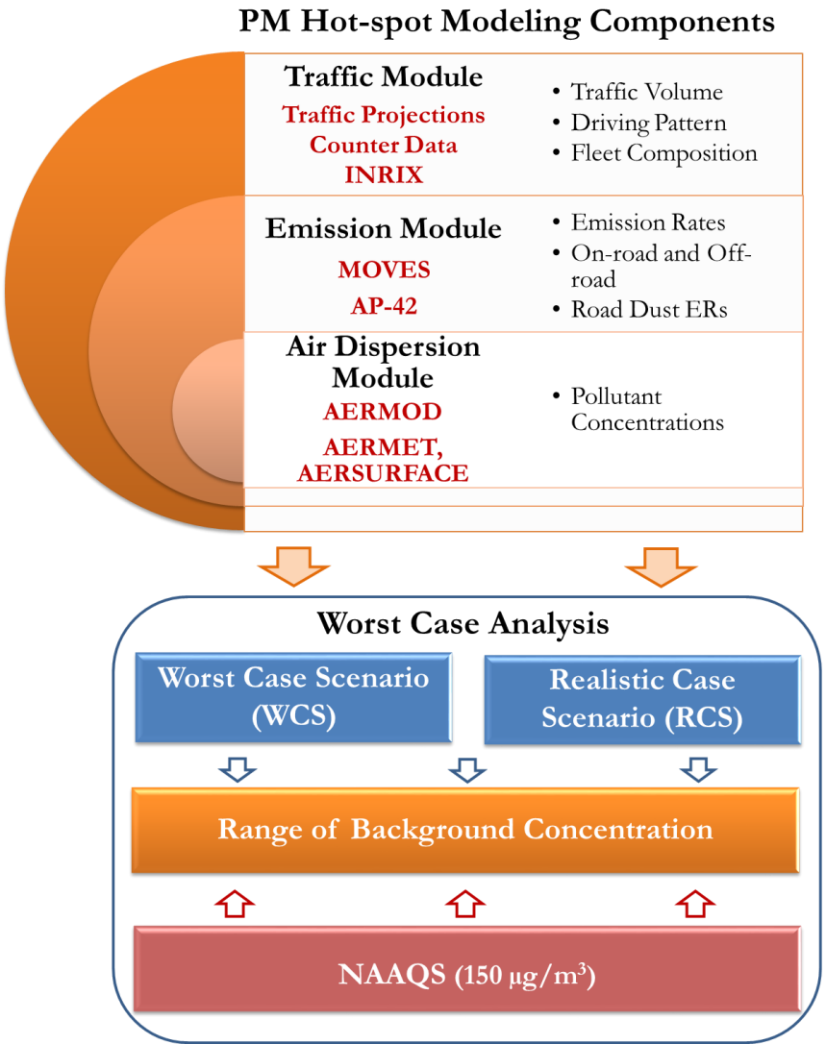

Figure 8- Modeling components involved in PM worst case analysis

3.1.2.4. Traffic Data

Traffic data was obtained from three data sources, namely (a) TxDOT traffic projections for I-10 project (also referred to as the "BOTA" study), (b) TxDOT traffic counts measured in 2015 and (c) INRIX *(91)* real-time traffic data for I-10-US-54 location collected in 2016. Traffic parameters for on-road sources (or links) required for PM hot-

spot analysis include traffic volume, fleet mix (or composition) and average speed. Sources of data utilized for each of these traffic parameters are listed below:

- Traffic volume: in from of AADT (annual average daily traffic) was obtained from the I-10 project projections and traffic counter data,
- Fleet mix: was obtained from regional conformity analysis specific to El Paso and traffic counter data, and
- Speed data: in form of average speed estimates was obtained from sensitivity analysis conducted as part of Phase 1 and the INRIX data set.

TxDOT's traffic projections for the case study, consisted of ADT (average daily traffic) for the existing (year 2012), base year (2017), 2037 (20-yr design year) and 2047 (30-yr pavement design year), for no build and build scenarios. The forecasts were developed using the Pivot Method with a combination of growth rate recommendations from TxDOT and Horizon model. Detailed information about the project can be found on TxDOT I-10 project website *(92)*. The WCS1 AADT for 2019 for select roadway links is shown in Figure 9.

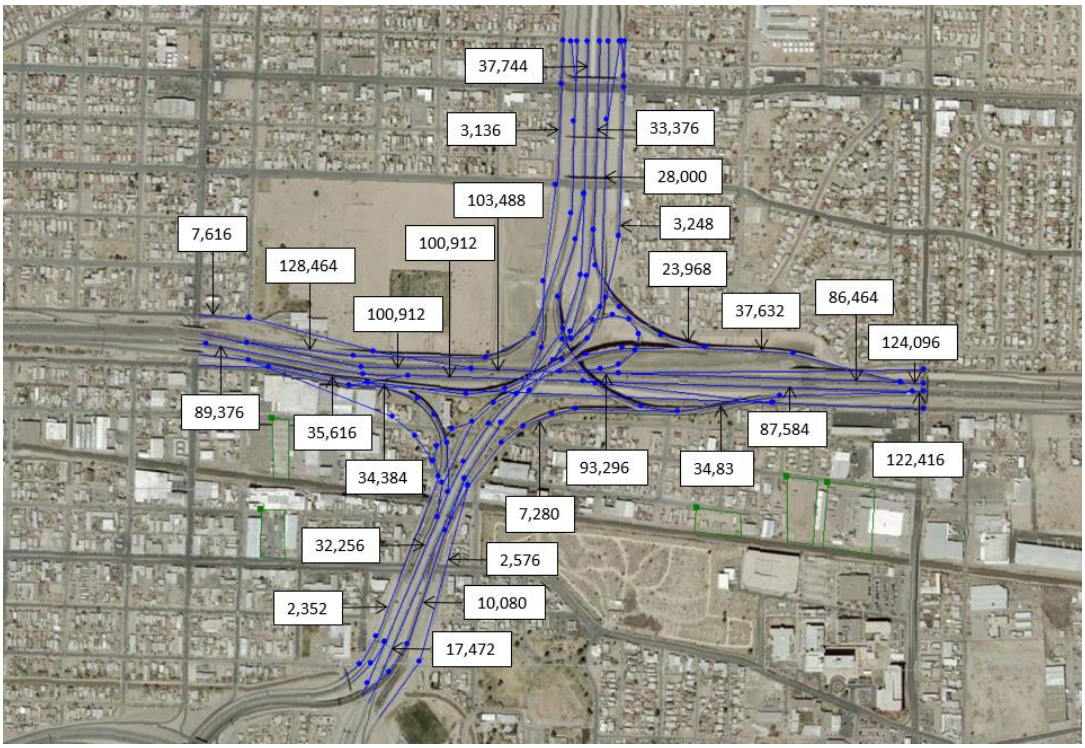

Figure 9- Worst case scenario AADT for select roadway links

3.1.2.5. Emissions (On-road, Off-road and Road Dust)

Emission estimates for on-road links and off-road network were obtained from EPA's MOVES2014a model, and road dust emission estimates from AP-42 model. The project scale of analysis in MOVES emission model was utilized for localized emission estimated involved in PM_{10} hot-spot analysis. The ERs obtained were post-processed to obtain total emissions (grams) for each link corresponding to the fleet mix, and traffic volume. For start emissions related to the off-network facilities, the ERs were combined with the distribution center facility specific hourly start distribution to get hourly total emissions. The total idle emissions obtained from MOVES was adjusted based on the truck duration and percentage idling of the dwell time distribution. Table 3 lists the input

data parameters for MOVES modeling. Road dust emission rates were calculated according to the method provided in AP-42 for paved roads.

3.1.2.6. Concentration Estimates

As the case-study includes highways, arterials and off-network links, the AERMOD dispersion model was selected for the air dispersion modeling. Vehicular emission sources were modeled using area representation. A total of 126 links were modeled with one or more area sources based on traffic activity, and geometry. Emission rates from MOVES, and AP-42 were combined for all links and normalized by the area of the AERMOD sources. The receptor height from the ground level was set to be 1.8 m based on the average human breathing height. The first group of receptors were located at a 25-meter spacing for a distance of 100 meter after allowing for the 5 meters (16.4 ft). The second group of receptors were located at a distance of 50 meter for a distance ranging between 100 and 300 meters, and the third set of receptors placed at 100 meters spacing for the remaining part between 300 to 800 meters (Figure 10).

The Texas Commission of Environmental Quality (TCEQ) produces pre-processed meteorological data for all counties in Texas. For each county, TCEQ produces three sets of meteorological data corresponding to three categories of surface roughness (low (0.001-0.1m), medium (0.1-0.7m) and high (0.7-1.5m)). Based on the surface roughness obtained through processing of case study site specific land use data, appropriate meteorological data is recommended to be used *(93)*. The surface roughness value for El Paso obtained by processing land cover data is 0.095 meter.

Table 5- Input parameters for MOVES model runs

Input Item	Description
Run Specification	
Scale	Project Scale (On-road), Inventory (off-road)
Calculation Type	Emission Rate
Geographic Bounds	El Paso, TX
Time Period	Analysis Years: 2019; Seasons: Winter (January) Time-of-day: Hourly
Road Type	Urban Restricted Access (highways) Urban Unrestricted Access (arterials) Off-network
Vehicle Type	13 vehicle types
Pollutant Type	PM_{10}
Emission Process	Highways: Running Exhaust, Crankcase Running Exhaust, Brake Wear and Tire Wear Off-network: Start and extended idling
Project Data Manager (Project Specific Input Data)	
Link Length	1 mile
Average Speed	• RCS Highway Off-peak: 65mph, Peak: 50mph Arterial Off-peak: 40mph, Peak :25mph • WCS1 Highway Off-peak: 55mph, Peak: 15mph Arterial Off-peak: 35mph, Peak :10mph • WCS2 Highway Off-peak: 55mph (overnight), 45mph (midday), Peak: 15mph Arterial Off-peak: 25mph (overnight), 10mph (midday), Peak :10mph • WCS3 Highway Off-peak: 55mph, Peak: 15mph Arterial Off-peak: 35mph, Peak :10mph
Fleet Composition	100% for each vehicle type
Age Distribution	Local specific data
Meteorology	Local specific hourly temperature and relative humidity
Fuel Supply	Local specific data
Inspection-maintenance program	Local specific data is

Figure 10- Source and receptor placement

Model outputs from AERMOD includes PM10 concentration estimates at 24-hour averaging time period at all receptors. Table 6 presents a summary of the key input data parameters from all three steps for the AERMOD model.

Table 6- Input data parameters for air dispersion modeling for AERMOD

Modeling Parameters	Inputs
Base Imagery	• Google Earth image covering the case study extent
Model Control Parameters	• Pollutant: PM_{10} • Averaging Period: 24 hours • Pollutant Properties: No deposition and settling
Meteorology	• Pre-processed meteorological data consisting of surface, upper air and land use data representative of case study location is obtained from TCEQ for five years (2008 to 2012)
Source Characterization	• Sources were defined based on the physical dimensions, and volume and speed as the traffic activity indicators. The case study site is modeled with a total of 126 links
Emission Factor	• ERs from MOVES and AP-42 • ERs are normalized with reference to time and source dimensions
Dispersion Parameters	• Initial vertical dispersion is computed based on a combination of initial vertical dispersion coefficient values weighted by traffic volumes • Release Height is computed based on a combination of release heights values weighted by traffic volumes
Receptor Characterization	• Receptors positioned at a height of 1.8, are placed at varying spacing of 25 – 100 meters extending to a distance of 800 meters • A total of 1,344 are placed
Output	• Sixth highest 24-hr average concentration values at all receptor locations are estimated

3.1.4. Results

The statistic required to determine compliance with the NAAQS for 24-hours PM10 was estimated using the 6th highest predicted concentration from the project and identifying the highest of these values (highest 6th highest value) across 5 years of meteorological data over all receptors. Concentration estimates were obtained for three sets of worst-case scenarios (WCS1, WCS2, and WCS3) and a realistic case scenario. Sensitivity analysis was performed to evaluate the difference in concentration estimates for different meteorological data sets processed for low and medium surface roughness. Difference in concentration values were also evaluated for different right-of-way distance from the roadway edge. In total, concentration estimates were obtained for a total of 12 scenarios based on the variation of the following parameters:

- Scenarios: (1) RCS, (2) WCS1, (3) WCS2, and (4) WCS4
- Surface Roughness: Meteorological data processed for low and medium surface roughness
- First row of receptors: placed at 5m and 15m from the edge of roadway links

Results obtained are shown in Table 7.

Among all scenarios, the WCS3 resulted in the highest estimates processed with low surface roughness meteorological data. The reduced friction from the low surface roughness to the wind blowing over the surface resulted in reduced dispersion of pollutants and thereby higher concentration estimates. As expected, higher estimates were observed at 5 meters first line of receptors compared to 15 meters is due to the peaking tendency of pollutant emissions released from vehicles.

Table 7- Highest 6th highest (H6H) PM_{10} concentrations

Scenario	First line of Receptors (m)	H6H (µg/m^3) *Low Surface Roughness*	H6H (µg/m^3) *Medium Surface Roughness*
RCS	5	30.59	29.02
RCS	15	24.49	21.57
WCS 1	5	45.07	40.85
WCS 1	15	35.2	30.32
WCS 2	5	44.9	42.2
WCS 2	15	33.7	29.8
WCS 3	5	**54.08**	**49.02**
WCS 3	15	42.24	36.38

Approximately a 20% reduction in the H6H values was observed by changing the first line of receptors between 5 and 15 meters. Between the RCS and WCS1, approximately a 30% increase in the H6H PM_{10} concentrations at 24-hrs averaging period was observed. The WCS1 and WCS3 have identical parameters except for a 20% increase in AADT, this 20% increase translated into a 20% increase in the H6H concentration estimates. Between WCS2 and WCS3, changes in AADT, fleet mix and speed resulted in significant differences in PM_{10} estimates.

Concentration maps showing the PM_{10} dispersion patterns for the WCS1 are shown in Figure 11. Higher concentrations were obtained near the major highway (Interstate I-10) that carries the highest traffic volumes during all time periods. Comparison of the PM_{10} concentration maps between all scenarios is shown in Figure 12. The dispersion patterns of PM_{10} concentrations was found to be similar for all scenarios, with the highest concentrations always obtained near the I-10 corridor.

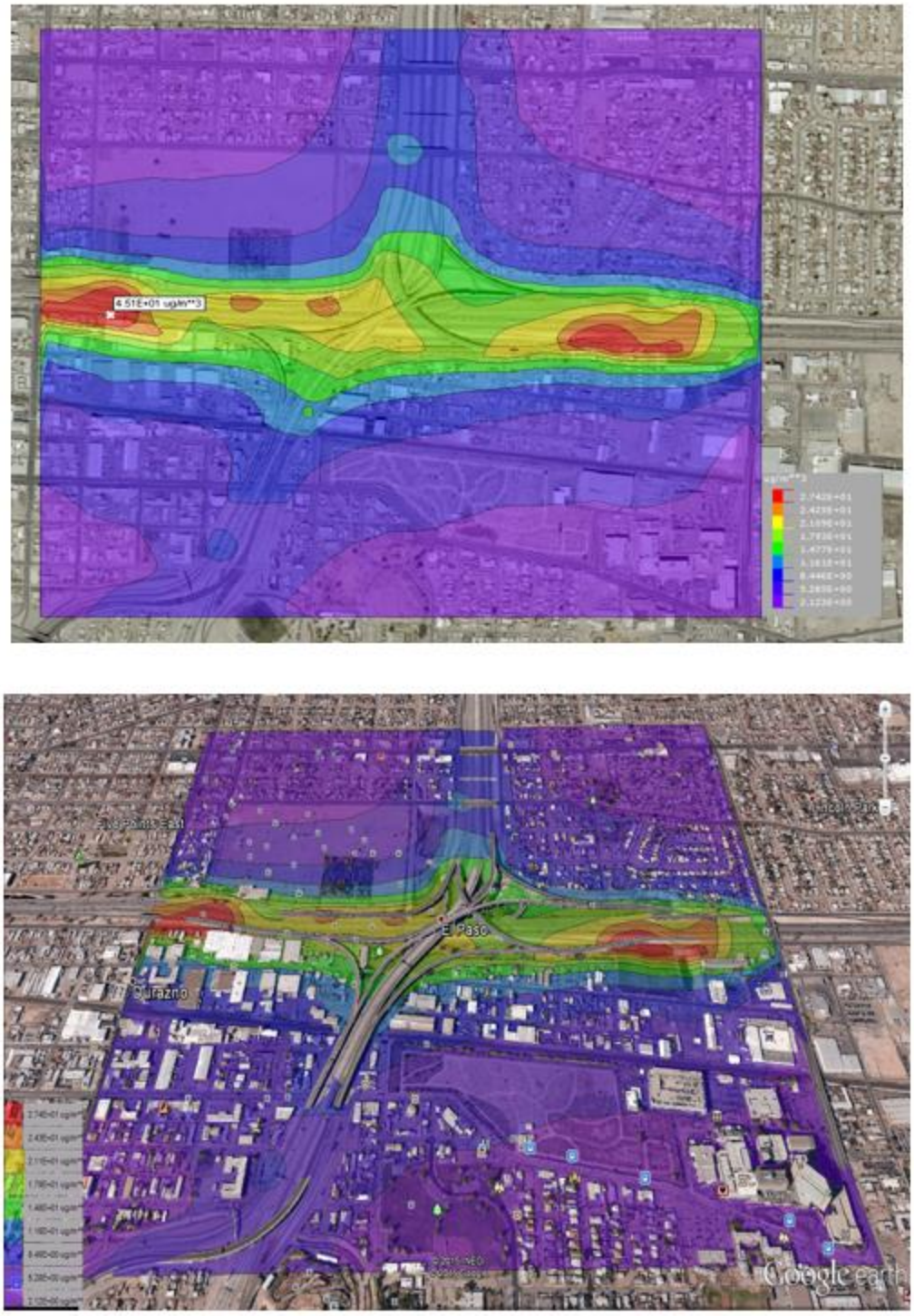

Figure 11- PM_{10} concentration map (WCS1)

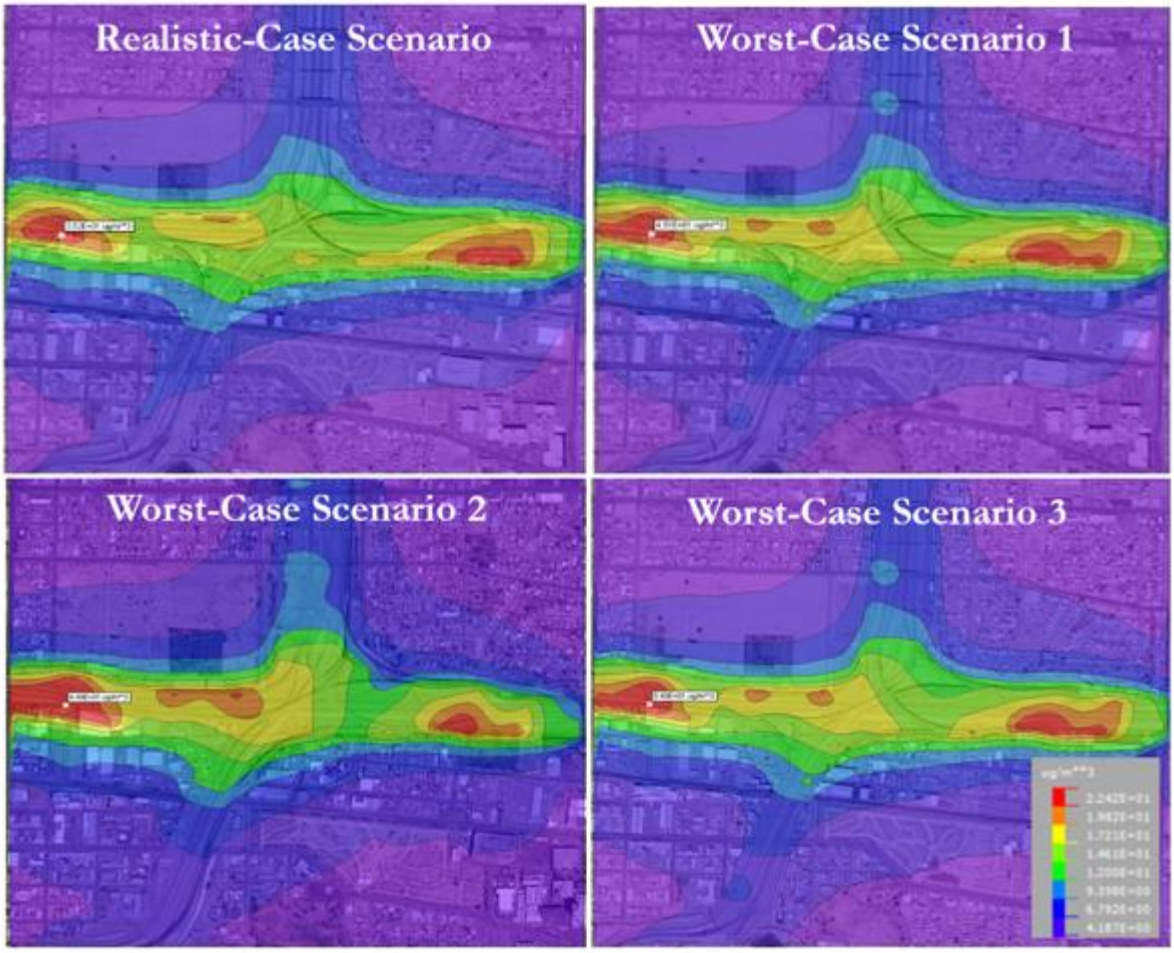

Figure 12- Comparison of concentration maps for different scenarios

According to the EPA guidance *(89),* compliance with the NAAQS for 24-hours PM_{10} is determined based on the calculation of the "design value." Design value (DV) is a measure that indicate the air pollutant concentration in a project area. Design value is compared to the NAAQS to determine compliance and it consists of two main components: (1) modeled concentration estimates from the project and (2) background concentration from all sources surrounding the project excluding the contribution from the project.

$$Design\ Value = Air\ Quality\ Modeling\ Results + Background\ Monitoring\ Data$$

Equation (2)

- Air Quality Modeling Results are calculated based on the 6th highest 24-hour modeled concentration and identifying the highest of these values (highest 6th highest value) across 5 years of meteorological data over all receptors
- Background Monitoring Data are calculated based on three most recent years data

Based on the modeled estimates from Table 7 and the NAAQS, the range of background concentration to achieve compliance for 24-hours PM_{10} is shown in Table 8. As seen in Table 8, as long as the background concentration is equal to or less than 95.92 for the WCS3 which produces the highest concentration estimate among all scenarios, the project conformity requirement with the NAAQS is met.

Table 8- Range of background concentrations to achieve compliance with NAAQS

Scenario	PM10 H6H (µg/m^3)	NAAQS	Background Concentration (µg/m^3)
RCS	30.59	150	≤ 119.41
WCS1	45.07	150	≤ 104.93
WCS2	44.89	150	≤ 105.11
WCS3	**54.08**	**150**	**≤ 95.92**

3.1.5. Conclusion

There are a number of insights that this study and its results yield and can be e helpful for conducting PM hot-spot analysis. First, the results emphasize the importance of careful selection and processing of input parameters for traffic, emissions and air dispersion components. As highlighted by the sensitivity analysis, quality assurance at every step of the modeling process is needed to avoid possible problems in prediction of air pollutant concentration.

Another important insight is the importance of background PM concentration. Background PM were typically much higher than the project contribution that was modeled, thereby dominating the design value. Similarly, uncertainties and sensitivities in the modeled project contribution may be dominated by those associated with the background concentration. This consideration is important for understanding the potential outcome of a design value that hinges predominantly on the background. Another insight gained is the importance of road dust emission characterization due to the importance of road dust as a major category in the PM emission inventory. Currently, road dust ERs are calculated using AP-42, which is outdated and based on aggregate estimates. Additional research is needed to improve the associated modeling techniques for this process.

3.1.6. Acknowledgement

This study was conducted at Texas A&M Transportation Institute (TTI) as part of a research project titled "*Conducting PM10 Hot-spot Worst-Case Analysis,"* funded by the Texas Department of Transportation (TxDOT). This study was supervised by Dr.

Vallamsundar and this article was submitted to Transportation Research Board (TRB) 2019 and was presented at TRB annual meeting. A group of TTI researchers (Suriya Vallamsundar, Mohammad Hashem Askariyeh, Chaoyi Gu, and Reza Farzaneh) contributed to this study.

3.2. Pregnant Women Exposure to Traffic-related Air Pollution in South Texas[3]

Given the significant public health and economic costs associated with the rapidly increasing prevalence of transportation-related health effects, there is a critical need to determine traffic-related emissions exposure at the individual level. Population groups vulnerable to adverse effects of traffic-related air pollution correspond to children, pregnant women and elderly because of their physiological conditions. Literature is limited in terms of studies focusing on these groups. A reason often cited is the limited information on mobility which is critical for exposure assessment at the individual level. Emerging datasets such as GPS and Bluetooth technologies continuously tracking human behavior are used for a wide variety of applications. The current study presents a method for assessing traffic-related emissions exposure by integrating mobility patterns tracked by GPS devices with dynamics of pollutant concentration modeled by regulatory models. The study is based on a pool of women (in their third trimester of pregnancy) residing in Hidalgo County, Texas who are equipped with wearable monitoring devices. The entire network-based transportation emissions and pollutant concentrations were estimated using EPA's MOVES and AERMOD models, respectively. The obtained $PM_{2.5}$ exposure levels exhibited considerable variation between time-periods within a day, with higher levels modeled during peak commuting periods, especially close to the U.S-Mexico border region and lower levels during midday periods. The study also assessed if there was any

[3] *Reproduced with Permission from:* Askariyeh, M.H., Vallamsundar, S., Zietsman, J., Ramani, T., International Journal of Environmental Research and Public Health, 16(13), 2433, Copyright 2019, MDPI.

difference between dynamic exposure, based on time-varying mobility patterns, and static exposure based solely on residential locations.

3.2.1. Background

Recent evidence shows traffic emissions to be a significant source of pollution *(94)* with several studies showing a strong association between elevated emissions levels and near-roadway areas *(95-97)*. Accordingly, epidemiology studies document adverse respiratory, and cardiovascular effects *(98-100)* for populations living in close proximity to major roadways. Studies show specific adverse health effects of people exposed to Particulate Matter (PM) including heart diseases *(101, 102)*, cancer risk *(103)*, and adverse birth outcomes *(104)*. Children, pregnant women, the elderly and people with existing health issues are some of the vulnerable population groups to PM that suffer from adverse health effects of traffic-related emissions exposure. Studies demonstrate a correlation between traffic-related emissions exposure with reduced fetal growth, preterm birth and post-term low birth weight and susceptibility to asthma *(105, 106)*.

Exposure to harmful concentrations of emissions depends on (1) the location and time of exposure; and (2) the emission concentrations in different microenvironments. Most epidemiological studies estimate exposure levels based on data from ambient monitors and census information *(107-110)*. Due to the spatial movement of individuals, fixed ambient monitoring data might not accurately capture the exposure levels *(1, 111)* as they are not at a sufficient spatial resolution and do not provide a source-specific contribution. This limitation can be overcome by employing personal exposure

monitoring, which is typically limited in terms of the sample size due to their higher cost of covering larger samples. Air dispersion models, on the other hand, use numerical techniques to predict the dispersion patterns of emissions based on the source strength, rate of emission release, meteorology, and land use. Several prior studies evaluated exposure levels based on air dispersion models *(112-114).*

Among the different population groups, there have been limited studies focused on assessing maternal exposure to air pollution *(115-117).* Exposure levels for pregnant women could vary compared to the general population because of their different activity patterns*(116, 118).* The National Human Activity Patterns Survey, an extensive survey conducted from the year 1992 to 1994 for 9386 people all over the US did not address pregnant women activity patterns *(119).* Limited studies *(116)* have determined the activity patterns based on self-reported assessments. These assessments could lead to inaccurate reporting of location or activity duration *(120)*. Emerging technologies such as smartphones and Bluetooth devices are able to provide highly resolved spatial and temporal information about people's activities. Anonymized data obtained from these technologies have the potential to improve the characterization of emissions exposure.

This study focused on evaluating the traffic-related emission exposure for a group of pregnant women across different microenvironments. The study is based on 17 third trimester pregnant women who were equipped with a portable global positioning system (GPS) tracking device for three days. Specifically, this study focused on exposure to fine particulate matter with a diameter less than 2.5 μm ($PM_{2.5}$). Exposure levels were modeled based on the active location information of people (also referred to as dynamic exposure)

compared to their fixed residential location of people (static exposure). The study used a combination of emerging techniques such as GPS technology, air dispersion modeling and spatial interpolation techniques to model dynamic population exposure to traffic-related pollution. This study was conducted in Hidalgo County, South Texas where the prevalence of childhood asthma is found to be the highest in the State of Texas. The key objective was achieved through the following steps:

1) Calculate emissions and pollutant concentrations from traffic emissions at a refined roadway link level for the entire county. The U.S. Environmental Protection Agency (EPA) regulatory models MOVES and AERMOD were employed for calculating the emission and pollutant concentration in the atmosphere.

2) Examine dynamic exposure by combining the interpolated pollutant concentrations with dynamic location information obtained from GPS devices

3) Examine variability in modeled traffic-related emission exposure levels during a day and

4) Compare the differences between dynamic and static exposure assessment.

3.2.2. Methodology

The emission module calculates emission rates based on traffic and other parameters. The emission data were modeled with EPA's microscopic MOVES emission model that utilizes site-specific traffic activity data and other local specific data corresponding to vehicle age distribution, fuel supply, and inspection/maintenance parameters, etc. These emission rates were combined with meteorological were land use

data in the dispersion module. Site-specific meteorological and land use data are obtained from closest surface data and upper air weather stations. The emission dispersion was modeled using the AERMOD model at discrete receptor locations. A spatial interpolation technique was applied to the discrete concentration levels to create continuous surfaces of $PM_{2.5}$ concentrations. Activity information of participants was tracked by GPS devices for 24 hours at a 10-second resolution. Specific details about the different modeling components are discussed in this section.

3.2.2.1. Air Dispersion Modeling

AERMOD is a Gaussian-based dispersion model which incorporates factors that account for the rate the plume disperses in each direction, reflection from the ground and plume rise *(121)*. The dispersion modeling process consists of three broad steps.

Step 1: consists of obtaining the base imagery, specifying model control parameters, securing emission, meteorological and land use data. Base imagery shows the geographical locations corresponding to the study area and helps in geographically coding the sources and receptors. The model control parameters refer to the specific pollutant type, pollutant properties, and averaging period etc. Three types of data are required for processing the meteorological data, namely: (1) land use data that represent surface characteristics, (2) surface data collected at airports by the National Weather Service (NWS), and (3) upper air sounding data collected by NWS. The land use data was obtained from the U.S. Geological Survey (USGS) Land Use database *(122)*. The raw data was processed by AERMOD preprocessors, (AERMET, AERMAP, AERMINUTE, and AERSURFACE) in a format compatible for AERMOD.

Step 2: consists of characterizing the emission sources (i.e., adjacent roadway links) and placing receptors. AERMOD area source characterization used to model the roadway links. Source (roadway link) dimensions were defined based on the roadway link orientation, geometry, and travel activity. Pollutant concentration levels were calculated at discrete receptor locations, placed at an average adult breathing height of 1.8m. To capture the peaking tendency of traffic-related emissions, receptors were placed at a higher density closer to roadways.

Step 3: Based on inputs assembled from Steps 1 and 2, AERMOD estimates pollutant concentrations at a desired averaging period at all receptor locations.

3.2.2.2. Spatial Interpolation

Emission concentrations estimated at discrete receptor locations are converted into a continuous surface by employing a spatial interpolation technique in a geographic information system (GIS) platform. The inverse distance weighting (IDW) technique was utilized which estimates the value at an unknown location based on computed values at nearby locations. Closer locations (or receptors) were given more weight than those farther away, and the weight rate of decrease with distance was dependent on the power value (a power value of 2 is used in this study).

3.2.2.3. Location-Allocation

Spatial-temporal dynamics of people's location was captured using portable GPS devices. The advantages of these techniques include minimum burden for participants, high-resolution continuous tracking of location and reduction of human errors in reporting the locations *(123)*. This study used portable GPS technologies to track location

information of participants at a 10-second resolution for 24 hours. The location information was overlaid over the continuous concentration maps generated by AERMOD to obtain dynamic exposure levels of the participants across the study area.

3.2.2.4. Exposure Assessment

Early researchers *(124, 125)* first established the mathematical formulation (Equation 3) for exposure assessment as the product of time and concentrations in different locations;

$$E = \int C(t)dt \qquad \text{Equation (3)}$$

where E is the cumulative exposure (concentration × time), C is the traffic-related emission concentration, and dt is the time spent in different locations. Time-weighted average exposure is estimated by dividing E by T (total time spent in all locations) *(126)*. Three classifications of microenvironments were considered in this study. Incorporating these microenvironments, Equation 3 was customized into Equation 4 considering indoors, outdoors and in-vehicle.

$$E = \sum(T_{ii}\, C_{ii} + T_{io}\, C_{io} + T_{iv}\, C_{iv}) \qquad \text{Equation (4)}$$

where C_{ii}, C_{io}, C_{iv} are indoor, outdoor and in-vehicle concentrations respectively; T_{ii}, T_{io}, T_{iv} are the time spent in corresponding microenvironment. To incorporate the change in concentrations microenvironment, Equation 4 is modified into Equation 5. The adjustment

factors are used to account for the difference in indoor and in-vehicle concentration compared to ambient concentration.

$$E = \sum(T_{ii}\, C_{io}\, A_o + T_{io}\, C_{io} + T_{iv}\, C_{iv}\, A_v) \qquad \text{Equation (5)}$$

where A_i, and A_v are the adjustment factors for indoor, and in-vehicle locations. The adjustment factors are obtained from the literature *(127, 128)*. An adjustment factor of 0.88 and 1.79 are used for indoor and in-vehicle microenvironments. Using this approach, cumulative exposure was calculated as a function of the person, time, and microenvironment.

3.2.3. Case Study

The case study is located in Hidalgo County (Figure 13), Texas. As of the 2010 census, the county had an estimated population of 774,769, making it the eighth-most populous county in Texas. The county has the highest prevalence of childhood asthma in the State and accounts for the greatest share of people receiving food stamps *(129)*. The largest city in Hidalgo is McAllen, while the county seat is Edinburg.

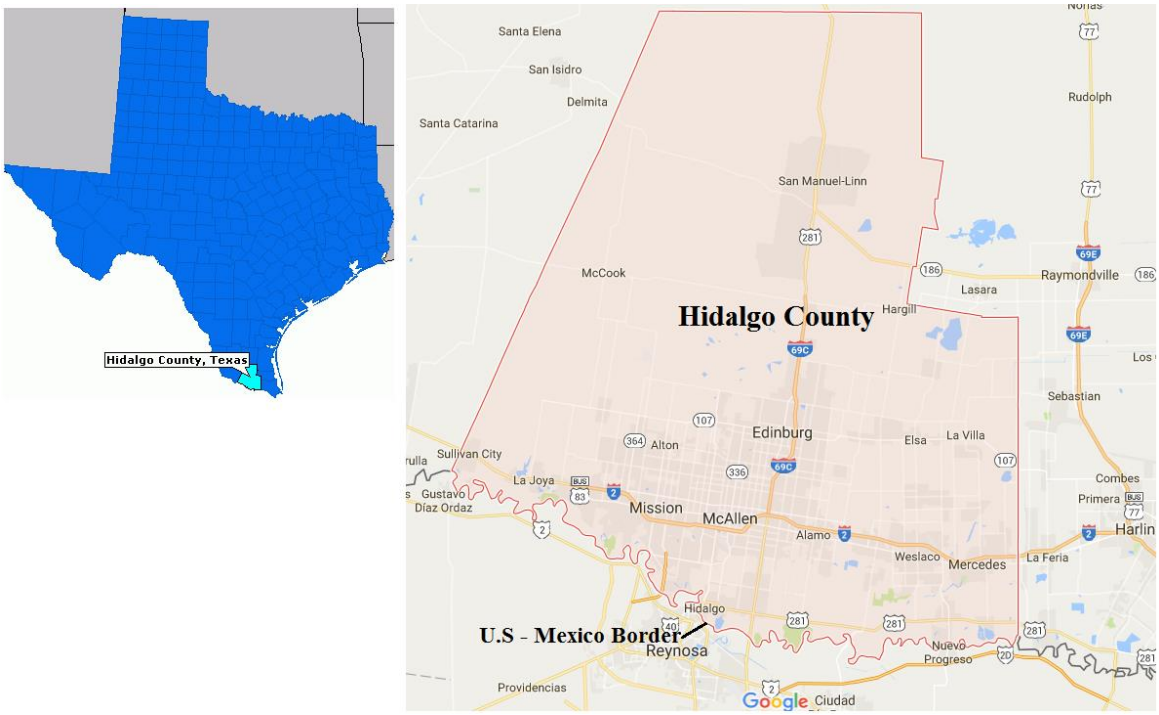

Figure 13- Case study location

Study participants consisted of women in their third trimester of pregnancy recruited from the Rio Grande Valley Regional OBGYN Clinics in McAllen and Edinburg, TX. A pool of 17 participants carried a portable GPS device from October 2015 to May 2016 for three non-consecutive 24-hour periods. This resulted in a total of 50 sampling days (16 participated in the sampling on days and 1 conducted the sampling in two days).

The $PM_{2.5}$ traffic-related emissions and concentration levels were assessed for the entire Hidalgo County. Traffic activity data for all roadway links (excluding minor collectors and local roads) were obtained from traffic counters. The activity data collected included average daily traffic volumes, average vehicle trajectory, and fleet composition at the roadway link level. The average daily traffic volume is converted into hourly

volumes using growth factors and hourly traffic percentages. These adjustment factors and regional level information (related to age distribution, fuel supply, and inspection/maintenance program) were obtained from the latest on-road mobile source inventories prepared for Texas *(130)*. Hourly distribution of traffic is shown in Figure 14. Traffic levels were found to be higher during morning and evening peak commuting periods and lower during overnight time periods.

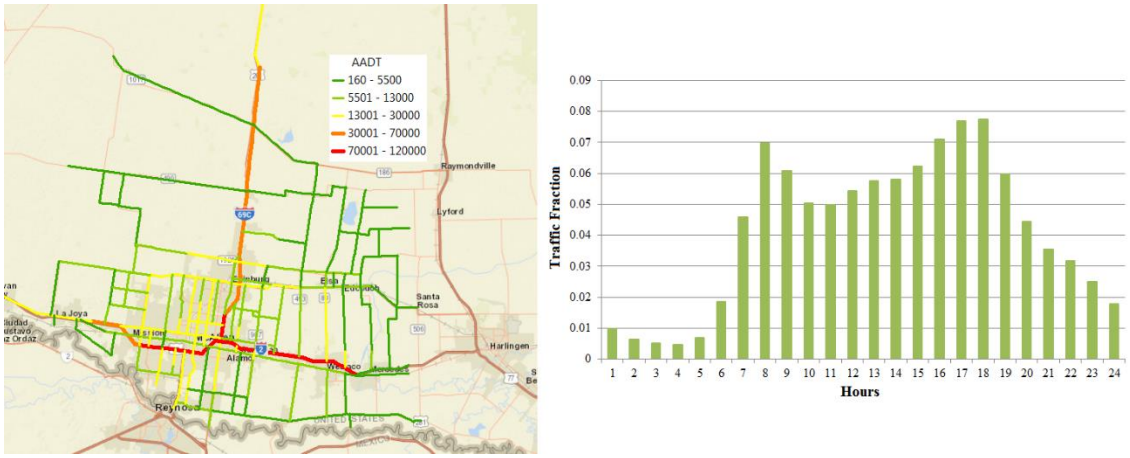

Figure 14- Distribution of AADT (left) and hourly traffic (right)

The composite $PM_{2.5}$ emission inventories for all roadway links were obtained from the latest version of MOVES emission model. Surface data was obtained from the McAllen International Airport and the upper air data from the Brownsville Airport. The wind rose diagram (Figure 15) shows the predominant wind direction to be in the south-east direction.

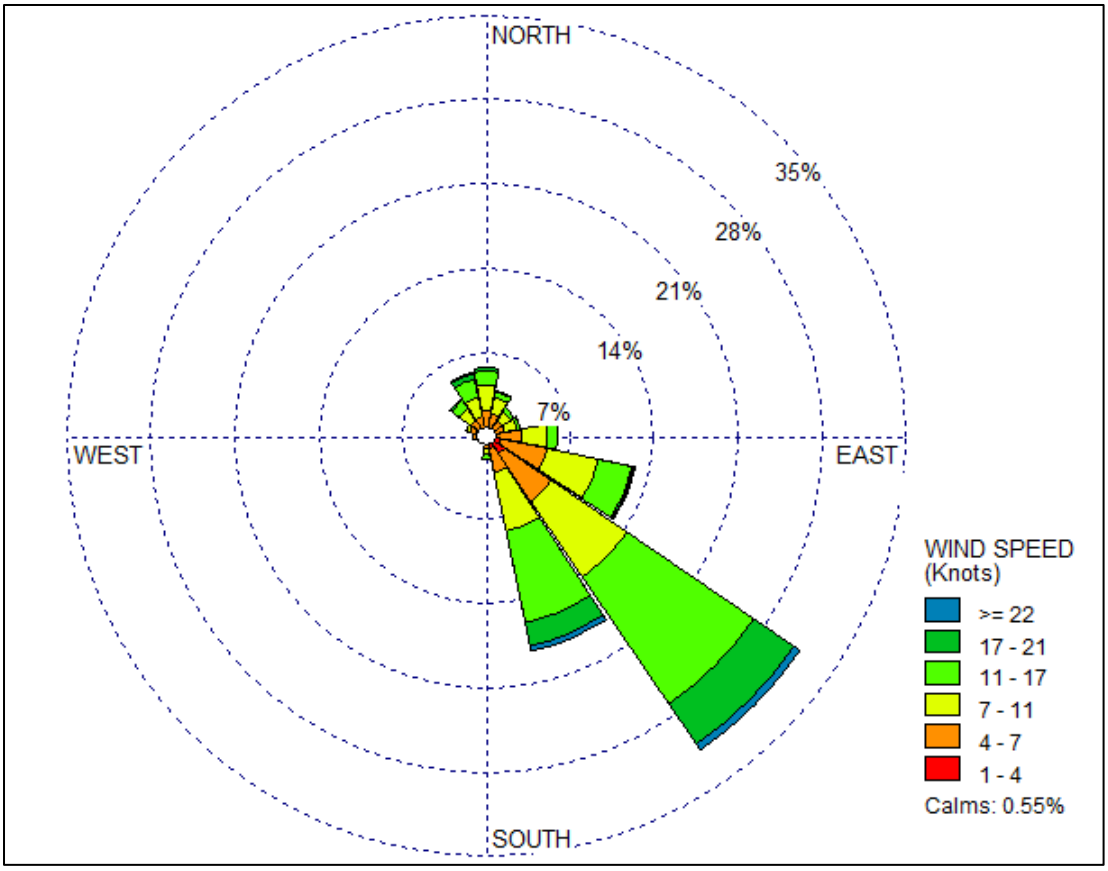

Figure 15- Wind rose diagram

Concentration estimates were obtained at discrete receptors placed at a density of 250m near the urban core area which is increased to 500 m away resulting in a total of 3,500 receptors for the study area as shown in Figure 16. The concentration levels were estimated at every receptor location at an hourly averaging period for 50 sampling days when the participants carried the GPS devices. Continuous surfaces of $PM_{2.5}$ concentrations were developed with inverse-distance weighted (IDW) interpolation based on concentration estimates at discrete receptor locations. Concentration maps generated for a total of 1200 hours (50 days × 24 hours) were then combined with the location

information of participants to assess their dynamic exposure. The spatial and temporal coordinates contained in the GPS information was used to identify the location and time spent by each participant in different microenvironments. Concentration data was extracted from the concentration maps by matching the location and time contained in the GPS data. Exposure values were calculated according to Eq (4) for all time steps within a day and are summed or averaged to obtain the participant's cumulative or average exposure over 24 hours.

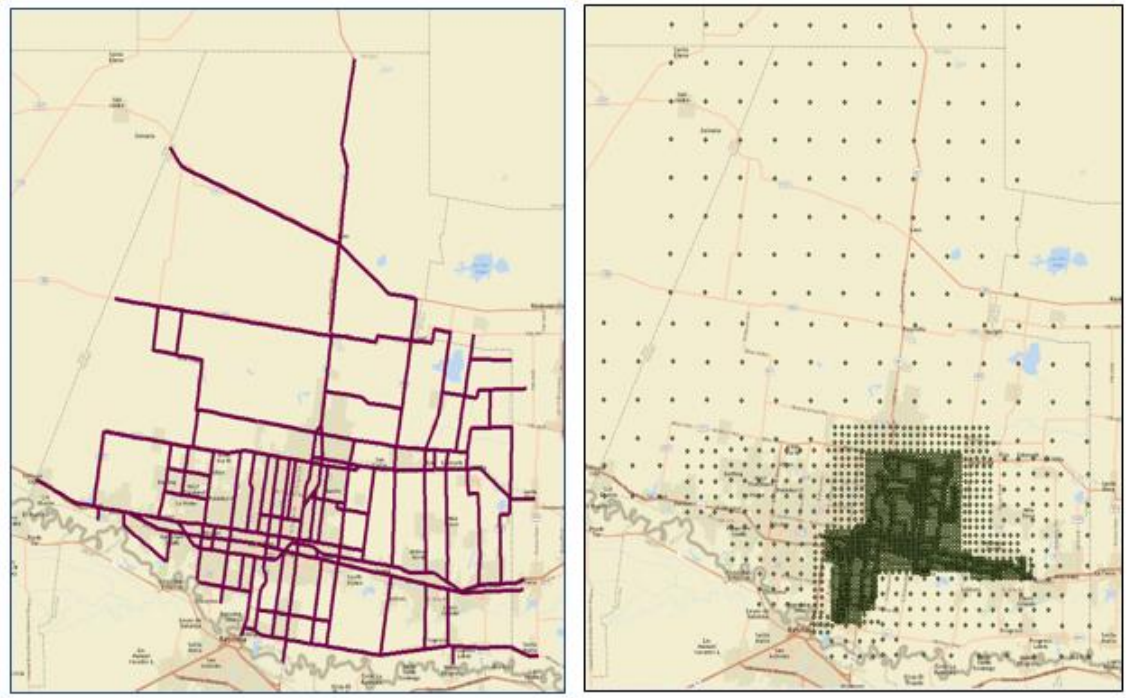

Figure 16- AERMOD emission source and receptor placement for case study site

3.2.4. Results

The case study extent and the participant's location tracked for all sampling days is shown in Figure 17. Color points categorize the participant's location as blue for indoor, yellow for outdoor, and red for in-vehicle microenvironments. The white circles indicate participant's residential location and have a high percentage of recorded locations indicating a majority of time spent at home. In total, participants are found to spend 6.8%, 88.1%, and 5.1% time outdoors, indoors and in-vehicle microenvironments, respectively.

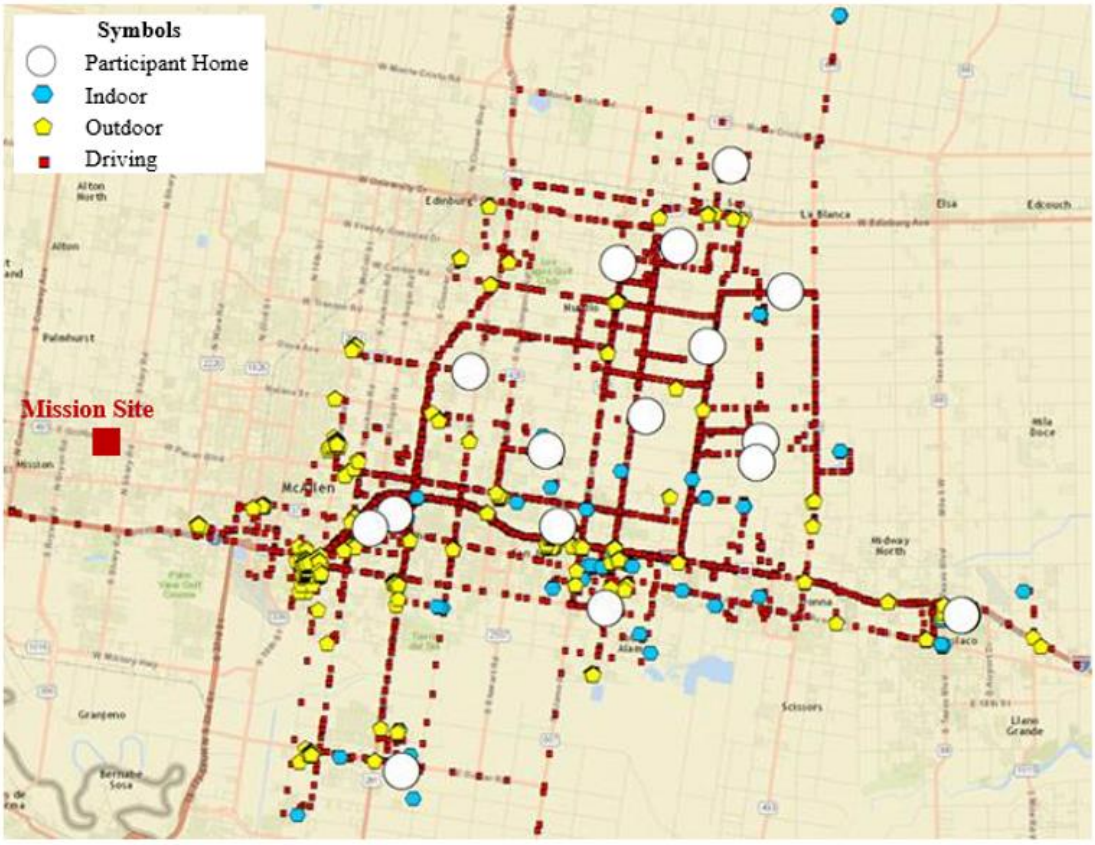

Figure 17- The time location trace from GPS coordinates for all 17 participants (50 sampling days)

A traffic-related emission concentration map is shown in Figure 18. Matching the concentration levels with the participant's location indicates higher levels of $PM_{2.5}$ concentrations along the driving location trace. This implies that participants experienced relatively higher exposure levels when they are traveling compared to the other microenvironments. This finding highlights the importance of incorporating participant's location information in exposure assessment to identify if any short-term exposure (such as commuting) contributed significantly to overall exposure levels.

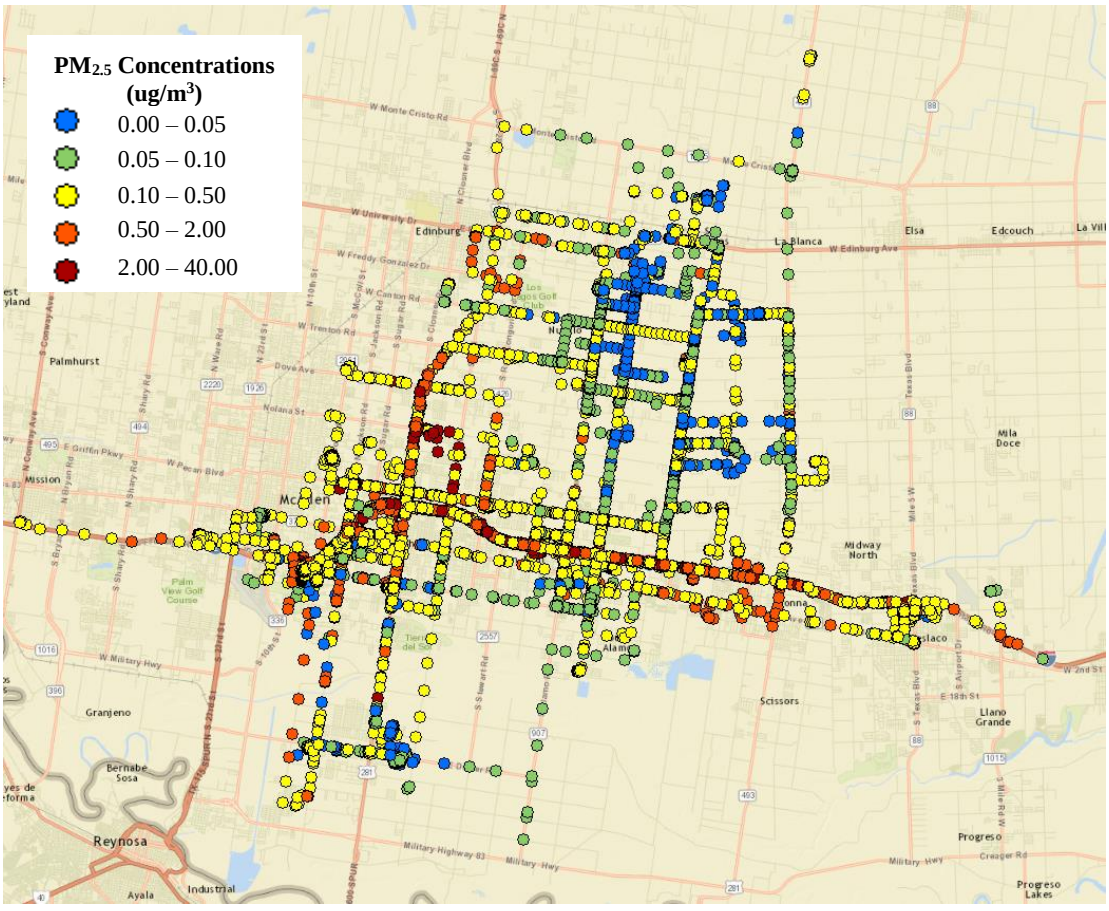

Figure 18- The traffic-related $PM_{2.5}$ mass concentration ($\mu g/m^3$) modeled by AERMOD as a function of time and GPS coordinates for all 17 participants

Table 9- Traffic-related $PM_{2.5}$ concentration ($\mu g/m^3$) in three microenvironments over the 50 measurement days

Micro-environment	Traffic-related $PM_{2.5}$ Mass to Time Ratio	Traffic-related $PM_{2.5}$ Daily Mean ($\mu g/m^3$)	Traffic-related $PM_{2.5}$ Standard Deviation	Range ($\mu g/m^3$)	95% Confidence Interval
Indoor	0.91	0.29	0.21	0.02 - 0.92	0.23 - 0.35
Outdoor	1.45	0.26	0.27	0.00 - 1.61	0.19 - 0.34
Driving	1.96	0.56	0.55	0.04 - 2.26	0.42 - 0.73
Total		0.32	0.22	0.02 - 1.04	0.26 - 0.38

Statistics of $PM_{2.5}$ emission exposure levels over the sampling period is shown in Table 9. Average daily in-vehicle concentration ranged between 0.02 and 1.04 $\mu g/m^3$, with a mean value of 0.32 $\mu g/m^3$. Table 9 presents the significant variation in exposure levels depending on the microenvironment visited and amount of time spent in the microenvironment. The mass-to-time ratios are estimated to be 0.91, 1.45, and 1.96 for indoor, outdoor, and in-vehicle microenvironments, respectively. The in-vehicle mass-to-time ratio is found to be doubled compared to the indoor microenvironment, due to the proximity to the emission source (roadway links) and the shielding offered by the buildings. The in-vehicle average concentrations obtained in this study are relatively low compared to other studies in literature. These values are attributed to low levels of traffic compared to other sources in the case study region. According to the EPA's emission based source sector classification for Hidalgo County (shown in Figure 19), the region is affected predominantly by dust and agricultural sources while mobile sources emissions account for 7% and fuel combustion accounts for 11%.

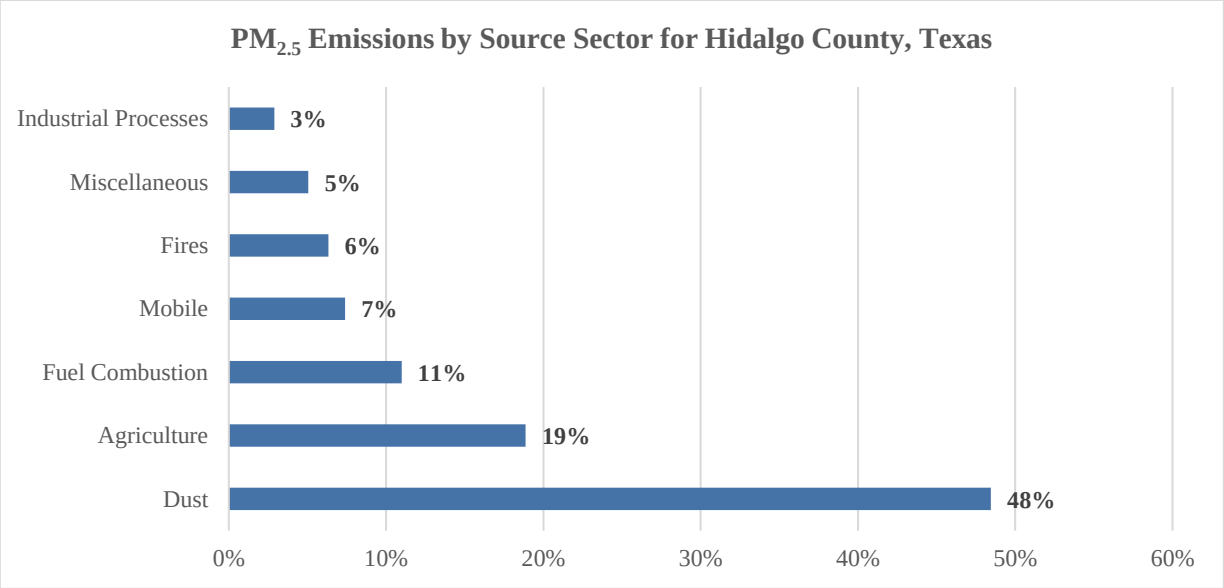

Figure 19- Emission based source sector classification for Hidalgo County (Source: USEPA, National Emission Inventory for 2014)

Spatial distribution of emission exposure for one sampling day (December 15, 2015) is shown in Figure 20. Higher concentration levels are observed near roadway links carrying higher traffic volumes. These links correspond to Interstate 2, one of the major east-west routes that traces the U.S-Mexico border and 69C which connects to the Mexican Federal Highway 97. Traffic and meteorological conditions have a dominating effect on the distribution of concentration levels. Traffic has a linear impact with higher concentration levels observed during peak morning (5 – 8 AM) and evening traffic hours (5 – 7 PM).

Key meteorological parameters governing the dispersion correspond to atmospheric stability, and wind speed and direction. Higher concentrations are typically found to coincide with the direction of the prevailing or dominant wind. In terms of wind speed, higher speed results in higher dilution, thereby reducing the concentration

estimates. Atmospheric stability characterized by a continuous measure of Monin-Obukhov length *(131)* in AERMOD can be broadly classified into unstable, stable and neutral conditions. Unstable conditions, occurring during early afternoon periods, decrease the concentration levels by increasing the atmospheric mixing effect. On the other end of the spectrum, stable conditions common during nighttime periods increase the concentration levels due to reduced atmospheric dispersion and neutral conditions are between the stable and unstable conditions. Due to stable atmospheric conditions, concentration levels during early morning periods, in spite of lower traffic conditions, are found to be higher. Lower concentration levels are observed during midday periods (10AM-4PM) due to low traffic volumes and high atmospheric dispersion. Dynamic exposure levels were calculated according to Eq. 4 that takes into account the location of the participant, the amount of time spent at different locations and modeled concentrations at the corresponding locations. The hourly exposure values calculated for each sampling day was summed over 24 hours to obtain cumulative exposure levels.

To highlight the importance of incorporating dynamic location information of participants, an additional analysis was performed based on fixed residential locations. The static approach adopted by a number of exposure studies assume people to be at static home locations *(107-110, 128)*. The dynamic approach, on the other hand, takes into account the dynamic location information of people for calculating their exposure levels. The distribution of static and dynamic exposure is shown in Figure 21. The average 24-hour static and dynamic exposure over the sampling period is found to be 0.29 $\mu g/m^3$ and 0.32 $\mu g/m^3$ respectively. The results indicate that, for the entire sample, mean dynamic

exposure is 7% higher than the mean static exposure. The reason for the modest difference between static and dynamic exposure assessments may be explained by the activity patterns of participants considered for the current study. These participants, being in their third trimester of pregnancy, were predominantly at their residential locations as indicated by their GPS coordinates.

3.2.5. Limitations of the Modeling Framework

Like any modeling analysis, the analysis presented in this paper has a number of assumptions and uncertainties. While quantifying these uncertainties is not within the scope of this study, an overview of the model assumptions and input data uncertainties associated with the analysis is provided in this section.

Firstly, the AERMOD model estimates concentration levels using a simplified Gaussian steady-state formulation. This formulation assumes steady-state meteorological conditions to exist throughout the case study location and within each hour. In addition, Gaussian models are not capable of capturing the chemical transformation of pollutants and are applicable only to primary non-reactive pollutants. These models are thereby better suited for near-field situations where the conditions do not change significantly such as in the case of traffic-related dispersion. Secondly, the average daily traffic volumes are converted using regional growth factors and traffic percentages. These regional factors are not site-specific and could introduce discrepancies in the emissions estimates and thereby exposure levels.

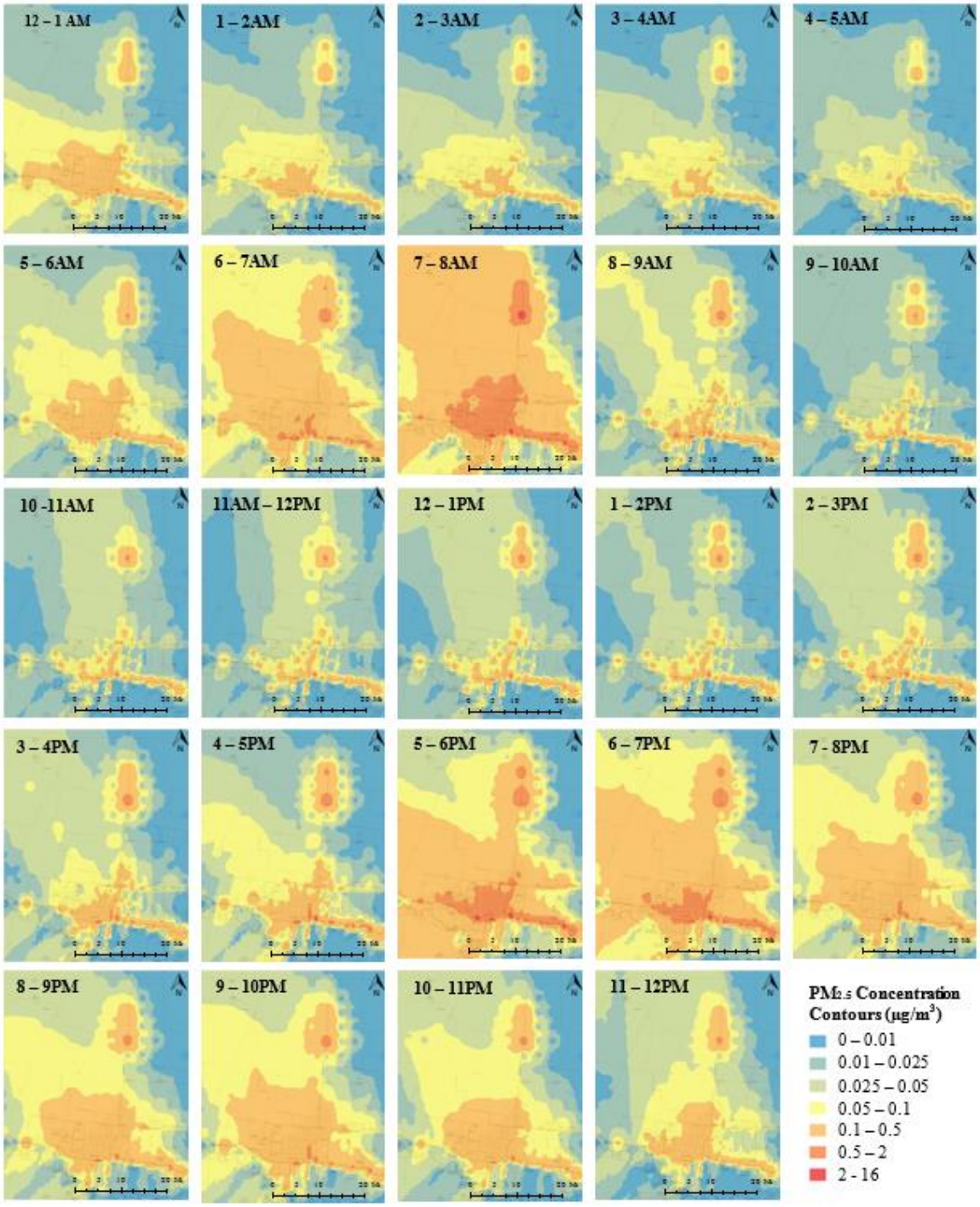

Figure 20- Spatial-temporal distribution of traffic-related $PM_{2.5}$ for a sampling day on December 15, 2015

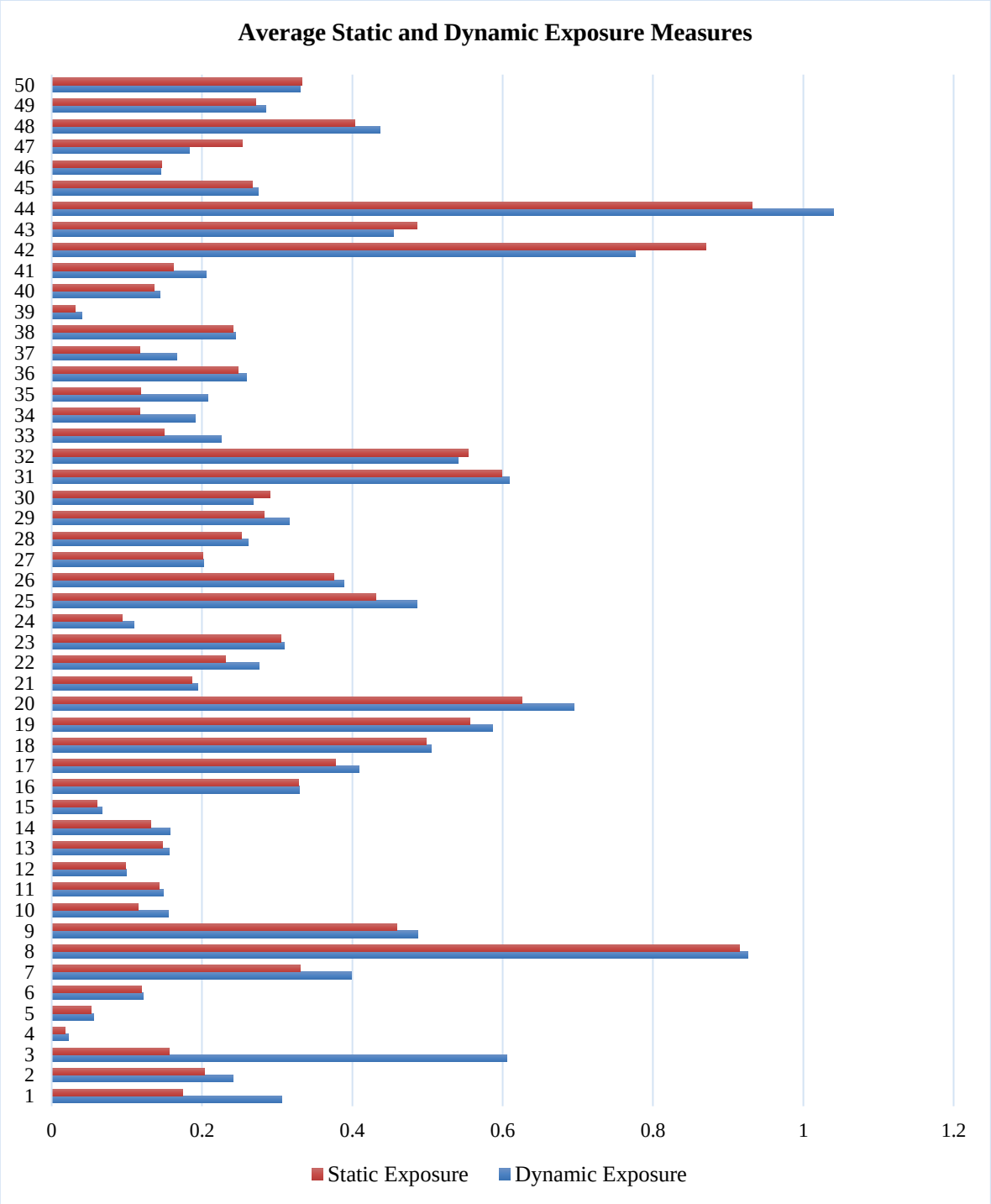

Figure 21- Static and dynamic exposure measures of traffic-related $PM_{2.5}$ concentrations ($\mu g/m^3$)

Thirdly, concentration estimates for indoor and in-vehicle microenvironment are obtained from the modeled outdoor concentration combined with ratios from the literature. These ratios are not specific to the study area or the population sampled and could introduce discrepancies in the exposure estimates. Finally, the study did not include roadway emissions from the Mexico side of the U.S-Mexico border mainly because the impact from across the border is found to be beyond the near-road zone of influence in the study area. Vehicular emissions tend to peak within a few hundred meters from the roadway edge and quickly drops to background levels. This near-zone of influence varies by pollutant and typically literature suggests this distance to be no more than 1640–3280 ft *(29, 132)* for most pollutants. The closest distance between a participant location and the border highway is 1.69 mi which is beyond the near-zone of influence.

3.2.6. Conclusion

The integration of health and transportation considerations is a topic of growing importance to transportation researchers and health practitioners. Quantifying the contribution of traffic-related emission exposure in the overall population exposure is a key first step to developing targeted policy and interventions to address this issue. The current study presented a method for integrating the dynamics of modeled pollutant concentrations with the location information of participants tracked using GPS devices. The results exhibited a significant variation of emission exposure across time periods and spatial locations, which cannot be captured by simpler metrics such as traffic density and near-road distance. The study evaluated measures of static exposure based on residential

location. Results showed an increase of 7% in overall exposure levels from static to dynamic assessment. While prior studies indicated significantly larger differences between dynamic and static exposure measures, current results do not indicate a significant improvement in accounting for dynamic location information of participants in exposure assessment. However, these results have to be interpreted in the specific context of this study as the participants involved were in their later stages of gestation and tended to increase the time spent at home.

The current study contributes to the literature on exposure assessment methods in important ways. Firstly, the dynamic exposure method developed based on GPS data and air dispersion models offers several advantages over traditional exposure assessment methods. The method overcomes restrictions of ambient and personal monitoring in terms of the sample size, higher cost, equipment failure, pollutant type and averaging time measured. Secondly, the study the explored the utility of novel data collection technologies for exposure assessment. Such technologies can be explored by analyzing peoples' behavioral patterns. Thirdly, the study has demonstrated the ability to capture the exposure levels in a vulnerable population group in a previously understudied and economically disparate region in South Texas. This is one of the early few studies that examined the activity patterns and emission exposure levels for a vulnerable population of pregnant women. In spite of increasing evidence linking traffic-related exposure and birth defects, there are limited studies examining maternal exposure levels. Recommendations for future research include investigating the impact of other emission

sources on the overall exposure levels and validate the modeled exposure levels with real-world data (in form of personal monitoring).

3.2.7. Financial Disclosure

The project is funded by Texas A&M Transportation Institute's (TTI's) Strategic Research Program in addition to additional funding from Texas A&M's Health Science Center (HSC). Faculty members from Johns Hopkins University (JHU) provided in-kind assistance, in the form of equipment use and faculty time.

4. DISPERSION MODEL SENSITIVITY ANALYSIS

4.1. Investigating the Impact of Meteorological Variables on Dispersion between Daytime and Nighttime Periods[4]

In urban areas in Texas and the United States, roadway work zone and construction activities are often conducted at night to reduce the disruptions to traffic and to prevent congestion caused by lane closures during peak hours. The reduced traffic delays due to nighttime construction have the potential to reduce traffic emissions. However, the air quality impacts associated with moving these activities from the daytime to the nighttime have not been studied in detail. Air quality impacts depend on two major factors, namely the traffic emissions and meteorological conditions. While the impact of traffic emissions between time periods have been studied in the literature, there is limited understanding of the impact that meteorological conditions have on the dispersion of mobile source pollutants. This study specifically addresses this gap by evaluating the impact of the meteorological condition on pollutant concentrations under different input settings related to the region, land use, distance from roadways and averaging periods. The assessment of the impact of metrological conditions indicated that for the same amount of emissions (mass per time), the nighttime period could result in higher pollutant concentration (mass per volume) levels. However, given that traffic congestion and overall traffic volumes are generally substantially lower in the nighttime period, the findings do not imply that

[4] *Reproduced with Permission from:* Askariyeh, M.H., Vallamsundar, S. and Farzaneh, R., *Transportation Research Record, Journal of the Transportation Research Board,* pp 1-12, DOI: 10.1177/0361198118796966. Copyright 2018, SAGE.

nighttime construction activities result in worse air quality in terms of pollutant concentrations. Thus, the relative difference in pollutant concentrations obtained from shifting construction activities to nighttime from daytime periods should be assessed based on a combination of meteorological and traffic conditions.

4.1.1. Introduction

Nighttime construction is being used increasingly by state Departments of Transportation (DOTs) and other highway agencies to conduct highway maintenance and reconstruction projects mainly to reduce the impacts on congestion and mobility. Nighttime construction has both favorable and unfavorable effects on many aspects to highway agencies and the public. Favorable aspects relate to reduction in congestion and delays during nighttime periods when traffic is at its lowest levels, less air pollution as it is believed that lower tailpipe emissions (emitted mass per time) lead to better air quality, lower traffic also related to lower fuel consumption and energy conservation, less inconvenience to traveling public caused by lane closures at work zones, and lower economic impact to the surrounding businesses due to the work being performed at nighttime periods. Negative issues associated with nighttime projects include safety issues to workers, premium worker wages, material costs, added traffic control costs, reduced visibility, noise disturbance to the surrounding communities, and reduced availability of materials and equipment parts. While some of these positive and negative effects are well known and have been studied in detail, others have not been sufficiently investigated. For example, most studies have focused on examining the safety of nighttime work activities and concluded that the crash rate on sections of the roadway near work activity was higher

than normal nighttime crash rates, and that crash rates were higher when lane closures were required compared to those when no lane closures were required *(133-136)*. Studies have also examined the noise and vibration effects from construction equipment and traffic congestion and found these issues to be detrimental especially if the construction activities are located closer to hospitals or schools *(137)*.

From an air quality perspective, when construction activities are shifted to nighttime, congestion will be lower compared to the same project undertaken during the daytime. In turn, this is thought to reduce fuel consumption and vehicle emissions associated with nighttime versus daytime projects. There are two major factors driving the pollutant concentrations in the atmosphere, namely (i) emissions released by the traffic and construction activities and (ii) meteorological conditions. While, emissions have a direct impact on pollutant concentrations, with higher concentrations being associated with higher emissions, the relationship between meteorology and pollutant concentrations is much more complicated. Meteorological conditions having an impact on pollutant dispersion relates to characteristics of the lower and upper layers of the atmosphere and land use conditions. Studies have shown the pollutant concentration levels to be significantly higher during pre-sunrise hours than during the daytime. The higher concentrations levels are associated with nocturnal surface temperature inversion, low wind speeds, and high relative humidity *(138)*. Ginzburg et al. *(23)* investigated the relationship between concentrations and meteorological parameters and found (a) an inverse relationship between concentrations and temperatures, (b) concentrations to decrease with increase in wind speed, (c) no significant correlation between wind direction

and concentrations and (d) higher atmospheric buoyancy to cause lower concentrations. In terms of seasonal variation, studies *(139)* found concentration levels to have a dominant peak in fall and winter seasons. Zhao et al. *(140)* found concentration variation to be greater in the summer season when temperature variations are also greater. Although meteorological conditions were found to have a dominating impact on pollutant concentrations, studies investigating the air quality effects of shifting construction activities between time periods examine the effects only from the traffic emissions point of view without considering the impact of meteorology *(141)*. This highlights a need to better understand how the impact of meteorological conditions affects the expected benefits of shifting construction activities from daytime to nighttime periods.

The overall goal of this study was to evaluate the impact of meteorological conditions on the dispersion of emitted pollutants by shifting daytime construction activities to nighttime. A series of sensitivity analyses was performed to evaluate the impact of meteorological and land use factors (for the same set of emission rates) on pollutant concentrations between daytime and nighttime periods. Sensitivity analysis is performed using EPA's approved AERMOD air dispersion model. This study is a part of a larger research project conducted to investigate the emissions and air quality impacts of nighttime construction through case studies and developed a decision-support framework. The study described in this paper aims at gaining a better understanding of air quality impacts specifically related to meteorological conditions that can be taken into account by public agencies in making informed decisions about whether to undertake nighttime construction. The rest of the paper is organized as follows. Section 2 presents the

methodology used to assess the relative differences in pollutant concentrations between time periods. Results and findings obtained are presented in Section 3, followed by discussion and conclusion in Section 4.

4.1.2. Methodology

This section outlines the methodology used to assess the relative difference in pollutant concentrations between daytime and nighttime periods. Two major factors that affect the dispersion of pollutants into the atmosphere are emission rates (mass per time at which the emissions are released from an emission source) and meteorological conditions (wind speed, wind direction, atmospheric stability, and surface roughness etc.). The modeling approach consisted of performing a series of sensitivity analysis that varied key input parameters (for same set of emission rates) to represent differences in nighttime and daytime conditions that may influence pollutant dispersion. Figure 22 illustrates the conceptual overview approach used for this study. The approach consists of the following major elements:

- Case study set-up
- Assess key input parameters for sensitivity analysis
- Perform air dispersion modeling and obtaining results

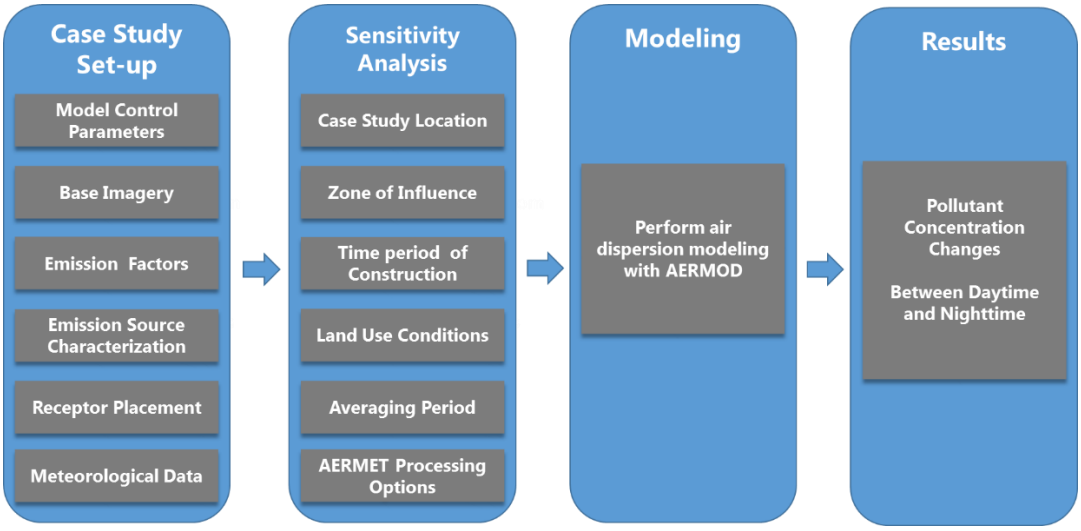

Figure 22- Conceptual methodology

4.1.2.1. Case-study Set-up

Sensitivity analysis was performed on a simplified representation of a roadway segment to isolate the impact of complicated roadway geometry, and emission rates. Figure 23 displays the source and receptor set-up of a hypothetical roadway line source with generic assumptions made for emission rates and source parameters.

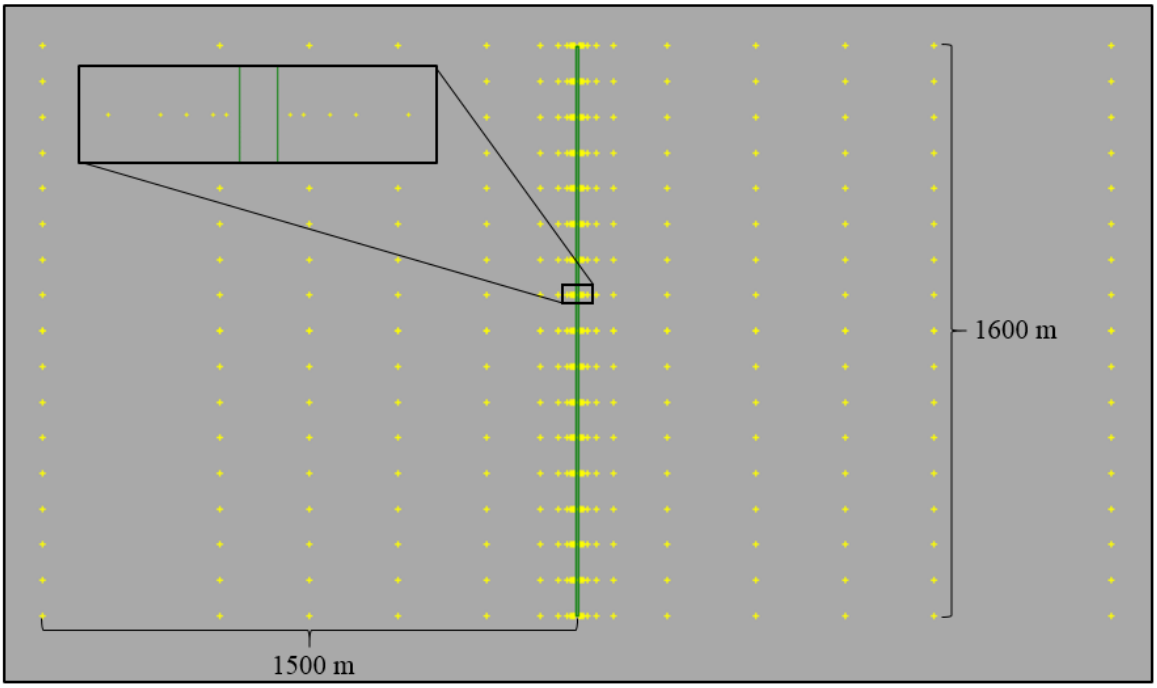

Figure 23- Source and receptor characterization

The emission source consisted of a two-lane, at-grade highway segment extending to a length of 1600 m (1 mile) and a width of 7.3 m (24 feet). Inputs of highway configuration data (except for emission rates) were defined according to the EPA project-level hot-spot analysis. The highway segment was characterized using AERMOD area source with a source elevation of 0 m, a release height of 1.3m, and an initial vertical dispersion parameter of 1.2 m. A unit emission rate was used for all modeling runs. Receptors were placed along the roadway from start of the roadway at 0 m and end of the roadway at 1600 m at a spacing of 100 m. At each of these locations along the roadway, receptors were placed at 2.5 m, 5 m, 10 m, 15 m, 25 m, 50 m, 100 m, 250 m, 500 m, 750 m, 1000 m, and 1500 m from the edge of the road. AERMOD, being a Gaussian-based dispersion model is capable of predicting the dispersion patterns of any primary non-

reactive pollutant with no chemical transformation. Accordingly, the dispersion patterns predicted by AERMOD applies to any primary non-reactive pollutant (such as carbon-monoxide (CO), primary particulate matter ($PM_{2.5}$ and PM_{10}), and primary nitrogen oxides (NO_x)).

4.1.2.2. Key Input Parameters for Sensitivity Analysis

The impact of meteorological conditions on pollutant concentrations between daytime and nighttime time periods were assessed for different input parameter settings as listed in Table 10.

Table 10- Key input parameters assessed for sensitivity analysis

Parameters Evaluated	Values
1. Case Study Location	• Dallas • Houston • El Paso
2. Zone of influence	• Near-road (0 – 250 m) from roadway edge • Far-road (> 250 m)
3. Time period of construction	• TxDOT Specification Handbook • Practical time period information from contractors
4. Land Use	• Rural • Urban
5. Atmospheric Stability	• Stable, Unstable and Neutral stability classes are classified based on Monin-Obukhov length
6. AERMET	• Regulatory default option • Beta option (LOWWIND, ADJ_U*)

Description about key input parameters and their parameter values considered for sensitivity analysis is provided below:

4.1.2.3. Case Study Location

As it is difficult to generalize the meteorological conditions between different case study sites, sensitivity analyses were performed based on local parameters for three urban areas in Texas, namely Dallas, Houston, and El Paso. Raw meteorological (surface and upper air) data specific to each case study location was processed using AERMINUTE, AERMET and AERSURFACE preprocessors to produce data in a compatible format for AERMOD. The prevailing wind rose diagrams for daytime and nighttime periods (on an annual averaging basis) are shown in Figure 24. The predominant wind direction was the same for both daytime and nighttime periods for Dallas and Houston. However, for El Paso, the predominant wind direction changed drastically from blowing from south-west (daytime period) to north-east (nighttime period).

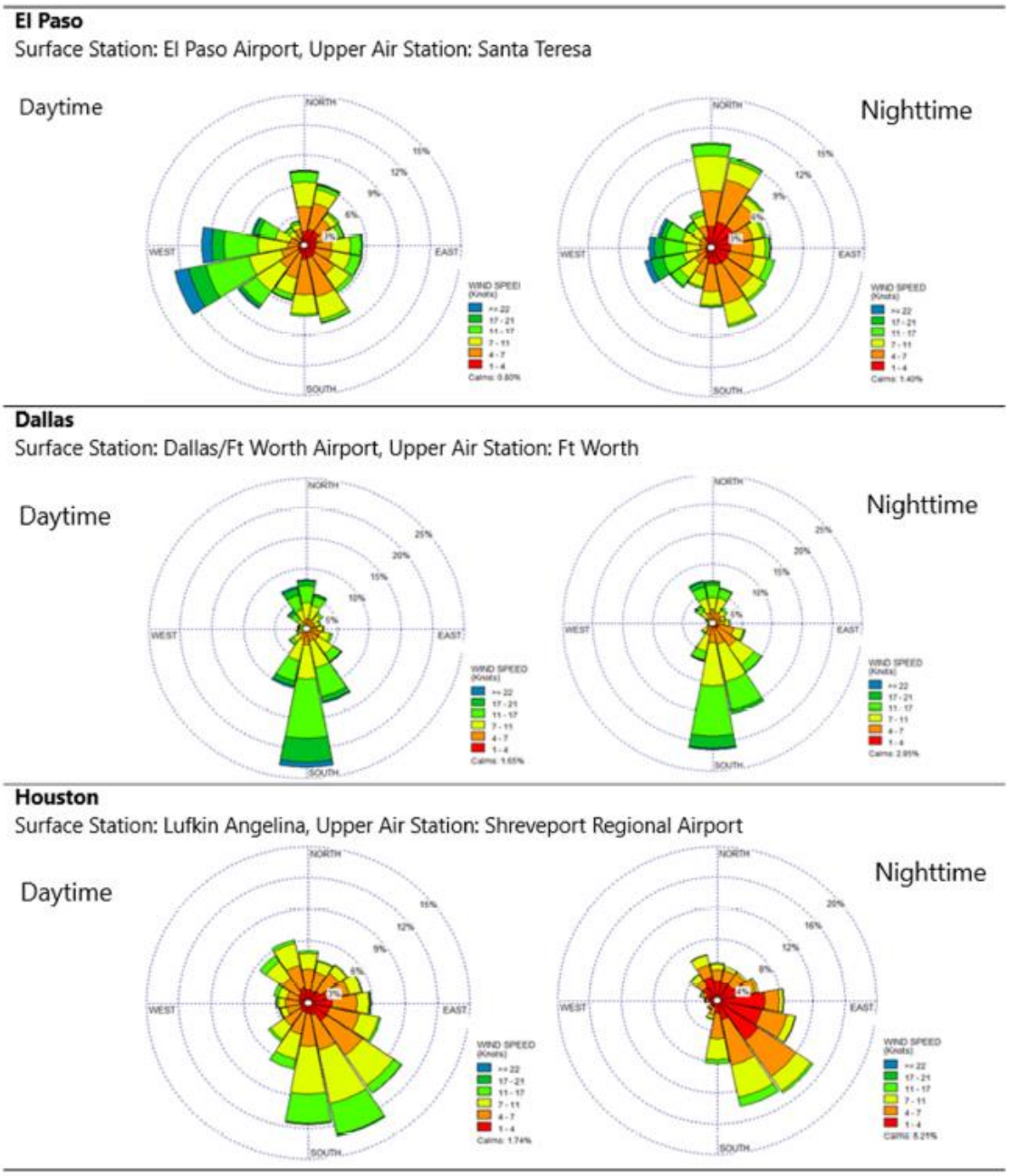

Figure 24- Wind rose diagram for case study areas

4.1.2.4. Time Period of Daytime and Nighttime Construction

Designation of time periods during which construction activities are performed during daytime and nighttime periods were obtained from two sources, namely (a) the TxDOT Standard Specification Handbook and (b) input obtained from construction contractors performing the activities. According to the TxDOT Standard Specification Book *(142)*, "nighttime work is defined as work performed from 30 minutes after sunset to 30 minutes before sunrise." Table 11 lists the designations of daytime and nighttime periods according to the seasonal sunrise and sunset times in Texas and based on the construction contractor's information.

Table 11- Daytime and nighttime construction time period

(A) Construction time period according to TxDOT specification handbook

Season	**Sunrise/Sunset**	**Daytime Construction Period**	**Nighttime Construction Period**
Winter (Dec., Jan., Feb.)	Sunrise 7:30 a.m., Sunset 5:30 p.m.	7 a.m.–6 p.m.	6 p.m.–7 a.m.
Spring (Mar., Apr., May)	Sunrise 7 a.m., Sunset 8 p.m.	6:30 a.m.–8:30 p.m.	8:30 p.m.–6:30 a.m.
Summer (June, July, Aug.)	Sunrise 6:30 a.m., Sunset 8:30 p.m.	6 a.m.–9 p.m.	9 p.m.–6 a.m.
Fall (Sep., Oct., Nov.)	Sunrise 7:30 a.m., Sunset 7 p.m.	7 a.m.–7:30 p.m.	7:30 p.m.–7 a.m.

(B) Construction time period according to construction contractors

Season	**Practical Daytime Construction Period**	**Practical Nighttime Construction Period**
Winter (Dec., Jan., Feb.)	6 a.m.–9 p.m.	9 p.m.-6 a.m.
Spring (Mar., Apr., May)	6 a.m.–9 p.m.	9 p.m.-6 a.m.
Summer (June, July, Aug.)	6 a.m.–9 p.m.	9 p.m.-6 a.m.
Fall (Sep., Oct., Nov.)	6 a.m.–9 p.m.	9 p.m.-6 a.m.

4.1.2.5. Land Use

The urban/rural land use representativeness of a case study site is found to have impact on the dispersed pollutant concentrations. Urban areas are generally hotter than nearby rural areas, especially at night, mainly because of heat retention by urban materials. Because of this heat retention, the vertical motion of the air is increased through convection, thereby leading to increased dispersion of pollutants *(143)*. This phenomenon is referred to as the urban heat island effect. The purpose of evaluating this key parameter was to assess the impact of land use on the relative difference in concentration estimates between daytime and nighttime periods, given the same traffic characteristics and site configuration.

4.1.2.6. Atmospheric Stability

Among the different meteorological parameters, atmospheric stability, responsible for mixing and dilution, is found to have a significant impact on pollutant concentration between different time periods. Hence, the variation of atmospheric stability was studied in detail. To evaluate the variation of pollutant concentration with atmospheric stability, pollutant concentrations were estimated at an hourly averaging period for four seasons (Spring, Summer, Fall, Winter) for El Paso.

4.1.2.7. AERMET Meteorological Data Processing

The EPA noted, in 2007, issues with high concentrations due to the treatment of light winds in AERMOD. AERMOD exaggerates the nighttime concentration estimates due to the way it handles low winds (low wind speeds <1 m/s) *(144)*. To overcome this

over prediction, the EPA, in 2012, developed non-default BETA options were developed for meteorological data processing in AERMET to improve AERMOD performance under low wind conditions *(144)*. This included the LOWWIND BETA options on the MODELOPT keyword in AERMOD, and the ADJ_U* option included in stage 3 of the AERMET meteorological processor. The LOWWIND option increases the minimum value of sigma-v, and replicates the centerline concentration accounting for horizontal meander, but utilizes an effective sigma-y and eliminates upwind dispersion. The ADJ_U* option adjusts the surface friction velocity (U*) to improve the performance of the model for low wind speed and stable conditions *(51)*. These non-default options are not approved for regulatory purposes but can be used for research purposes with the approval of appropriate reviewing authority. Meteorological data was processed using these non-default options to assess the impact on pollutant concentrations between different time periods.

4.1.2.8. Performing Air Dispersion Modeling and Obtaining Results

Among the different air dispersion models, the EPA approves AERMOD for a wide range of regulatory applications including roadways and off-road networks (i.e. construction sites) in all types of terrain. AERMOD is a steady-state Gaussian plume model and uses an advanced method to characterize stability compared to its processor models. AERMOD uses a continuous function called Monin-Obukhov length to characterize atmospheric stability. The two regulatory components of AERMOD include the meteorological preprocessor (AERMET) and the terrain data preprocessor (AERMAP). AERMET processes the meteorological data from the National Weather

Station (NWS) and onsite data. AERMET produces output files containing the surface scalar parameters and the vertical profile of meteorological data. AERMAP preprocesses complex terrain data and generates receptor grids, using USGS digital elevation data *(145)*. AERMOD model requires emission factors to be specified for all hours of the day. As such, AERMOD model was set to run for the daytime and nighttime time periods as follows:

- Daytime model runs: emission rates were assigned a value of 1 for the daytime period hours and were given a value of 0 for nighttime period hours
- Nighttime model runs: emission rates were assigned a value of 0 for the daytime period hours and were given a value of 1 for nighttime period hours

Whenever a given hour is specified a value of 0, AERMOD does not compute concentration estimates for that hour. For example, in a daytime model run AERMOD concentration estimates were based only on emissions occurring during daytime period and a nighttime model run AERMOD concentration estimates were based only on nighttime period emissions. The resulting pollutant concentrations obtained were normalized by the corresponding time periods.

4.1.3. Results and Discussion

To evaluate and compare the effects of different time periods, time period designations, land use, areas, and zones of influence from the roadway edge on pollutant concentrations, different combinations of these factors were defined to model pollutant dispersion using AERMOD. Figure 25 shows the variation in normalized concentration

predictions as a function of time period designation, zone of influence or distance from the roadway, and land use. Results shown in Figure 25 are based on the default regulatory option in AERMOD.

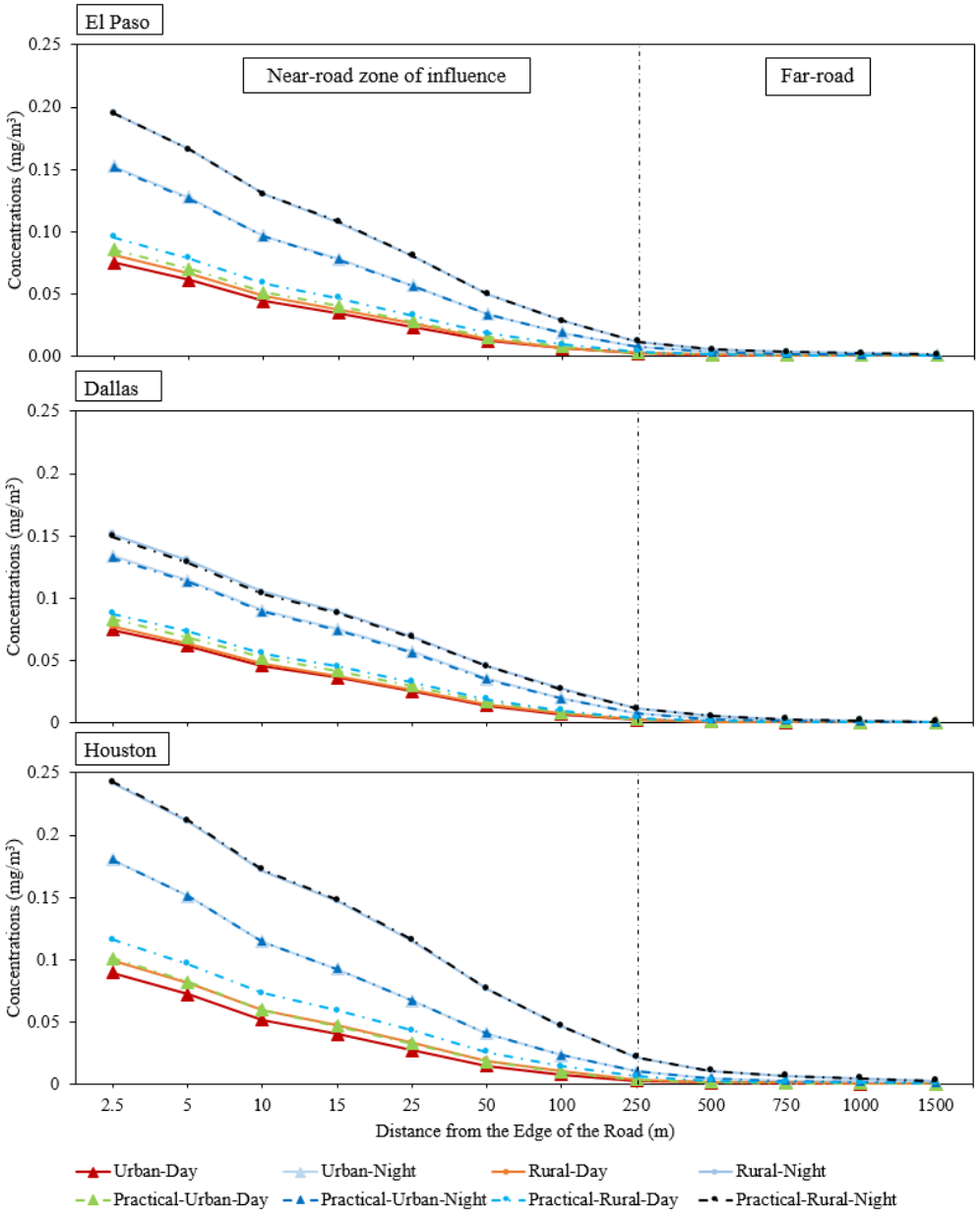

Figure 25- Normalized concentrations with distance from roadway edge, land use and time period designation for (a) El Paso, (b) Dallas and (c) Houston

4.1.3.1. Effect of Distance from Roadways

As shown in Figure 25, concentration estimates were found to be the highest near the roadway link edge and then gradually decreased with distance from roadway links edge. The decrease in concentration estimates was found to be steep for a distance of 250 m and the concentration estimates flattened for distances beyond 250 m. These findings were found to be consistent with the literature *(29, 146-149)*. Karner et al. *(29)* analyzed 41 roadside monitoring studies between 1978 and 2008 and concluded that almost all pollutants decrease to background levels at a distance of 115 m to 570 m from the edge of the road and the decrease varies from one pollutant to another. Venkatram et al. *(16)* analyzed data from three near-road pollution measurements and AERMOD dispersion model and found the concentration of an inert pollutant to decrease rapidly to less than one-fifth of its initial concentration from roadway edge.

4.1.3.2. Effect of Time Period

For all the case study areas (El Paso, Dallas, and Houston) concentration estimates were found to be higher for nighttime periods compared to daytime and rural land use compared to urban land use conditions. The reason for high concentration estimates during nighttime compared to daytime periods was because of the stable atmospheric conditions during nighttime periods. Sunlight during the daytime helps in the mixing/dispersion of pollutants in the atmosphere. When the sunlight strikes the Earth's surface during the day, it heats up more quickly and the heat is transferred to the air immediately above the ground, causing the warm air to rise and mix with the cooler air above. When the sun sets during the evening and nighttime periods, the Earth's surface cools down much faster than

air, resulting in cooler (heavier) air near the ground and warmer (lighter) air staying on top. This fairly stable atmospheric condition during nighttime periods leads to much reduced mixing and dispersion of pollutants and thereby higher concentrations. Thus, the low atmospheric transport and dispersion characteristics were the reason for higher concentration estimates *(121)* during nighttime periods.

4.1.3.3. Effect of Land Use

Lower concentration estimates observed in an urban land use setting compared to a rural setting was because of the urban heat island effect. In this regard, buildings, roads, and structures in urban areas absorb more radiation and energy compared to almost flat terrain conditions in rural areas. Because of this heat retention, the vertical motion of the air was increased through convection, yielding better mixing, stronger vertical air flux, and eventually better dilution resulting in increased dispersion of pollutants *(121)*.

4.1.3.4. Effect of Modeling Options in AERMOD

In addition to the default regulatory option, AERMOD was run with the BETA option (meteorological data processed with LOWWIND option in AERMOD and use of ADJ_U* in AERMOD). Concentration estimates obtained using BETA option were compared with the regulatory option. The regulatory option was found to predict higher concentrations compared to BETA option, but the difference was minor in concentration levels ranging between two to four percent. A potential reason for the low difference could be that the BETA options are more impactful for studies involving tall stacks *(150)*.

4.1.3.5. Effect of Atmospheric Stability

To investigate the variation of pollutant concentration with atmospheric stability, pollutant concentrations were estimated at an hourly averaging period for El Paso. Hourly concentrations are further classified by seasons and are shown in Figure 26. The higher concentration values in Figure 26 are because of the lower averaging period of an hour compared to Figure 25, which is based on an annual averaging period

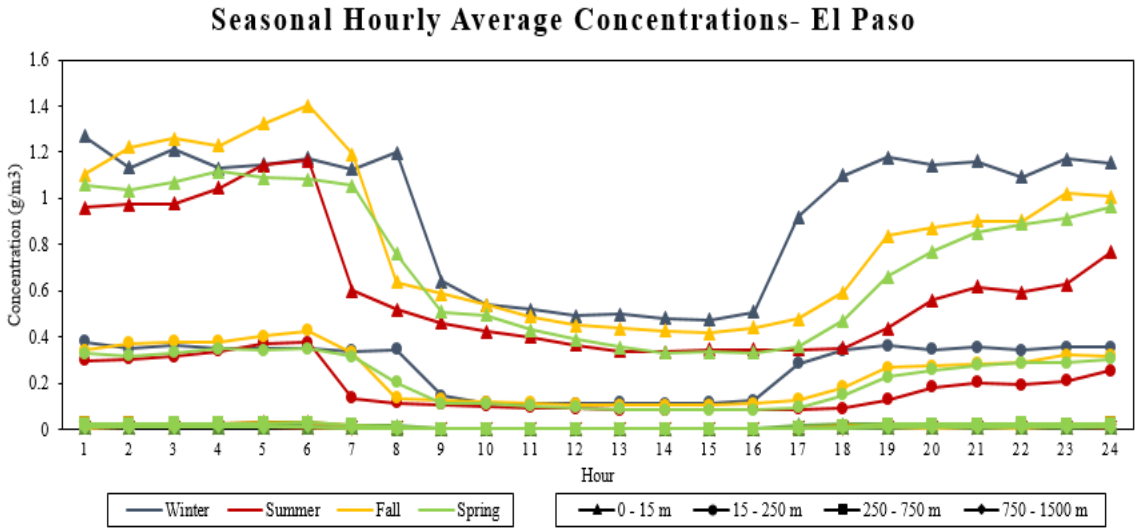

Figure 26- Pollutant concentrations at an hourly averaging period varied by season for El Paso

Atmospheric stability affects the dispersion of vehicle emissions downwind of the highway and is governed by heat and momentum forces in the environment. AERMOD provides a continuous measure of atmospheric stability based on an energy balance in the planetary boundary layer. The energy balance is represented by the sensible heat flux, which depends on net radiation and surface characteristics such as available surface

moisture. Atmospheric stability in AERMOD is represented as a function of the Monin-Obukhov length [L(m)] *(151)*. The atmospheric stability is obtained from the surface and upper air data processed by AERMET. Unstable atmospheric conditions refer to convective conditions when the atmosphere is not stable leading to increased dispersion and lower pollutant concentration estimates. Stable atmospheric conditions, typically observed during nighttime periods, have low atmospheric transport and dispersion leading to higher pollutant concentration estimates and neutral conditions are in the middle between stable and unstable conditions.

The hourly distribution of atmospheric stability conditions, based on AERMET provided Monin-Obukhov length, for all seasons specific to El Paso is shown in Figure 27. The, Monin-Obukhov length ranging from 0 to -10^5 is classified as Unstable, followed by 0 to 10^5 m classified as Stable and values greater than 10^5 m is classified as Neutral stability class *(152)*. Comparing Figure 26 with Figure 27, the variation of concentration estimates closely followed the variation in atmospheric stability conditions. Concentration levels were lower between hours 08:00 to 17:00, coinciding with the unstable atmospheric conditions. Concentration levels were higher between hours 01:00 to 08:00 and 17:00 to 24:00 due to the presence of predominantly stable conditions and limited neutral conditions. The concentration levels were higher during winter and fall seasons compared to summer and spring seasons. This was because of the higher prevalence of stable atmospheric conditions (less sunlight time compared to summer and spring) leading to reduced levels of mixing and pollutant dispersion during fall and winter season. Considering seasonal atmospheric conditions, concentration estimates were found to be

higher for winter and fall nighttime periods, followed by summer and spring nighttime periods, winter and fall daytime periods, and summer and spring daytime periods.

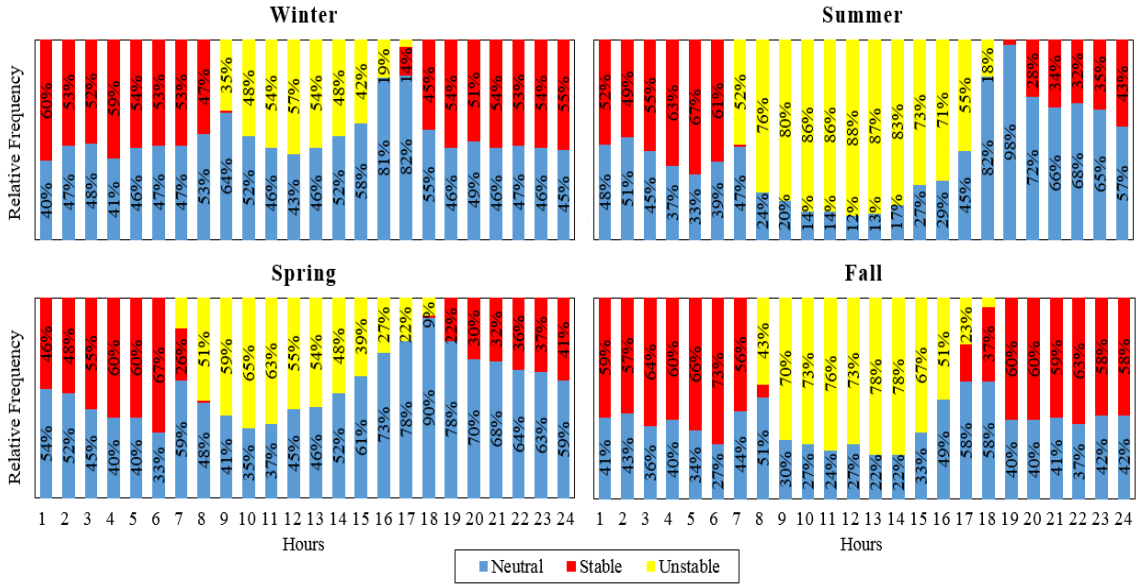

Figure 27- Distribution of atmospheric stability conditions for El Paso

The relative difference (expressed as a percentage) in average concentration levels between nighttime and daytime periods is summarized in Table 12. The relative difference expresses how much the concentration estimates are higher in nighttime periods compared to daytime periods for the same traffic activity, and source characterization. The relative difference was found to increase with distance from roadway edge because of the very low concentration values obtained at distances greater than 250 m. A higher relative difference was observed for rural land use conditions with time periods defined by the TxDOT specification handbook. The difference in concentration estimates between case study regions (i.e. El Paso, Dallas, and Houston) was due to their different meteorological conditions.

Table 12- Relative difference in average pollutant concentrations between nighttime and daytime periods

Relative Difference[5] in Average Concentration Levels (expressed as a percent)				
S: TxDOT specification handbook, P: Construction contractors information				
El Paso				
Distance from roadway	0–15 m	15–250 m	250–750 m	750–1500 m
Urban – S	110%	176%	269%	267%
Rural – S	151%	254%	370%	367%
Urban – P	81%	119%	166%	164%
Rural – P	109%	167%	226%	228%
Dallas				
	0–15 m	15–250 m	250–750 m	750–1500 m
Urban – S	88%	172%	326%	366%
Rural – S	109%	237%	496%	589%
Urban – P	67%	117%	189%	197%
Rural – P	80%	154%	275%	296%
Houston				
	0–15 m	15–250 m	250–750 m	750–1500 m
Urban – S	106%	174%	302%	333%
Rural – S	159%	300%	495%	536%
Urban – P	80%	121%	183%	191%
Rural – P	118%	194%	274%	281%

Combining all estimates from Table 12, on average for any urban area, annual average pollutant concentrations dispersed during nighttime conditions were higher by 100 to 120 percent compared to daytime periods. This relative difference increased to 150 to 200 percent for rural land use conditions. This finding was found to be consistent with other near-road studies examining the difference between daytime and nighttime air pollutant impact. Ultrafine particle (UFP) concentrations at night were reported by Zhu et

[5] Relative difference is expressed as (Nighttime Concentration – Daytime Concentration)/Daytime Concentration

al. *(138)*, who conducted measurements upwind (300 m) and downwind (500 m) of a freeway from 22:30 to 04:00. Although traffic volumes were much lower at night (about 25 percent of peak) particle number concentrations were about 80 percent of the daytime peak concentrations along a major freeway in Los Angeles. Hu et al. *(153)* measured air pollutant concentrations along the I-10 freeway in west Los Angeles, one-two hours before sunrise in the winter and summer months using an electric vehicle mobile platform equipped with fast-response instruments. Although traffic volumes during the pre-sunrise hours were lower than during the day, the UFP concentrations were significantly higher in the pre-sunrise period due to strong atmospheric stability, low wind speeds, low temperatures and high humidity values. They found the combination of sufficient traffic flow with meteorological conditions during pre-sunrise hours to result in elevated concentrations of UFP, nitrogen-oxides and polycyclic aromatic hydrocarbons during pre-sunrise hours.

4.1.4. Conclusion

Key findings from the series of sensitivity analyses performed to evaluate the impact of meteorological conditions on pollutant concentrations between daytime and nighttime periods include the following:

- Peaking effects in pollutant concentrations were observed near-road and concentrations declined with distance from roadway edge. The decrease was dependent on meteorological conditions and varied by season.

- Concentrations were higher in rural areas when compared to urban land use conditions due to the retention of heat by urban materials that increased the vertical motion of air, leading to increased pollutant dispersion in urban conditions.
- Concentrations were higher during nighttime compared to daytime (when emissions levels from the source are held equal) due to stable atmospheric conditions, lower mixing heights, and lower wind speeds leading to higher concentrations of pollutants at the near-ground level during nighttime periods.
- Considering all combinations of input parameters, concentration estimates were found to be higher for the rural-night time period, followed by urban-night, rural-night and rural-day.
- The Higher relative difference in concentrations between daytime and nighttime periods were observed in far-road areas (i.e. farther than 250 m from the roadway) because of extremely low values when the concentrations fall back to background levels.
- On average, for any urban area, annual average pollutant concentrations dispersed during nighttime conditions were higher by 100 to 120 percent compared to daytime periods. This relative difference increased to 150 to 200 percent for rural land use conditions.

In summary, from a pollutant dispersion perspective, the assessment of the impact of meteorological conditions indicated that for the same amount of emissions (i.e., if traffic volumes were held equal between daytime and nighttime) higher pollutant concentration levels are expected overnight. However, given that traffic congestion and overall traffic

volumes are generally substantially lower during the nighttime period, the findings do not imply a net increase in pollutant concentrations in the region due to nighttime construction. Thus, the relative difference in pollutant concentrations obtained from shifting construction activities to nighttime from daytime periods should be assessed based on a combination of meteorological and traffic conditions.

Authors acknowledge the limitations of the results, as they were based on hypothetical case study settings evaluating the impact of meteorological conditions with no change in traffic activities. However, a review of the literature shows the conclusions and findings of this study, with regards to the difference in dispersion patterns between daytime and nighttime periods, and land use, were consistent with other studies. For future work, the authors recommend a methodology based on actual traffic data and near-road ambient air monitoring observations collected for daytime and nighttime to validate the findings obtained from the sensitivity analysis.

4.1.5. Acknowledgement

This study conducted as part of a research project titled "*Investigate the Air Quality Benefits of Nighttime Construction in Non-attainment Counties,"* is funded by the Texas Department of Transportation (TxDOT). The authors would like to thank members of the TxDOT Project Committee for their guidance and support in conducting this research.

4.2. The Effect of Re-suspended Dust Emissions on Near-Road Traffic-Related Air Pollution

In recent years, there has been a focus on adverse health effects of near-road long- and short-term exposure to traffic-related fine particulate matter ($PM_{2.5}$). Traffic-related $PM_{2.5}$ emissions can be attributed to tailpipe exhaust, brake wear, tire wear, and re-suspended road dust. Previous field and modeling studies have shown the considerable contribution of re-suspended $PM_{2.5}$ emissions from traffic-related activity. The U.S. EPA provides guidelines to predict traffic-related $PM_{2.5}$ concentrations. While tailpipe exhaust, brake and tire wear are estimated using EPA's MOVES modeling tool, re-suspended dust calculations utilize AP-42 factors which have gone through limited updates. There are limited studies that explore the sensitivity of EPA quantitative analysis results to re-suspended $PM_{2.5}$. In addition, the nonlinear relationship between emissions and concentrations due to the effect of meteorological variables and network geometry was under-investigated in prior studies. In this study, the effect of including re-suspended road dust due to near-road traffic-related $PM_{2.5}$ on near-road traffic-related concentrations was investigated based on EPA's guidelines. The results showed that the inclusion of re-suspended dust increased traffic-related $PM_{2.5}$ emissions by 139-208% on arterials and 16-19% on highways, and increased near-road $PM_{2.5}$ concentrations by 49-74% for different time periods in the four seasons evaluated. These estimated increases emphasize on the importance of re-suspended dust in long- and short-term traffic-related exposure studies, particularly in areas surrounded by arterials. These areas are where human exposure can

be more important than near highways as people tend to live, work and congregate near many arterials.

4.2.1. Introduction

In recent years, there has been a focus on the adverse health effects of near-road long- and short-term exposure to traffic-related air pollutants *(154, 155)*. Fine particulate matter ($PM_{2.5}$) is an EPA regulated criteria air pollutant *(156)*. $PM_{2.5}$ is emitted from different emission sources including the transportation sector and studies demonstrated the elevated $PM_{2.5}$ concentrations in near-road environments *(17, 24)*. A growing body of literature shows associations between higher exposures to $PM_{2.5}$ due to proximity of residential areas to major roadways and adverse health effects *(8-10)*. Approximately 11-19% of the U.S. population lives within a few hundred meters of major roads *(10, 11, 157)* which can effect more than 40 million people exposed to high levels of $PM_{2.5}$ in the U.S. The global population exposed to elevated levels of $PM_{2.5}$ is even higher. Hence, monitoring and modeling $PM_{2.5}$ emissions from the transportation sector and subsequently the dispersion in ambient air is highly important for exposure studies. In addition, the emission and dispersion modeling of $PM_{2.5}$ is a requirement of a regulatory quantitative analyses for federally supported new transportation projects in nonattainment and maintenance areas *(67)*. The $PM_{2.5}$ emissions from the transportation sector result from tailpipe exhaust, brake wear, tire wear, and re-suspended dust and are explained in the U.S. EPA developed MOtor Vehicle Emission Simulator (MOVES) guidance and transportation conformity guidance for $PM_{2.5}$ quantitative hotspot analyses *(67, 158)*.

The tailpipe $PM_{2.5}$ exhaust emissions have decreased considerably as different exhaust emission control measures have been deployed. However, current non-exhaust emissions from road vehicles are unabated making the contribution of re-suspended road dust to traffic-related particulate matters even more significant *(159, 160).* An intensive mass and chemical measurement included study showed that the $PM_{2.5}$ emission rate from re-suspended dust is significant and can exceed the tailpipe contribution in Reno, Nevada *(161).* Kundu et al. compared composition of $PM_{2.5}$ in rural and urban areas and concluded that unpaved roads can contribute to a significantly higher level of $PM_{2.5}$ at five sampling sites in Iowa *(162).* Amato et al. performed an extensive field measurement study and showed that a poor state of pavement can double the road dust loading *(159).* While these studies show the importance of including re-suspended $PM_{2.5}$ in air pollution studies, other studies did not conclude that re-suspended dust is a significant source of $PM_{2.5}$ rather on-road emission sources were more significant *(163).*

In emission and dispersion modeling for regulatory purposes, a procedure including specific guidelines to estimate $PM_{2.5}$ emission from transportation and perform dispersion modeling should be followed *(67).* In this procedure the $PM_{2.5}$ emissions from tailpipe exhaust, brake wear, tire wear, and re-suspended dust emissions should also be modeled. EPA's MOVES2014a on-road model and current AP-42 paved road re-suspended dust model are recommended to estimate $PM_{2.5}$ emission rates ($PM_{2.5}$ mass per time) as per the hotspot guidance *(67, 164, 165).* While tailpipe exhaust (running, idling, and start), brake, and tire wear are estimated using EPA's MOVES modeling tool *(158),* re-suspended dust calculations utilizes AP-42 factors which has gone through limited

updates. MOVES is a microscopic emissions model that uses a fine-scale modal-based approach to generate emission and energy consumption factors at different temporal geographical scales (national, county, and project) *(158).*

The emission factors obtained from the MOVES can be used with transportation activity to estimate total emissions from all roadway links. For project level emissions assessment, MOVES requires inputs from two broad categories: a) Site-specific traffic information, including traffic volumes, fleet composition, and vehicle activity at the roadway link level, and b) Local-specific inputs, including regional-level vehicle age distribution, meteorological variables, fuel characteristics, and parameters related to the inspection/maintenance (I/M) program. The modeled emission rates can then be used for dispersion modeling to consider the effect of meteorological variables and predict near-road $PM_{2.5}$ concentrations. Air pollutant dispersion for regulatory purposes needs to be modeled using the American Meteorological Society- United States Environmental Protection Agency Regulatory Model (AERMOD) *(41, 67).* AERMOD is a Gaussian steady-state dispersion model that predicts concentration of air pollutants emitted from characterized emission sources.

Many different studies around the world have shown the effect of re-suspended road dust on traffic-related $PM_{2.5}$ emissions. However, sensitivity of regulatory quantitative analyses to re-suspended $PM_{2.5}$ has not been investigated. The effect of using a network with and without road-dust on the dispersion models' predictions of near-road $PM_{2.5}$ concentrations is a less investigated area. Also, previous show a nonlinear relationship between emission rates and near-road air pollutant concentrations due to the

effect of meteorological variables on dispersion mechanisms *(23, 138, 140)*. A constant emission rate yields different concentrations under different meteorological conditions over time *(24)*. However, the effects of a certain change in $PM_{2.5}$ emissions due to inclusion of re-suspended road dust on near-road $PM_{2.5}$ concentrations over different time periods have not been evaluated.

In this study, the increase in PM2.5 emission rates that includes of re-suspended road dust in Fort Worth, Texas was investigated, following regulatory guidelines. Additionally, the dispersion modeling was performed using a 2016 dataset of monitored meteorological variables to evaluate the sensitivity of predicted traffic-related $PM_{2.5}$ concentrations in a near-road environment at different seasonal day time periods. As such, this study quantifies the sensitivity of dispersion modeling to a significant increase in $PM_{2.5}$ emission rates in a network by including re-suspended $PM_{2.5}$. In addition, this study evaluates the results using regulatory guidelines for traffic-related $PM_{2.5}$ emission and near-road dispersion modeling.

4.2.2. Materials and Methods

4.2.2.1. Theoretical Premise

The road dust $PM_{2.5}$ emission rate is a function of vehicle weight, road type (paved vs unpaved), and meteorological variables (precipitation) which will be multiplied by traffic volume for re-suspended dust emissions estimation. The $PM_{2.5}$ emissions from tail pipe exhaust, brake wear and tire wear (exhaust and other) are functions of traffic speed, road type, fleet characteristics and mix, fuel quality, and meteorological variables in the respective county which will be multiplied by traffic volume for vehicular (exhaust, brake,

and tire wear) emissions estimation. Adding the re-suspended $PM_{2.5}$ emissions to the vehicular (exhaust, brake, and tire wear) $PM_{2.5}$ emissions will be influenced by meteorological variables as a function of time when dispersion mechanisms occur. Also, adding the re-suspended $PM_{2.5}$ emission rate to various segments of a network with associated $PM_{2.5}$ emission rate (due to vehicular sources with different characteristics and speeds) cannot be interpreted as a linear increase of the total $PM_{2.5}$ emission rate in a network. Hence, it can be concluded that there is a nonlinear relationship between traffic-related emission rates and near-road traffic-related air pollutant concentrations over different time periods. Changes in emission rates will not necessarily result in the same changes in concentrations. In this study, the traffic-related $PM_{2.5}$ emissions (mass per time per area of roadway) and near-road traffic-related concentrations (mass per area), were estimated for different time periods of four seasons of the year 2016 for two types of roadways (highways and arterials). Finally, the emission rates and predicted near-road concentrations were averaged over daily time periods for each season to compare the effects including or not including re-suspended $PM_{2.5}$ emissions. Through this procedure, the increment of near-road traffic-related $PM_{2.5}$ concentrations including re-suspended $PM_{2.5}$ in traffic-related emissions was investigated.

4.2.2.2. Area of Study

In response to recent EPA requirements for near-road air pollution monitoring, the Texas Commission on Environmental Quality (TCEQ) determined six locations near major highways to monitor air quality using Federal Reference Method (FRM) in Texas *(166)*. One of these six locations is in Fort Worth, Texas, and this was selected for

emission, meteorological, and dispersion modeling in this study *(167)*. The near-road continuous air monitoring station (CAMS) 1053 is located 15 meters away from the edge of I-20 in Tarrant County (EPA Site Number: 484391053, 1198 California North, TX 76115), as shown in Figure 28. The highway and arterial segments within a 600 m radius *(24)* of this near-road point (roadways segments are shown by navy links and the near-road environment by red dot in Figure 28) were considered for dispersion modeling. The hourly wind speed, wind direction, and temperature monitored at this point (CAMS 1053) were used as the onsite meteorological data for data processing in the meteorological modeling.

The Dallas -Fort Worth (DFW) regional travel demand model (TDM) results were obtained from the North Central Texas Council of Governments and post-processed to estimate hourly traffic activity on each link for the target area. The modeled hourly traffic volume and speed were mapped into different daily time periods such as Morning Peak (6:00- 9:00 am), Midday (9:00 am- 4:00 pm), Evening Peak (4:00- 7:00 pm), and Overnight (8:00 pm- 6:00 am) periods. The hour that corresponds to the maximum volume in each period was selected for the analysis. Traffic volume and speed were not adjusted for different seasons.

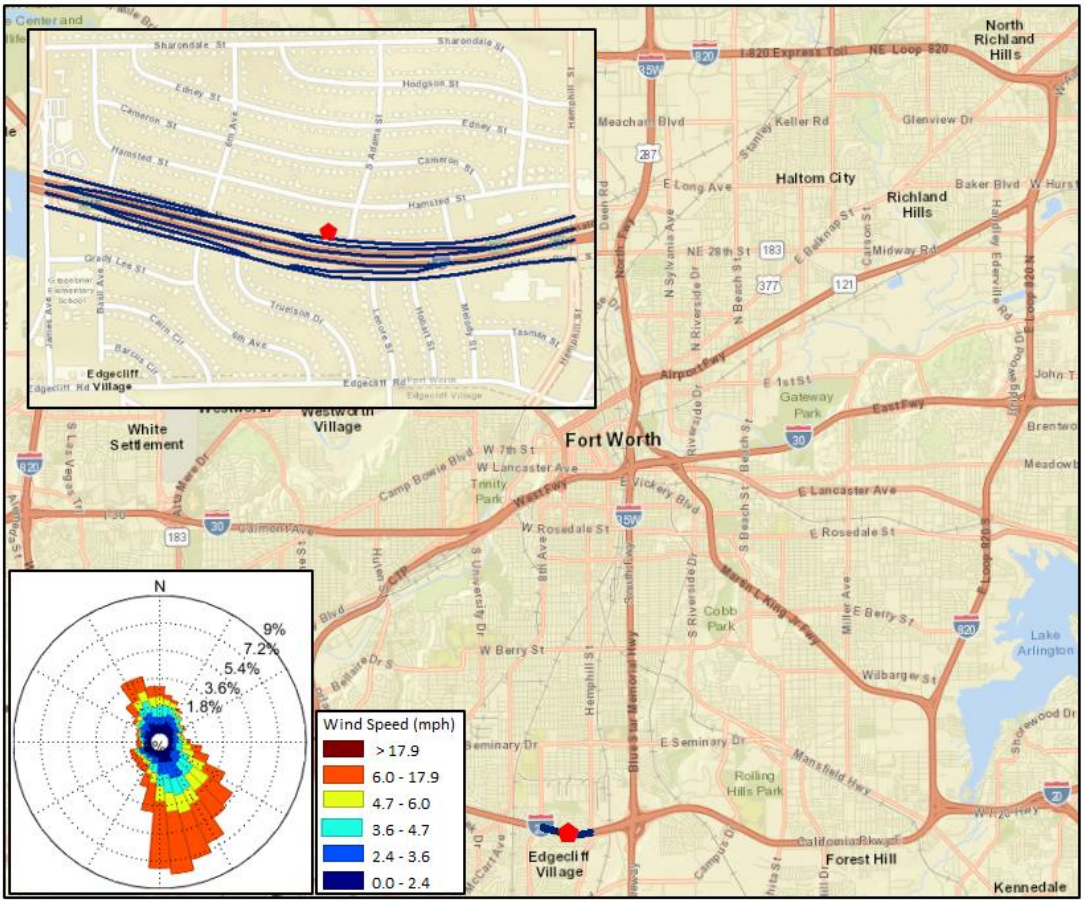

Figure 28- Study area (I-20: Ronald Reagan Memorial Highway shown by navy lines), near-road environment (shown by red mark) and corresponding wind rose based on monitored values in Fort Worth, Texas

4.2.2.3. Emission Modeling using MOVES

The $PM_{2.5}$ emission factors due to all traffic-related sources other than re-suspended dust (exhaust, brake and tire wear) were modeled using MOVES for 2016 Tarrant County. MOVES requires information for vehicle types, ages, fuel types and the emission parameters to estimate emission factors. To estimate composite emission factors

for each link in the target network, the vehicle miles traveled (VMT) mix was obtained for two road types: highways and arterials.

The VMT mix indicates contribution of each vehicle type to the total VMT. The VMT mixes were estimated using a previously developed method and expanded to produce the four-daily time period estimates for four months *(168, 169)*. The four daily time periods included morning peak, midday, evening peak, and overnight. The four months were January, April, July, and October and represent emissions in Winter, Spring, Summer, and Fall, respectively. Composite emission factors were estimated using MOVES emission factors for different vehicle types and VMT mix for two road types (arterials and highways) based on Equation 6 *(168)*, in which i represents vehicle types.

$$\text{Composite Emission Factor} = \sum_{i} \text{Emission Factors} \times \text{VMT mix} \qquad \text{Equation (6)}$$

4.2.2.4. Re-Suspended Dust Emission Estimation

No unpaved road emissions factor analyses were performed because there were no unpaved roads in the target network. Re-suspended dust emission factors from paved roads (i.e., TDM and intra-zonal links) were developed according to Equation 7 from the AP-42 section 13.2.1 *(165)*.

$$E = k\,(sL^{0.91})(W^{1.02})\left(1 - \frac{P}{4N}\right) \qquad \text{Equation (7)}$$

where:

k = Particulate Size Multiplier (g/VMT)

sL = Road Surface Silt Loading (g/m^2)

W = Average Vehicle Weight (tons)

P = Number of wet days (>= 0.01" of rain) (days)

N = Number of days in the period (days)

The input parameters to estimate re-suspended $PM_{2.5}$ emission are $PM_{2.5}$ multiplier, a factor indicating road surface silt loading, the average weight of fleet, days with 0.01 inches precipitation and more (wet days) for the seasonal period, and number of days in the seasonal averaging period. The number of wet days for the seasonal periods of Tarrant County was obtained from Community Collaborative Rain, Hail and Snow Network database *(170)*. The $PM_{2.5}$ particle size multiplier from the referenced EPA AP-42 guidance was used *(165)*. The average vehicle weight values were estimated using the current Tarrant County VMT mix and respective MOVES vehicle types weights. Because control programs (i.e., street sweeping) affect the road surface silt loading and controlled silt loading values are not available, no control programs were included in the development of the re-suspended $PM_{2.5}$ emissions factors for this analysis.

4.2.2.5. Dispersion Modeling using AERMOD

Dispersion modeling requires an input set including meteorological variables and emission source characteristics. The meteorological inputs were obtained from running a meteorological module developed by EPA for regulatory dispersion modeling, AERMET *(171)*. The onsite data including wind speed, wind direction, and temperature obtained from hourly near-road monitoring (CAMS 1053) was incorporated with upper air data and surface air data for 2016. Surface characteristics including Albedo, Bowen ratio, and also surface air and upper air representative station name for Tarrant County were obtained from TCEQ meteorological database for air dispersion modeling *(172)*. The surface air data of Dallas Fort Worth Airport (Station ID: 3927) was obtained from National Oceanic Atmospheric Administration (NOAA) surface air database *(173)* and upper air data of Fort Worth (Station ID: 3990) was obtained from NOAA Radiosonde Database *(174)*. AERMET was run including these raw input sets to model meteorological variables in hourly time resolution for target near-road environment in 2016.

To model the target network as the emission source in AERMOD, the network highways and arterials were split into smaller segments (to represent the roads curvature) and were defined as the area sources of $PM_{2.5}$ emissions. The $PM_{2.5}$ quantitative hotspot analyses was used to define the details of area sources of emissions *(67)*. The release height and initial vertical dispersion coefficient were estimated based on EPA's guidance for each of the four daily time periods for arterial and highway segments (approximately 1.4 m, and 1.3 m, respectively). The $PM_{2.5}$ concentrations were modeled for one receptor

located at 15 meters from the edge of the highway (32.66^0 N, -97.34^0 W, elevation: 214.9 m) representing the near-road environment.

4.2.3. Results and Discussion

4.2.3.1. Traffic-Related $PM_{2.5}$ Emission Rates on Highways and Arterials

The $PM_{2.5}$ emission rates due to re-suspended dust and also exhaust emissions as averaged over four time periods of the day are shown for highways and arterials for four seasons in Figure 29. The predicted $PM_{2.5}$ re-suspended emissions are greater than exhaust, brake, and tire wear combined at arterials emphasizing the need to include re-suspended dust in emission modeling when in close proximity to arterials. However, the re-suspended $PM_{2.5}$ emissions are significantly lower than exhaust, brake, and tire wear combined at highways which can be explained by the higher quality of highway pavement leading to smaller factors used in highway re-suspended $PM_{2.5}$ emission estimation. Results do not show significant changes in emission rates between morning peak, midday, and evening peak, but considerable decrease during nighttime due the lower traffic activity.

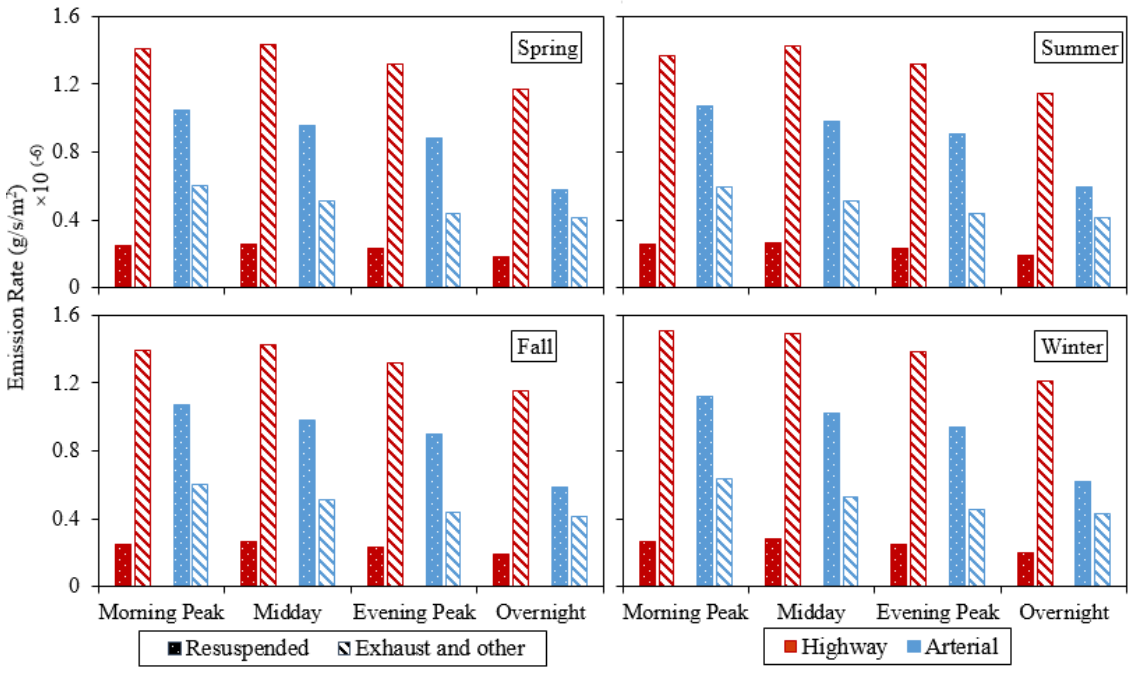

Figure 29- Predicted $PM_{2.5}$ emission rates

To investigate the $PM_{2.5}$ emission rate increment due to inclusion of re-suspended emissions in different seasonal and daily time periods, the ratio of re-suspended $PM_{2.5}$ to the tail pipe exhaust, brake wear, and tire wear emissions for highways and arterials was calculated (Table 13). The percentages are consistently higher than 100% for arterials. For arterials, results also show that the percentage is highest during evening peak followed by midday, morning peak, and overnight, respectively, which shows the importance of considering re-suspended dust in $PM_{2.5}$ emission estimation in the same order. Among different daily time periods for highway emissions, re-suspended to exhaust, brake, and tire wear $PM_{2.5}$ emissions percentage is highest for midday, followed by morning peak, evening peak, and overnight, respectively. As far as seasonal variation, this percentage is highest for

summer, followed by fall, winter, and spring, respectively. The overall evaluation of modeled emission rates show that the increase in average $PM_{2.5}$, due to the inclusion of re-suspended dust emissions, will vary from 15.7% to 18.7%, and 138.9% to 207.6% for highways and arterials in Fort Worth, Texas.

Table 13- Predicted $PM_{2.5}$ emission increment due to inclusion of re-suspended dust (Ratio of re-suspended $PM_{2.5}$ to exhaust and other $PM_{2.5}$ emission rates)

	Highway				Arterial			
Time Period	**Spring**	**Summer**	**Fall**	**Winter**	**Spring**	**Summer**	**Fall**	**Winter**
Morning Peak	17.4%	18.4%	18.1%	17.5%	172.7%	181.3%	178.4%	175.6%
Midday	18.1%	18.7%	18.6%	18.6%	187.4%	193.0%	192.2%	193.1%
Evening Peak	17.3%	17.8%	17.8%	17.8%	202.1%	207.6%	206.8%	207.3%
Overnight	15.7%	16.4%	16.2%	16.2%	138.9%	144.1%	142.9%	144.8%

4.2.3.2. Traffic-Related $PM_{2.5}$ Concentrations from Highways and Arterials

The $PM_{2.5}$ emission rates were applied to the study network with focus on highways and arterials to predict the average $PM_{2.5}$ concentrations in four daily time periods of each season during 2016, as shown in Figure 30. In line with the emission results discussed above, comparison of modeled concentrations shows a lower contribution of re-suspended dust from highways and higher contribution from arterials when compared with exhaust, brake, and tire wear emissions. However, modeled $PM_{2.5}$ concentrations resulting from traffic activity in highways and arterials show significant variation across the different daily time periods and the four seasons. This variation in $PM_{2.5}$ concentrations is a result of various meteorological variables in different time periods caused by nonlinearity between traffic-related emissions and near-road concentrations over time, which cannot be detected by investigating daily and seasonal emission rates (Figure 29). The overnight traffic-related

$PM_{2.5}$ concentrations are typically highest, followed by morning peak, evening peak, and midday, respectively (Figure 32). The higher overnight near-road traffic-related $PM_{2.5}$ consistent with previous literature based on field *(138)* and modeling studies *(24)*.

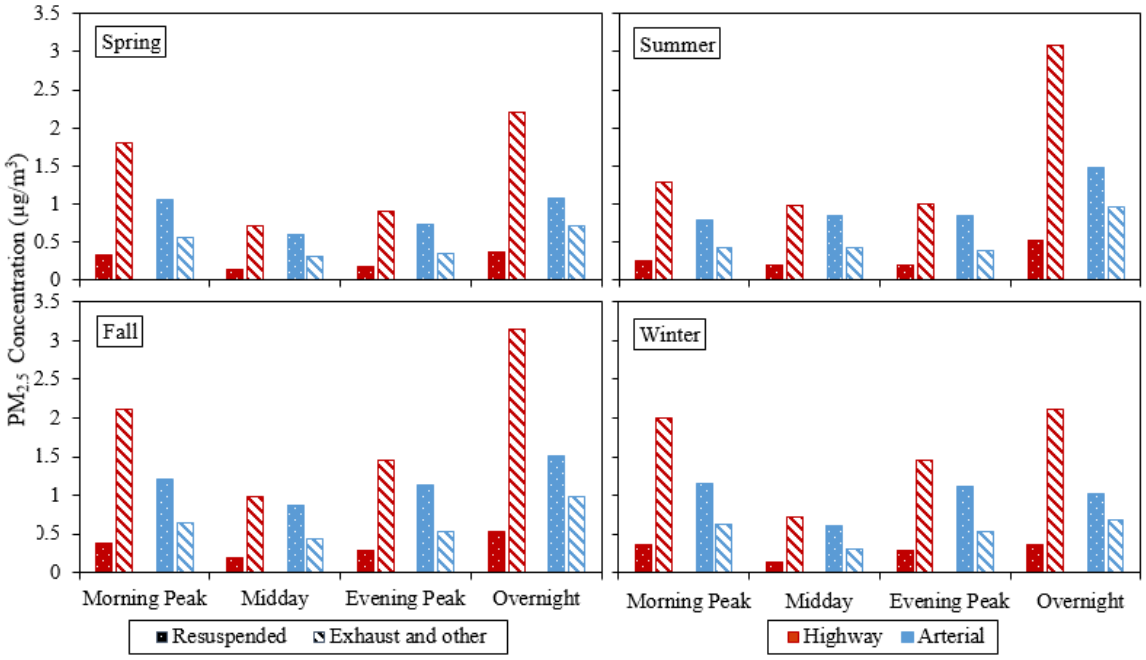

Figure 30- Predicted $PM_{2.5}$ concentrations

4.2.3.3. Overall Traffic-Related $PM_{2.5}$ Concentrations

The near-road environment is located at different distances from various segments (highway and arterial with corresponding traffic count and speed) which comprise the whole target network and influence associated near-road traffic-related air pollution. The influence of different segments of the network on the target near-road environment depends on the geometry of the network and near-road environment, which will be combined with meteorological variables' effect on emissions. This effect is the other source of nonlinearity

between traffic-related emissions and near-road concentrations in dispersion modeling. Table 14 shows the increase in average near-road $PM_{2.5}$ concentrations due to inclusion of re-suspended dust emissions and dispersion modeling in different time periods and seasons. The results show that adding re-suspended $PM_{2.5}$ emissions to the whole network (highways and arterials) yields significant increases (between 49% and 74.3%) in near-road traffic-related $PM_{2.5}$ concentrations. The variation between different seasons is minimal. However, the increases is highest for midday and evening peak, followed by morning peak and overnight periods, respectively. The increments shown in Table 14 are different to those presented in Table 13 due to the nonlinearity of near-road traffic-related emission and concentration relationship due to the effect of meteorological variables and network geometry.

Table 14- Overall percent of hourly average $PM_{2.5}$ concentrations increment due to considering re-suspended dust compared with those of a network without re-suspended dust

Season	Morning Peak	Midday	Evening Peak	Overnight
Spring	58.5%	73.1%	72.2%	49.6%
Summer	60.2%	73.8%	74.4%	49.4%
Fall	57.8%	74.3%	71.1%	49.5%
Winter	58.3%	73.3%	70.2%	49.8%

4.2.4. Conclusions and Recommendations

Using EPA regulatory guidelines and tools, the $PM_{2.5}$ emission rates due to re-suspended dust and exhaust, brake, and tire-wear were modeled for two road types (highway and arterial), four time periods of the day, and four seasons in year 2016. The increase in traffic-related $PM_{2.5}$ emission and near-road concentrations due to inclusion of re-suspended dust in estimations was evaluated and compared in different daily and seasonal time periods for a near-road environment in Tarrant County, Fort Worth, Texas. The estimated increase in traffic-related $PM_{2.5}$ emissions was not proportional to the estimated near-road traffic-related $PM_{2.5}$ concentrations at the different time periods. The nonlinearity between emission rates and concentrations due to the effect of meteorological variables and geometry of the network with unevenly scattered traffic-related emission rates (due to different link traffic speeds) was evident.

Increases in $PM_{2.5}$ emission rates due to re-suspended dust inclusion was considerably higher than the sum of tail pipe exhaust, brake wear, and tire-wear emissions on arterials and its relative percentage ranged between 139% and 208%, while it was lower on highways and ranged between 16% and 19%. The comparison of emission rates showed the importance of the inclusion of re-suspended $PM_{2.5}$ particularly when dealing with traffic-related $PM_{2.5}$ in a near-road environment surrounded by arterials. These are areas where human exposure can be more important than near highways as people tend to live, work and congregate near many arterials. All $PM_{2.5}$ emission rates overnight were lower than those modeled for other three daily periods during the year (which is expected due to the lower traffic counts), while modeled $PM_{2.5}$ concentrations were highest overnight. The

overall increase in near-road traffic-related $PM_{2.5}$ concentrations for the whole network varied between 49% and 74%, an important percentage from an exposure and health point of view. A similar study using monitored hourly vehicle classification, traffic counts and speeds and also near-road speciation data would be more reliable and useful for evaluation of regulatory guidelines in re-suspended dust emission estimation and the exposure and health effect scenarios. In addition, the explained nonlinearity can be quantified using a monitored dataset and would be helpful to have a better understanding of influential variables and parameters in dispersion modeling. The study utilized AP-42 re-suspended dust $PM_{2.5}$ factors which has a rating of D *(165)* for application, this shows further studies are required to corroborate or update the existing AP-42 re-suspended dust $PM_{2.5}$ factors.

4.2.5. Acknowledgement

This research was conducted as part of the Texas A&M Transportation Institute's (TTI) Center for Advancing Research in Transportation Emissions, Energy, and Health (CARTEEH) activities. A group of TTI researchers (Mohammad Hashem Askariyeh, Madhu Venugopal, Haneen Khreis, Andrew Birt, and Joe Zietsman) contributed to this article.

4.3. AERMOD for Near-Road Pollutant Dispersion: Sensitivity to Source and Dispersion Related Parameters

Near-road traffic-related air pollutant dispersion modeling is important for regulatory purposes and exposure assessment studies. The sensitivity of the EPA regulatory dispersion model, AERMOD, was evaluated for the dispersion parameters. Model predictions were obtained for dispersion parameters at different vertical and horizontal distances from the edge of the road and for different wind speeds. Statistical measures were used to perform a quantitative evaluation of the model's predictions using observations obtained from a tracer study and assessed potential improvement of the model's performance due to changes in the regulatory suggested parameters. Results of sensitivity analysis showed an increase in release height, initial vertical dispersion coefficient (σ_{zo}), and minimum standard deviation of horizontal concentration distribution ($\sigma_{v,min}$), decreases predicted concentrations at the near-ground level and increases at 9.5 m from ground level located at downwind. Near-road dispersion modeling under low-speed winds is sensitive to dispersion parameters. Using alternative parameters yields negligible improvement in quantitative performance measures in different classes of wind speed and wind direction suggests that different input sets can be used to model dispersion under different wind cases.

4.3.1. Introduction

The transportation sector accounts for a major emission source of air pollutants in urban areas *(94)*. Numerous studies have shown that the level of air pollutants are elevated at near-roadways *(95-97)*. A higher level of air pollutants dictates a higher level of exposure to the transportation-related air pollutants for near-roadway populations *(141)*. Long-term exposure to air pollution is proven to cause various adverse health problems *(175, 176)*. Epidemiological and toxicological studies identify adverse respiratory *(177, 178)*, premature mortality *(179, 180)* and cardiovascular effects *(98-100)* for near-roadway populations are interpretable as the consequences of long-term exposure to the transportation-related air pollutants. Understanding the temporal and spatial distribution of near-roadway air pollutants has an instrumental role in the assessment of exposure to transportation-related air pollutants. Air dispersion models are generally being used to estimate the temporal and spatial variation of transportation-related air pollutants under near-roadway conditions for research and regulatory purposes *(34)*. Several air dispersion models are available to estimate temporal and spatial dispersion of air pollutants *(35-38)*. The **A**merican Meteorological Society –**E**PA **R**egulatory **MOD**el (AERMOD) is the current regulatory dispersion model by the EPA for estimating the spatial and temporal distribution of pollutants in stable and convective boundary layers for both simple and complex terrains *(39-41)*.

Considering increasing interest in transportation-related air pollutant exposure, the performance of air dispersion models in predicting near-roadway air pollutants has been evaluated using different field studies (for example *(141)*) and tracer studies (for example

(26, 28)). Comprehensive studies on influential factors on near-roadway air pollutants show the significant role of wind direction in dispersion modeling using the Gaussian distribution equation *(16)*, which was also observed in field studies *(18)*. Evaluation of AERMOD showed the determinant effect of wind direction *(28)* and speed on model performance and revealed overprediction of concentrations under low-wind conditions *(51, 52)*. Limitation of surface layer similarity theory in explaining dispersion mechanism in low-wind speed *(34, 53)*, and a lack of reasonable vehicles induced turbulence (VIT) *(54-59)* can be the main reasons for issues with dispersion models. VIT has shown a determinant role in dispersion mechanism under low-wind conditions *(56, 59, 60)*.

Different dispersion mechanisms and turbulences including VIT are usually considered in air dispersion models using parameterized forms *(61)*. In particular, AERMOD estimates a meander component, vertical and horizontal wind velocity fluctuation due to turbulence (σ_w and σ_v (m/s)), and standard deviations of the vertical and lateral concentration distributions (σ_z and σ_y) *(62)*. It also uses release height, the initial vertical dispersion coefficient (σ_{zo}), and the initial lateral dispersion coefficient (σ_{yo}) while modeling transportation-related emission sources as volume sources *(62)*.

AERMOD allows for arbitrary low-wind speed in the input data and can use a meander component on top of a coherent plume to account for the additional effective lateral pollutant dispersion caused by random wind direction shifts. In such cases, the overall concentration is calculated as the weighted average of the meander and coherent plume as shown in Equation 8 *(181)*.

$$C_{\text{Total}} = (1 - f) * C_{\text{Coherent Plume}} + f * C_{\text{Random}} \qquad \text{Equation (8)}$$

In Equation 8, C stands for concentration and f is the plume state weighting factor which is determined by the ratio of the random component of the horizontal turbulent energy to the total wind energy and varies between 0.5 and 1 *(181)*. The pollutant concentration due to the meander component in the stable boundary layer (SBL) or convective boundary layer (CBL) is computed using the same governing equations for the coherent plume but a different form of the horizontal distribution function is used in these equations.

The AERMOD model calculates vertical profiles of vertical and horizontal wind velocity fluctuation due to turbulence (σ_w and σ_v (m/s)) using EPA meteorological processor, AERMET, provided information including u_* *(62)*, aiming at considering the effect of variation in turbulent intensity with height to model the turbulent dispersion of near-surface air pollutants *(51, 182)*. It also applies a minimal σ_v ($\sigma_{v,min}$) to increase lateral dispersion in very light winds under stable conditions. By default, the $\sigma_{v,min}$ is taken as 0.2 m/s. Three additional user-selectable low-wind (LW) options are included in the current version of AERMOD, each with different choices for the $\sigma_{v,min}$ values and treatment of the meander component *(183)*. In summary, LW-1 disables the horizontal meander component and increase $\sigma_{v,min}$ to 0.5 m/s; LW-2 keeps the horizontal meander component and slightly increases $\sigma_{v,min}$ to 0.3 m/s; LW-3 eliminate upwind dispersion but uses the $\sigma_{v,min}$ to 0.3 m/s as in LW-2. In addition, LW-3 introduces an additional "effective" lateral standard deviation of concentrations (σ_y) to account for the enhanced horizontal dispersion in other directions due to meander. Moreover, LW-2 and LW-3 set an upper limit of 0.95

on the plume state weighting factor which is called FRANmax in the model description *(40)*. The $\sigma_{v,min}$ and FRANmax can also be set for values other than the default ones within corresponding ranges.

Standard deviations of vertical and lateral concentration distributions (σz and σy (m)) were used in AERMOD to calculate spatial distribution of air pollutants. AERMOD calculates these parameters as the combined effect of ambient and plume buoyancy turbulence. Considering the variation of ambient turbulence induced vertical dispersion and its near-surface strength, the main assumption in the estimation of vertical and lateral dispersion parameters, due to ambient and plume buoyancy turbulence, is that the effects are independent of each other. The AERMOD uses specific parameters to characterize a volume emission source in addition to the emission rate. These parameters include release height, the initial vertical dispersion coefficient (σ_{zo}), and the initial lateral dispersion coefficient (σ_{yo}). The final dispersion coefficient including initial standard deviation of vertical and lateral concentration distribution is calculated using Equation 9, where σ_o is initial standard deviation, σ_l is standard deviation before accounting for initial dispersion, and σ is the total vertical or lateral concentration distribution (dispersion coefficient).

$$\sigma^2 = \sigma_l^2 + \sigma_o^2 \qquad \text{Equation (9)}$$

General Motors (GM) conducted an experiment in 1975 to study the near-road dispersion of pollutants emitted specifically by on-road vehicles under different meteorological conditions *(13)*. This unique dataset was previously used to evaluate AERMOD's performance using different main options for near-road dispersion modeling at three different levels *(28)*. Results showed the dramatically better performance of

volume sources to represent vehicular emission sources compared with area sources. AERMOD also showed better performance to model transportation-related air pollutants dispersion using LW-3 option. Results also indicated the reasonable performance of the model to predict concentrations at ground level (0.5 m), but relatively weak performance at higher levels (3.5, and 9.5 m) downwind. A general over prediction occurs using volume sources at upwind was another finding of this study *(28)*.

In the present study, the GM near-road pollutant concentration and meteorological data were used to evaluate the sensitivity of AERMOD to the vehicular emission source's characteristics and dispersion coefficients using volume sources representation. The objectives of this study determined the sensitivity of AERMOD to the release height and initial vertical dispersion coefficient (σ_{zo}) (as the vehicular source characteristics) and determined the minimum value of lateral wind velocity fluctuation due to turbulence ($\sigma_{v,min}$), and FRANmax (characteristics of dispersion treatment) in predicting concentrations at different heights (from ground level), different distance from the vehicular emission source, and different wind speeds. In this study, the effect of these parameters and possible improvement of AERMOD performance to account for different influential parameters on near-road transportation-related dispersion modeling are being studied. The results of this study will assist researchers and model practitioners by providing a better understanding of model performance to account for ambient and vehicular emission source's characteristics and dispersion treatments. The results will also help researchers to use dispersion parameters accounting for near-road transportation-

related air pollutant distribution and eventually dispersion models more effectively in exposure studies.

4.3.2. Methodology

4.3.2.1. General Motors Dispersion Study

In 1975, GM conducted an experiment with the participation of the EPA and other government agencies to critically assess the validity of dispersion models in predicting near-road transportation-related air pollutants *(13)*. This comprehensive experiment included measurements of a gas tracer (SF6) dispersion and meteorological variables. The experiment was conducted at GM Proving Ground in Milford, Michigan, in the morning hours (between 7:00 and 11:00 am) of 17 selected days in October and September 1975. The time period of the experiment was chosen based on the meteorological variables recorded in the previous year (Fall of 1974) to include the most records with low-wind speed blowing from west direction. The GM Proving Ground test track has two five-km long tracks and each track includes two lanes. To simulate the transportation-related air pollutant from a highway, a fleet consists of 32 packs of 11 (352) passenger cars were driven at the speed of 80 km/h. The tracer was released from cylinders of Matheson CP grade SF6 (sulfur hexafluoride) mounted vertically on the back of eight (or seven) pickup trucks each day of the experiment. The SF6 concentrations, wind speed, wind direction, and temperature were measured at three different heights from ground level (0.5, 3.5, and 9.5 m) on six towers (T1-T6) and also at one height from ground level (0.5 m) on two stands (S1 and S2). Figure 31 shows the relative location of test track and measurement points (perpendicular distance of measuring points from the edge of the road and also

ground level) in GM Proving Ground. During this experiment, 50 sets of 30-min average concentrations of SF6, wind speed, wind direction, and temperature were collected for 20 measuring points (total of 1000 data points).

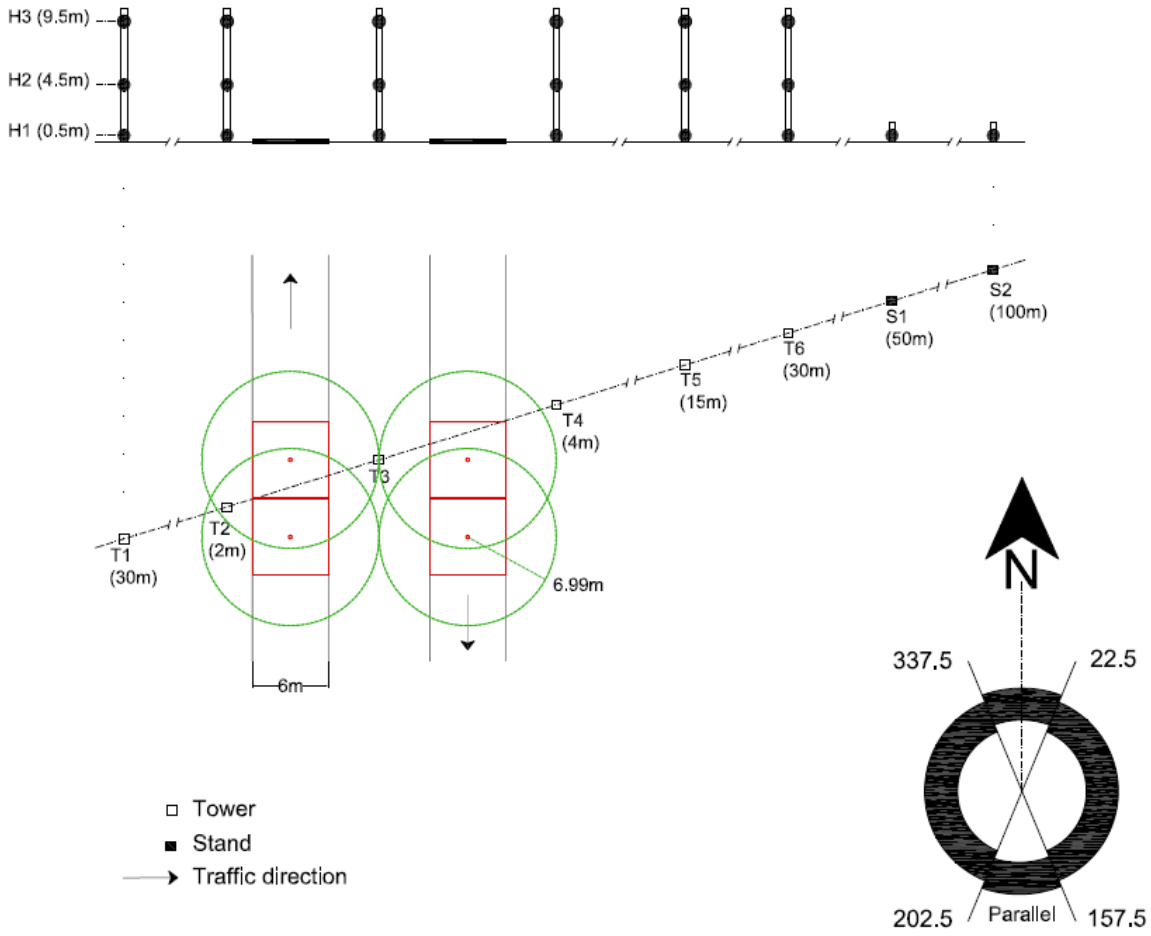

Figure 31- Locations of the tracks, towers, and stands where SF_6 and local meteorological conditions were measured during the GM Sulfate Dispersion Experiment.

4.3.2.2. Dispersion Model Set-Up

AERMOD, using its LW-3 option with different dispersion parameters, was used to evaluate the effect of release height, initial vertical dispersion coefficient (σ_{zo}), minimum value of lateral wind velocity fluctuation due to turbulence ($\sigma_{v,min}$), and FRANmax on the dispersion of near-road transportation-related SF_6 in GM study. The test track was modeled as a series of volume sources, based on the better performance of volume sources compared with area sources in our previous study *(184)*. The SF_6 emission rate was calculated based on the total recorded emission rates from SF6 cylinders mounted on trucks for each day of the experiment and assumed to remain constant and continuous *(13)*. The average emission rate was 7.90 ± 0.51 μg m^{-2} s^{-1}.

For simulating vehicular emission sources as the volume sources in this study, emission sources are being considered to be cubes with a base dimension of 6 m. The EPA guidance for hot-spot analysis *(185)* recommends estimating the fleet release height using a weighted average of light-duty (1.3 m) and heavy-duty vehicles (3 m) while using volume sources. In this study, the variation of SF6 release height between 0.3 and three for GM experiment fleet *(13)* is being taken into consideration. The initial vertical dispersion coefficient (σ_{zo}) also was assumed to vary between one m and 3.5 m above the dispersion height, based on weighted average of light-duty (1.2 m) and heavy-duty vehicles (3.2 m) recommended by the EPA guidance for hot-spot analysis *(185)*. Based on this guidance, the initial horizontal dispersion coefficient (σ_{yo}) was assumed to be 2.79 m (volume source width divided by 2.15).

To model meteorological conditions, the off-site raw data obtained from Bishop International Airport Station (AWS: 726370) - the nearest regional weather station - as well as the on-site meteorological data, measured during GM study, formed input set of AERMET (meteorological processor) to obtain processed meteorological inputs of the dispersion model (AERMOD). The on-site meteorological data included reading of wind speed, wind direction, and temperature, and included a total number of 20 measurement points (three heights (0.5, 3.5, and 9.5 m) of six towers and one height (0.5 m) of two stands). The location-dependent surface parameters including surface albedo and Bowen ratio were taken as 0.18, and 0.92 based on consulting with experts in the Michigan Department of Transportation for fall of 1975. To evaluate the AERMOD performance, dispersion modeling results were obtained at the total number of 20 measurement points for each hour (50 hours) of the experiment (1000 observation and modeling records).

To evaluate the model performance at different wind directions, the dataset was classified either as parallel wind or perpendicular wind direction. The cases with a wind direction of 337.5° to 22.5° and 157.5° to 202.5° (from the north) were classified as cases with parallel and the rest as perpendicular wind direction (Figure 31). The perpendicular wind cases were grouped into upwind and downwind cases based on westerly or easterly wind direction. Therefore, data corresponding to Towers 1 and 2 (T1 and T2) were considered as upwind for westerly perpendicular wind cases and Towers 4 to 6 (T4-T6) as well as both Stands (S1 and S2) as upwind for easterly wind cases. Hence, the results were evaluated in three categories of upwind, downwind, and parallel wind cases, to consider the effect of wind direction on dispersion modeling using different parameters.

4.3.2.3. Model Performance Measures

To evaluate model performance using different parameters, all parameters were kept constant and equal to the default values unless the parameters desired to focus on. In this regard, the whole dataset or some representative cases were selected to evaluate the specific effect of the focus parameter, and corresponding two-dimensional figures were used to illustrate the results and identify any systematic patterns. Moreover, the model predicted and on-site observed concentrations were paired in time and space and the statistical measures were used to quantify model performance with variation of desired parameters.

The quantitative measures of comparison include the fractional bias (FB), the fraction of predicted values within a factor of two of observed values (FAC2), normalized mean error (NME), the normalized mean square error (NMSE), and the correlation coefficient (R). The definitions of the above-mentioned measures are shown in Equations 10 to 14*:*

$$\mathrm{FB} = 2\frac{(\overline{C_O} - \overline{C_P})}{(\overline{C_O} + \overline{C_P})} \qquad \text{Equation (10)}$$

$$\mathrm{FAC2} = \text{fraction of points within } 0.5 \leq \frac{C_P}{C_O} \leq 2.0 \qquad \text{Equation (11)}$$

$$\mathrm{NME} = \frac{\sum_1^n |C_O - C_P|}{\sum_1^n C_O} \qquad \text{Equation (12)}$$

$$\mathrm{NMSE} = \frac{\overline{(C_O - C_P)^2}}{\overline{C_O}\,\overline{C_P}} \qquad \text{Equation (13)}$$

$$R = \frac{\overline{(C_O - \overline{C_O})(C_P - \overline{C_P})}}{\sigma_{C_O}\sigma_{C_P}} \qquad \text{Equation (14)}$$

In the above equations, C indicates concentrations, while subscripts O and P denote observed and predicted concentrations, respectively. The overbar represents the arithmetic mean and sigma (σ) represents the standard deviation. FB represents the normalized value of model bias and therefore indicates if the model results are systematically biased. Ideally equal to zero, FB varies between -2 and +2. NME is also the conventional statistics measure which shows how the overall normalized model's predictions are biased and scattered relative to the observation. NME varies between 0 and +∞ and ideally equals zero. NMSE measures the mean scatter of the model relative to the observations and provides an estimation of deviations between model predictions and observations. R is the linear correlation coefficient between model results and observations. This would equal one when observations and predictions are positively correlated perfectly and it typically varies between -1 and +1.

4.3.3. Results and Discussion

4.3.3.1. Sensitivity to Dispersion Parameters in a Low-Wind Speed Case

To evaluate the sensitivity of near-road transportation-related air pollutants to the variation of $\sigma_{v,min}$, σ_{zo}, and release height, a representative low-wind case perpendicular to the roadway was selected. In this specific case, wind speed is 0.7 m/s and the wind direction is 273° (from the north). The predicted concentrations at twenty receptors located at different distances from the edge of the road and different heights can be seen in Figure 32. An increase of $\sigma_{v,min}$ from 0.1 to 0.4 m/s does not change the prediction, while the increase of $\sigma_{v,min}$ from 0.4 to 0.7 m/s decreases predicted concentrations at 0.5 and 3.5 m heights and increase those of 9.5 m at downwind. The same pattern in the reduction of predicted concentrations at 0.5 and 3.5 m and increase at 9.5 m heights at downwind due to increase in σ_{zo} (1.5 to 3.5) and release height (1 to 3).

It should be noted that least changes can be seen upwind due to changes in $\sigma_{v,min}$ and σ_{zo}, while increase in release height yields an increase at immediate upwind points. The consequence of increase in all three parameters of $\sigma_{v,min}$, σ_{zo}, and release height is a decrease in predicted concentrations at 0.5 and 3.5 m and increase at 9.5 m from ground level, located at downwind. The higher level of mixing of transportation-related air pollutants at near-road sources leads to dilution (lower concentrations) at the near-ground level and more mass transport to higher levels (higher concentrations).

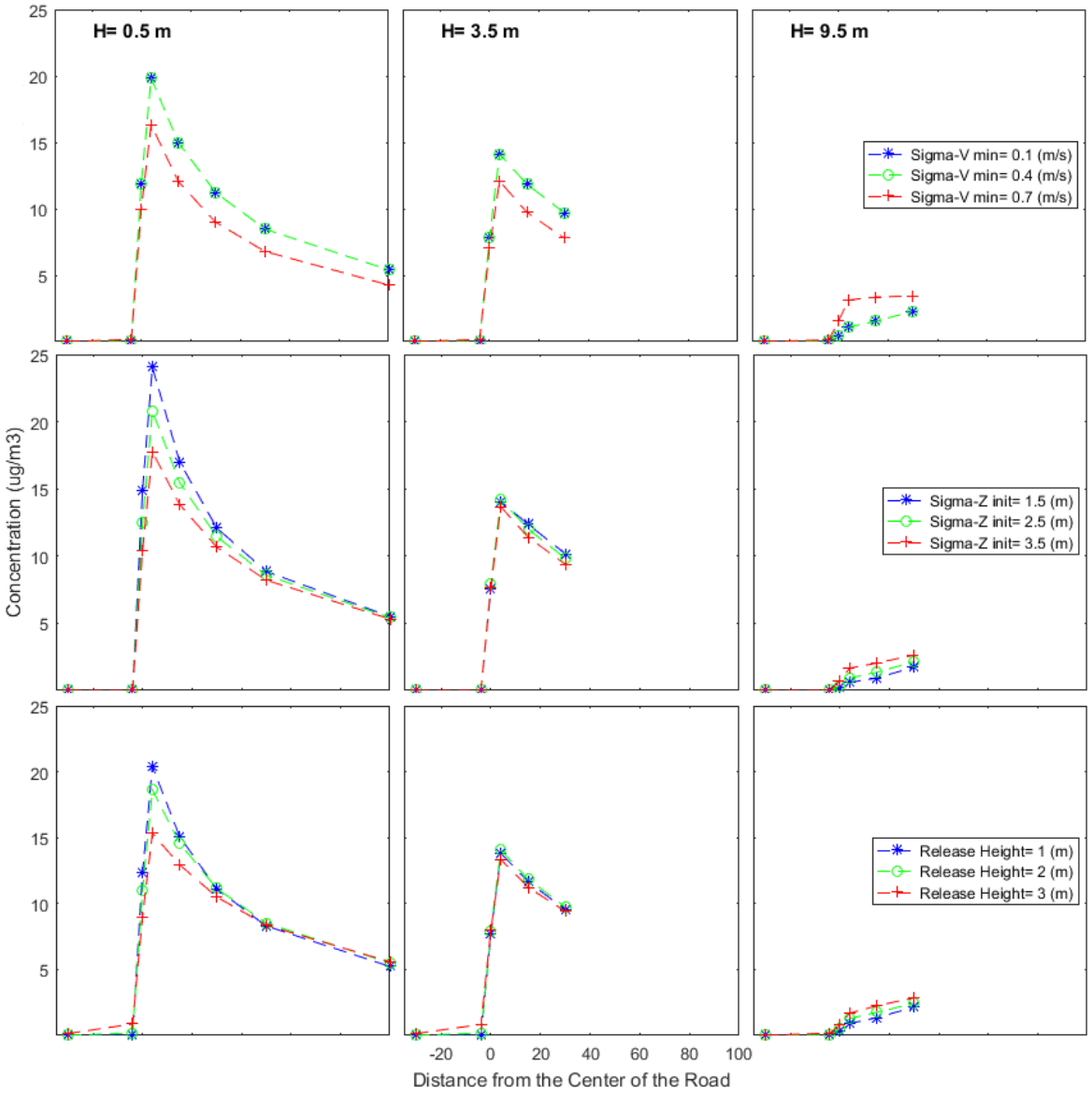

Figure 32- Sensitivity of AERMOD using volume sources and LW-3 option to $\sigma_{v,min}$, σ_{zo}, and release height in a representative perpendicular low-wind case (wind speed: 0.7 m/s, wind direction: 273°)

4.3.3.2. Sensitivity to Dispersion Parameters in Different Wind Speeds

To better understand of the sensitivity of near-road transportation-related air pollutants to dispersion parameters, the effect on the modeling results of variations in these parameters at different wind speeds was evaluated. Figure 33 illustrates the difference between predicted concentrations using maximum and minimum values of $\sigma_{v,min}$, σ_{zo}, and release height used in previous part, at three heights located at Tower 4 (immediate downwind tower) under different wind speeds.

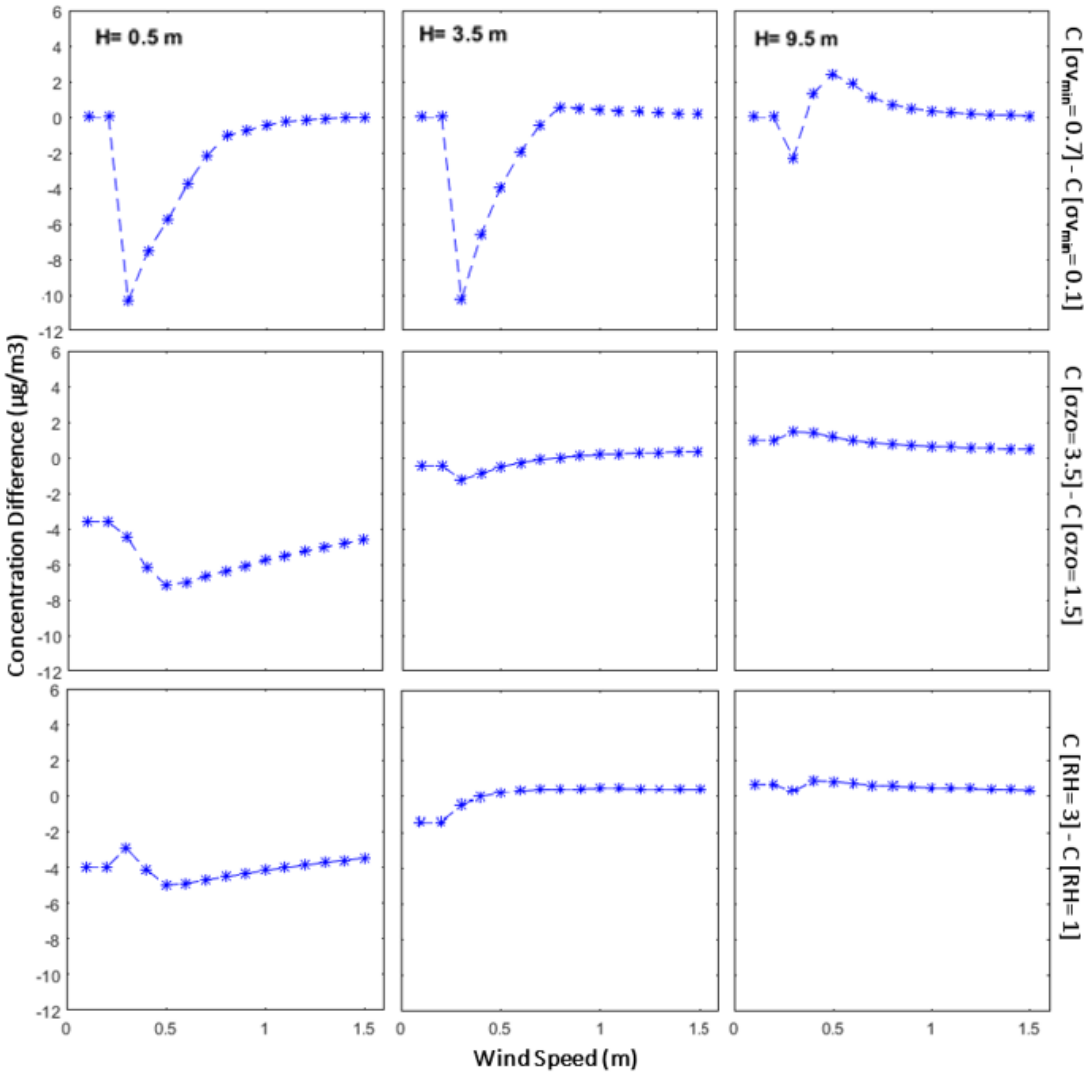

Figure 33- Sensitivity of AERMOD prediction at downwind near-roadway using volume sources and LW-3 option to $\sigma_{v,min}$, σ_{zo}, and release height (RH) in a representative perpendicular wind direction and different wind speeds

An increase in wind speed generally decreases the difference between predicted concentrations using maximum and minimum used parameters of $\sigma_{v,min}$, σ_{zo}, and release height. Moreover, this difference decreases the further away from ground level. Obtained results show a relatively higher effect of $\sigma_{v,min}$, particularly at wind speeds about 0.4. It

should be noted that the shift in concentration difference, corresponding to wind speeds lower than 0.3 m/s, is related to AERMOD treatment for cases with wind speeds below the minimum that does not consider advection due to meteorological condition and do not use meteorological inputs.

4.3.3.3. Statistical Analysis

Previously described quantitative measures (FB, FAC2, NME, NMSE, and R) were used to evaluate the model performance using a variety of dispersion parameters through comparison of predicted against observed concentrations in different categories of wind directions and the results are shown in Figure 34 and Figure 35. Figure 34 illustrates changes in quantitative measures, based on dispersion modeling using a set of σ_{zo}, and release height (as the vehicular source characteristics), for four categories including all cases and cases at upwind, downwind, and parallel wind cases. The model provides a better quantitative measure set for downwind cases, which is indicated by lower FB, NME, and NMSE as well as higher FAC2 and R.

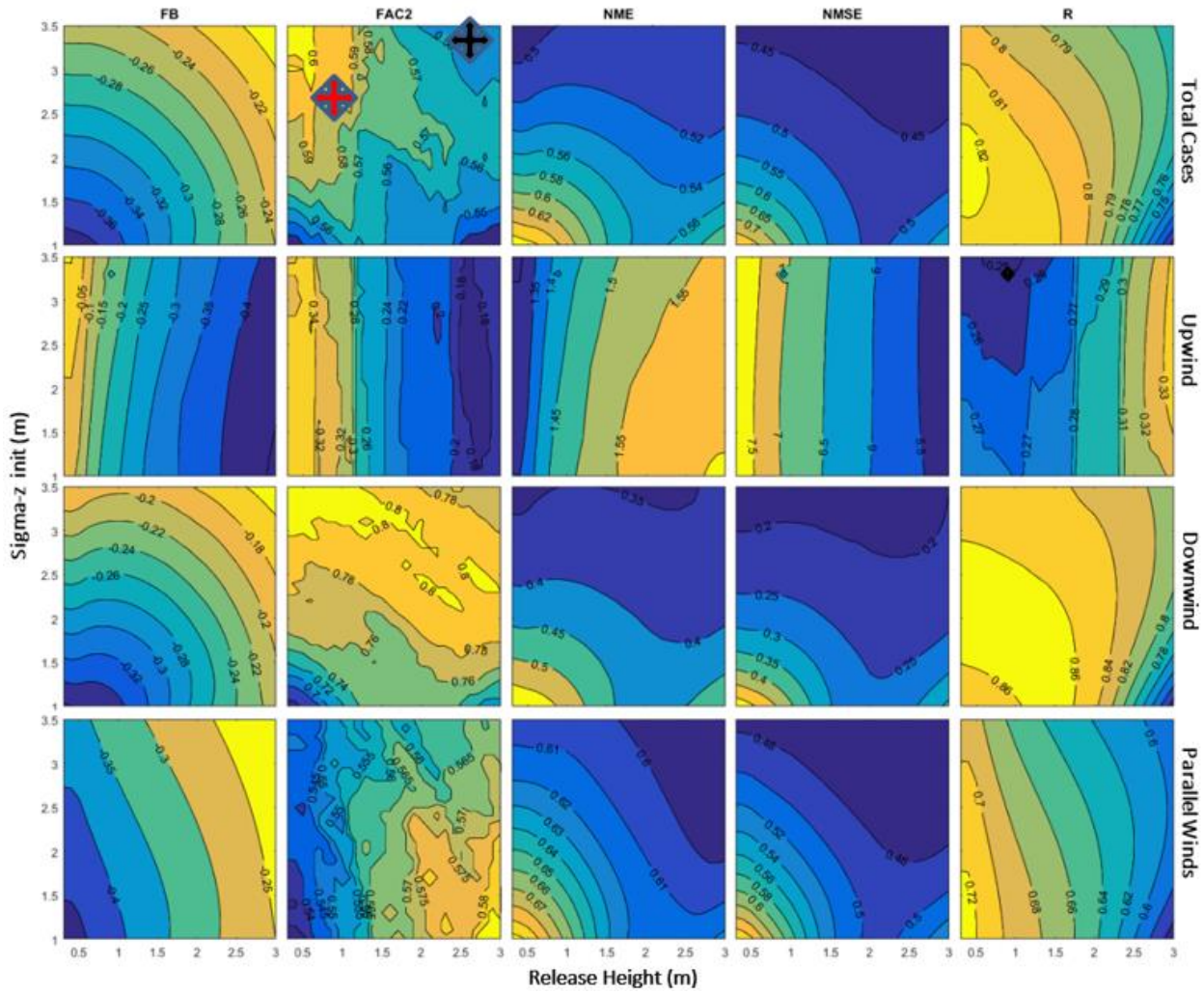

Figure 34- Statistic measures of model performance (each column) with a variation of σ_{z_0} and release height at different wind categories (each row), red and black signs show default and alternative values

Figure 36 shows that the release height has more effect on quantitative measures compared with σ_{zo}. It should be noted that the five provided quantitative measures do not necessarily suggest a pair of σ_{zo} and release height value that yields the best model performance. For instance, three measures (FB, NME, and NMSE) indicate that an increase in σ_{zo} improves model's performance, while R shows vice versa for total cases. However, considering small changes in R and FAC2, and considerable changes in FB, NME, and NMSE for total cases, it can be concluded that higher values of σ_{zo} and release height may enhance overall model performance (shown by black sign) compared with EPA guidance default ones (shown by red sign in Figure 34).

The same analysis was performed to evaluate the effect of $\sigma_{v,min}$ and FRANmax (characteristics of dispersion treatment) on model performance (sensitivity of AERMOD to $\sigma_{v,min}$ and FRANmax) and corresponding results are shown in Figure 35. It illustrates a relatively better model performance in predicting concentrations at downwind compared with other categories. Results show the higher sensitivity of model prediction to $\sigma_{v,min}$ rather than FRANmax and a higher effect of change in $\sigma_{v,min}$ at values greater than 0.5 m/s on model results. It can be seen variation of $\sigma_{v,min}$ and FRANmax has the least effect on model performance in parallel winds.

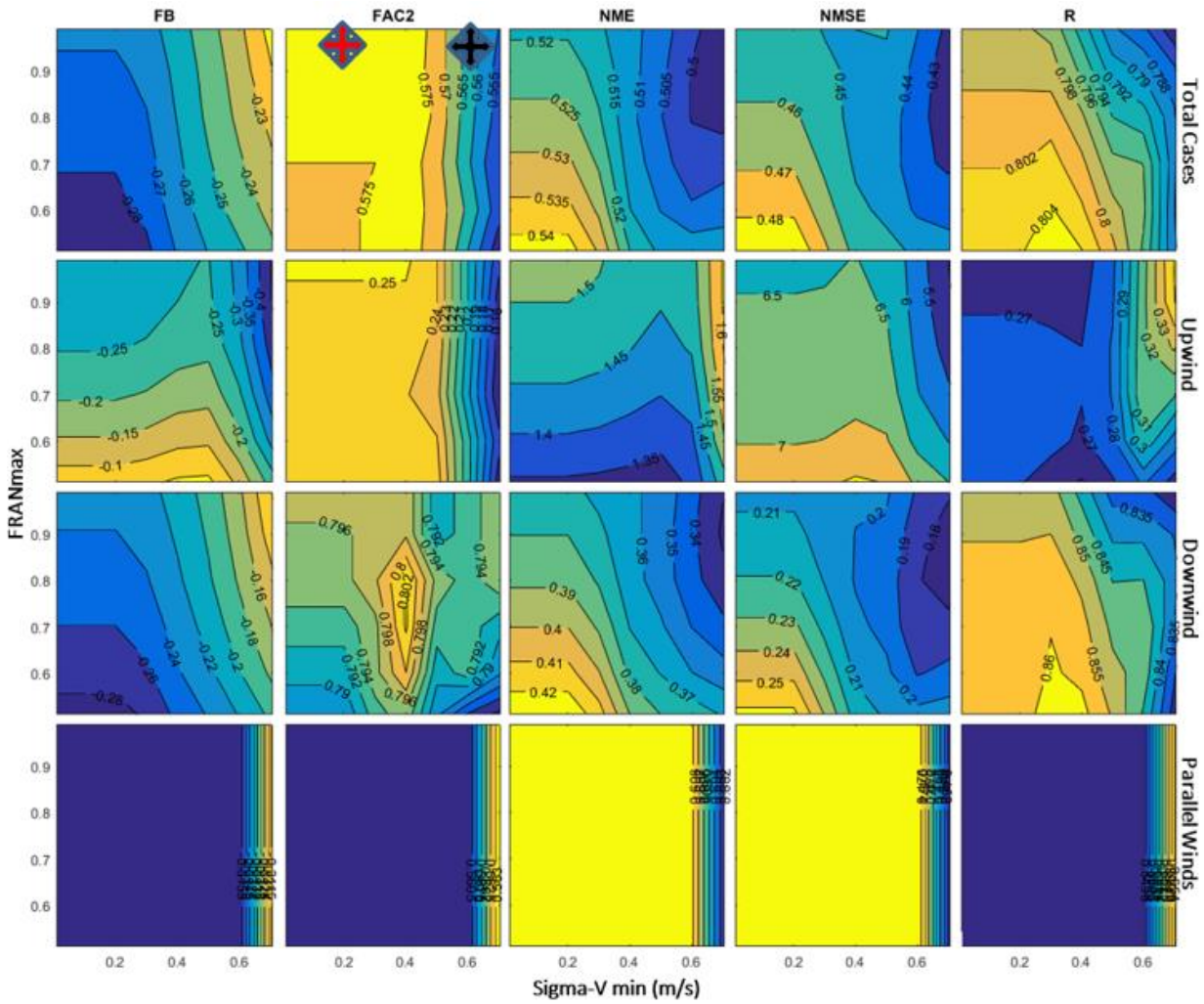

Figure 35- Statistic measures of model performance (each column) with variation of $\sigma_{v,min}$ and FRANmax at different wind categories (each row), red and black signs show default and alternative values

4.3.3.4. Model Performance with Alternative Parameters

To investigate potential improvement in model's performance with a specific set of σ_{zo} and release height (as the alternative) in comparison with default ones, the model's results obtained using two sets (of σ_{zo} and release height) were compared together. Model predictions using alternative σ_{zo} and release height (the highest values of σ_{zo} and release height that perceived to be able to generate a better result set based on Figure 34) were compared with those of EPA guidance default values. Figure 36 shows model predictions using the alternative values of σ_{zo} and release height (3.5 and 3 m) versus EPA guidance default ones (2.8 and 1.5 m) under different wind directions, wind speeds, and at different heights. Using these alternative values instead of default values yields an increase in upwind predictions at all three heights. It also increases high-level (9.5 m) and decreases near-ground level (0.5 m) predictions at downwind and parallel winds. Results show changes for some of the low-wind speed cases at upwind, but not systematic difference between low- and high wind speed cases at downwind and parallel wind cases.

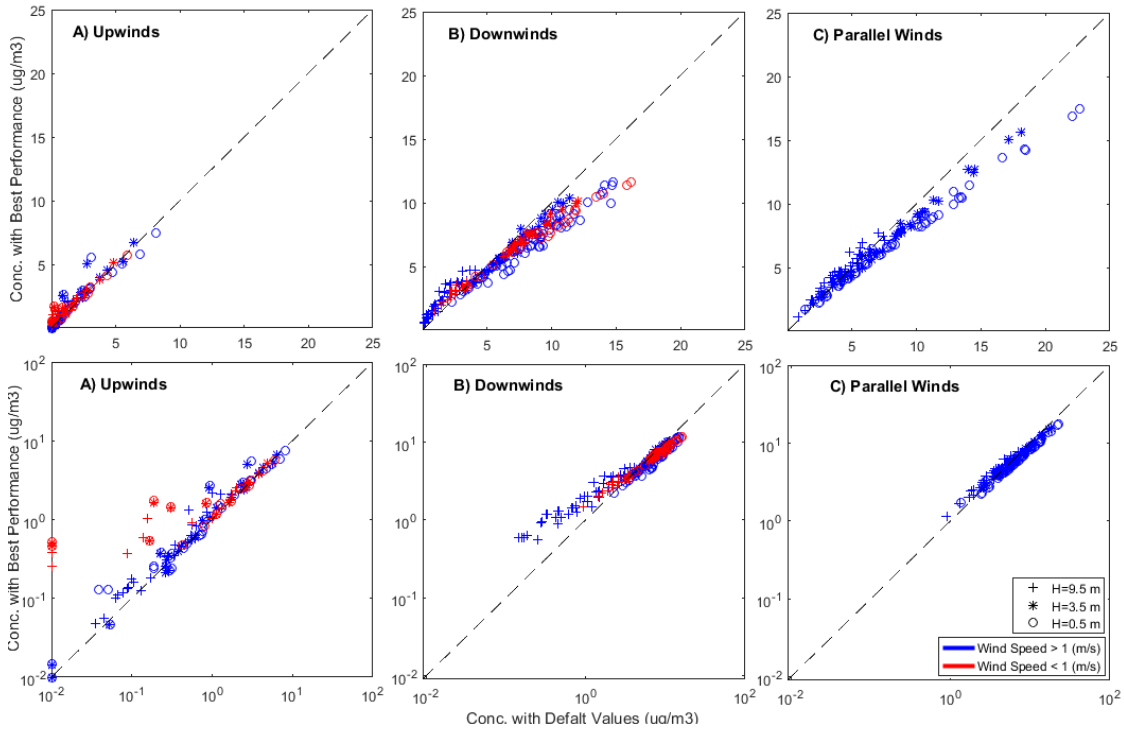

Figure 36- Performance of model with alternative values of σ_{z0} and release height versus default values at three wind direction categories, two wind speed classes (low- and high wind speeds), and three heights.

Considering improvement of model performance at higher $\sigma_{v,min}$ based on FB, NME, and NMSE, model performance at $\sigma_{v,min}$=0.707 m/s (as an alternative) was compared with that of default value ($\sigma_{v,min}$=0.3 m/s using LW-3 option). Figure 37 shows model predicted values using $\sigma_{v,min}$=0.707 m/s compare with those of $\sigma_{v,min}$=0.3 m/s in different categories. As it can be seen in Figure 37, increase in $\sigma_{v,min}$ (from 0.3 to 0.707 m/s) leads an increment in predictions at upwind which is mainly related to high-wind speed cases. The alternative value for $\sigma_{v,min}$ decrease near-ground level (0.5 m) predictions and clusters predicted values at 9.5 m in low-wind speeds around 1 $\mu g/m^3$. Using alternative $\sigma_{v,min}$ yields some slight changes in parallel wind cases results those are not systematic.

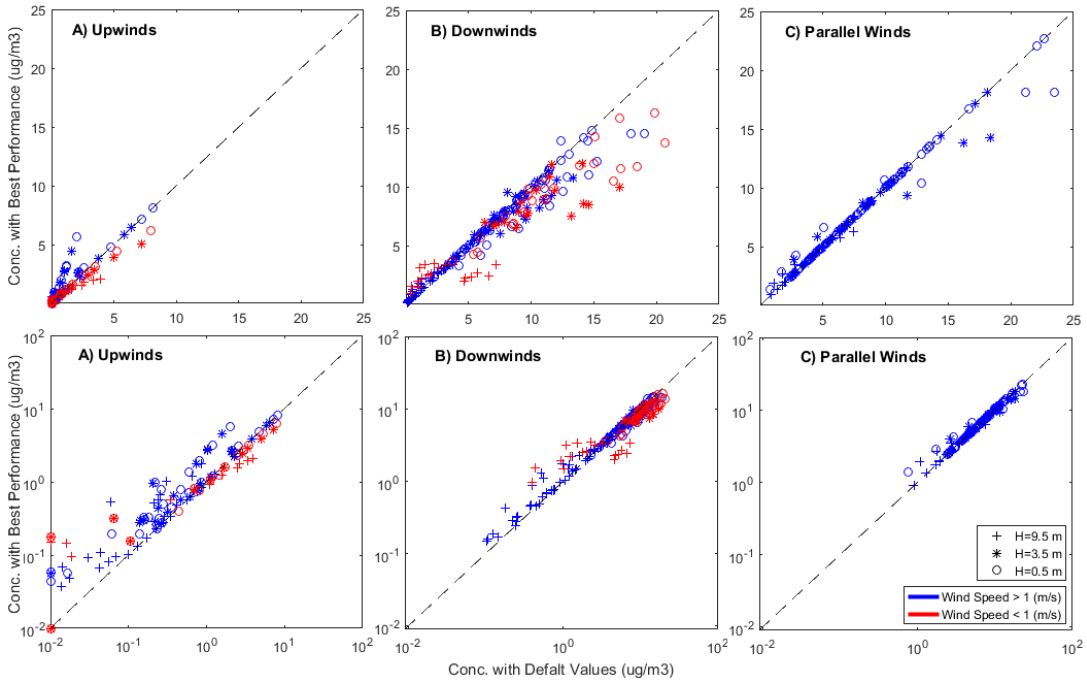

Figure 37- Performance of model with alternative values of $\sigma_{v,min}$ versus default values at three wind direction categories, two wind speed classes (low- and high wind speeds), and three heights.

The same quantitative measures were used to get a better understanding of model performance using alternative σ_{zo} and release height versus default ones which are provided in Table 15 for different categories of wind directions and wind speeds. Alternative σ_{zo} and release height significantly improve FB but have negligible improvement on NME and NMSE and worsen FACT2 and R considering the whole dataset. The detailed factors for model's performance at different categories show improvement in some of the measures related to downwind and parallel wind cases due to use of alternative σ_{zo} and release height instead of default ones.

Table 15- Quantitative measures to evaluate model performance using Alternative σzo and release height versus Default ones

							Upwind				Downwind				Parallel	
	Total	Total	HW		LW		High WS		Low WS		High WS		Low WS		High WS	
Stats	Def	Alt	Def	Alt	Def	Alt	Def	Alt	Def	Alt	Def	Alt	Def	Alt	Def	Alt
FB	-0.27	-0.19	-0.27	-0.19	-0.25	-0.18	-0.19	-0.33	-0.44	-0.57	-0.23	-0.15	-0.23	-0.14	-0.32	-0.21
FAC2	0.58	0.55	0.56	0.55	0.65	0.58	0.23	0.18	0.30	0.19	0.76	0.75	0.88	0.83	0.56	0.57
NME	0.52	0.51	0.55	0.54	0.42	0.37	1.48	1.53	1.57	1.60	0.40	0.40	0.32	0.27	0.61	0.59
NMSE	0.45	0.44	0.51	0.62	0.57	0.60	8.24	12.74	9.54	9.43	0.25	0.37	0.19	0.23	0.46	0.40
R	0.80	0.76	0.76	0.72	0.92	0.91	0.24	0.30	0.35	0.43	0.82	0.75	0.91	0.89	0.65	0.59

Table 16- Quantitative measures to evaluate model performance using Alternative σv,min and FRANmax versus Default ones

							Upwind				Downwind				Parallel	
	Total	Total	HW		LW		High WS		Low WS		High WS		Low WS		High WS	
Stats	Def	Alt	Def	Alt	Def	Alt	Def	Alt	Def	Alt	Def	Alt	Def	Alt	Def	Alt
FB	-0.27	-0.22	-0.27	-0.26	-0.25	-0.05	-0.19	-0.53	-0.42	-0.26	-0.23	-0.18	-0.23	-0.03	-0.32	-0.31
FAC2	0.58	0.55	0.56	0.55	0.65	0.58	0.23	0.14	0.29	0.20	0.76	0.78	0.88	0.83	0.56	0.56
NME	0.52	0.50	0.55	0.53	0.41	0.36	1.48	1.74	1.53	1.35	0.40	0.35	0.32	0.28	0.61	0.60
NMSE	0.45	0.42	0.51	0.57	0.57	0.73	8.24	10.30	9.78	13.00	0.25	0.34	0.19	0.26	0.47	0.37
R	0.80	0.79	0.76	0.77	0.92	0.87	0.24	0.35	0.36	0.39	0.82	0.84	0.92	0.82	0.65	0.65

However, none of the categories have all five quantitative measures improved or worsened. Quantitative measures to evaluate the effect of using alternative $\sigma_{v,min}$ for different categories (Table 16) show improvement of FB, NME, and NMSE and negligible impact on FAC2 and R considering the whole dataset. Some considerable improvement in FB can be seen but they are not associated with the improvement of other measures in the same category.

4.3.4. Conclusion

In this study, the sensitivity of AERMOD to vehicular source characteristics (initial vertical dispersion coefficient (σ_{zo}) and release height) and dispersion treatment characteristics (minimum value of lateral wind velocity fluctuation due to turbulence ($\sigma_{v,min}$), and FRANmax) were investigated. The sensitivity of the model's prediction was evaluated at different vertical and horizontal distances from the road, as well as different wind speeds. Results showed an increase in $\sigma_{v,min}$ (0.4 to 0.7 m/s), σ_{zo} (1.5 to 3.5 m) and release height (1 to 3 m) and a decrease in predicted concentrations at 0.5 and 3.5 m and an increase at 9.5 m from ground level located at downwind. This can be explained by a higher level of mass transfer from the vehicular emission source to the surrounding environment. The fewest changes were seen at upwind due to changes in $\sigma_{v,min}$ and σ_{zo}, while an increase in release height yields an increase in immediate upwind points near-ground level.

Results showed that the parameters of focus have a significant effect at near-ground level (0.5 m) and near-road predictions under low-speed wind, while their effects

dramatically decrease with increased distance from the roadway and as wind speed increases. Results put an emphasis on the high level of dispersion modeling sensitivity to both vehicular source and dispersion treatment characteristics when predicting near-road concentrations, which is a requirement for both regulatory purposes and exposure assessment studies.

Considering quantitative measures of FB, FAC2, NME, NMSE, and R, the model generally performs better at downwind, varying four input parameters of focus. Model performance using alternative parameters was compared with the one using regulatory guidance suggested parameters in different wind speed and wind direction categories. Using alternative parameters improved some, but not all, of the quantitative measures and yielded negligible overall model improvement. Obtained results showed that variation of some of the investigated parameters to improve one measure may not be followed by improvement in other statistical measures. Hence, using different input sets of source and dispersion treatment characteristics might be required to be able to predict different classes of wind direction and speed.

4.3.5. Acknowledgement

The authors would like to thank Dr. Tony Held for providing the GM dataset and related documentation, as well as the original research team that conducted the General Motor Sulfur Dispersion Experiment. The authors would also like to thank the Michigan Department of Transportation for providing guidance on selecting proper input parameters for AERMOD.

5. EVALUATION OF DISPERSION MODEL PERFORMANCE

5.1. AERMOD for Near-Road Pollutant Dispersion: Evaluation of Model Performance with Different Emission Source Representations and Low Wind Options[6]

The performance of the regulatory dispersion model AERMOD in simulating vehicle-emitted pollutant concentrations near-roadway using area or volume source representation of emissions and with different low wind options was assessed using the SF6 tracer data from the General Motors (GM) Sulfur Dispersion Experiment. At downwind receptor locations, AERMOD, using either area or volume source emissions, can reasonably predict the tracer concentrations near the surface (0.5 m) but the model performance decreases at higher elevations (3.5m and 9.5m above the surface). For upwind receptors, using an area source representation leads to significant under-predictions due to AERMOD's lack of treatment of lateral plume meander, but using volume source representation leads to over-predictions of upwind concentrations regardless of the low wind options for plume meander. Among the three low wind options currently available in AERMOD, best model performance is obtained with low wind option 3, which treats plume meander with a higher minimal standard deviation of the horizontal crosswind component ($\sigma_{v,min}$ = 0.3 m s^{-1}), eliminates upwind component of dispersion and uses an effective lateral dispersion parameter (σy) to replicate centerline concentration. The optional adjustment of the surface friction velocity in the

[6] *Reproduced with permission from:* Askariyeh, M.H., Kota, S., Vallamsundar, S., Zietsman, J. and Ying, Q., Transportation Research Part D, Vol. 57, pp 392-402. Copyright 2017, Elsevier.

meteorological preprocessor AERMET does not lead to obvious improvements in predicted near-road concentrations for this application.

5.1.1. Introduction

Near-road air pollution could potentially affect 11% of the population in the United States, which lives within a 100-m radius of highways *(157)*. To evaluate population exposure to traffic-related emissions as a function of time and distance to roadways under various meteorological and geographical conditions, several widely used near-road dispersion models have been developed, including CALINE3 *(42)*, CALINE4 *(15)*, ADMS *(43, 44)*, RLINE *(45)*, and the American Meteorological Society– United States Environmental Protection Agency (US EPA) Regulatory Model (AERMOD) *(41)*.

The capability of these models needs to be evaluated so that their predictions can be used with confidence in exposure and health effects analyses. Heist et al. (2013) *(26)* conducted a model inter-comparison study to assess the abilities of different near-road dispersion models using surface level on-site data from the Caltrans Highway 99 tracer experiment and the Idaho Falls tracer study. Heist et al. found that all models have similar overall performance statistics except CALINE3, which produces a larger degree of scattering in concentration estimates. AERMOD appeared to have the best performance among all the dispersion models, especially for the highest concentrations. AERMOD results using volume sources were slightly better than the models using area sources. Based in part on the findings of Heist study, the US EPA proposed replacing CALINE3 with AERMOD for all future transportation-related air quality analysis *(46)*.

In contrast, some other model validation studies show that AERMOD might not give as good model performance as expected. For example, Chen et al. (2009) *(47)* found that CALINE4 and CAL3QHC predictions of airborne particulate matter (PM) matched well with observations while AERMOD led to under-predictions at a near-road site. Claggett and Bai (2012) *(48)* found that both CAL3QHCR and AERMOD under-predicted the observed PM2.5 concentration at a signalized intersection, but CAL3QHCR had more data points within a factor of two of observations than AERMOD. The performance of AERMOD might be sensitive to the representation of vehicle emissions (i.e., volume vs. a resource). Claggett and Bai (2012) *(48)* and Claggett (2014) *(49)* found that higher concentrations of PM were predicted by AERMOD when emission sources were characterized as area sources as opposed to volume sources. In contrast, Schewe (2011) *(50)* reported 1.8 to 3.8 times higher concentration predictions from AERMOD for highways configured as volume sources compared with those configured as area sources. More studies are needed to further evaluate the performance of AERMOD for near-road predictions using different model configurations.

The main objective of this study was to evaluate the performance of various source representation options in AERMOD for near-road inert tracer concentrations. Data collected by General Motors (GM) during the GM Sulfate Dispersion Experiments in 1975 *(13, 186, 187)* were used for the modeling analyses. Emissions of the inert tracer (SF6) and the vehicle fleet volume and speed were well characterized and meteorological parameters (wind speed, wind direction, and temperature) were well determined in the GM study. In addition, concentrations were determined not only as a function of distance

to the roadway near ground level but also at two additional higher elevations, making this unique data set useful for evaluating the performance of dispersion models in near-road applications *(35, 38, 188)*. The model performance with different source representations is statistically characterized for different wind directions, wind speed groups, and elevations. The results of this study provide researchers with an improved understanding of the capability and limitation of AERMOD to model near-roadway pollutant concentrations in future applications. The GM dataset in electronic format and input files for the simulations described in the study are available upon request.

5.1.2. Observation Data and Model Setup

5.1.2.1. The General Motors (GM) Dispersion Study

In 1975, General Motors (GM) conducted a study to evaluate the dispersion of vehicle emissions in a near-road environment, using SF6 emitted from its own designed on-road fleet at the GM Proving Ground in Milford, Michigan *(13)*. The test track consisted of a long straightway loop, which included two 5-km long tracks with vehicles running in opposite directions. The vehicles were running in two lanes on each track. The fleet was comprised of 352 passenger cars, 32 packs of 11 cars each, and pickup trucks evenly spaced around the track in both traffic directions. SF6 was released from eight pickup trucks equipped with cylinders and mounted nozzles on the back of their cabs. The trucks were evenly distributed in the passenger cars fleet which means they were spaced 4 packs apart. Wind speed, wind direction, ambient temperature and SF6 concentrations were measured at three levels (9.5 m, 3.5 m, and 0.5 m from ground level) on six towers (T1-T6), as well as at one level (0.5 m from ground) on two stands (S1 and S2) in 30-min

intervals. The various locations of the towers and stands, as well as their perpendicular distances to the nearest track edge, are illustrated in Figure 38. The alignment of the towers and stands was purposefully designed to reduce the possible influence of the small hills and trees located in the test track's vicinity on pollutant dispersion *(13)*. The experiments were conducted by driving the vehicles at a constant speed of 80 km/h. Thus, in each 30-min experiment, the 11 packs of cars were separated by a 29-s internal, leading to a traffic density of 5462 cars per hour. All experiments were conducted during the morning hours (between 7:00 and 11:00 am) of 17 selected days in September and October 1975. The aim in selecting this time period was to collect a dataset that would include the most diverse wind directions and lowest wind speeds, based on the recorded meteorological data for the previous Fall of 1974. A total of 50 sets of 30-min average SF6 concentrations, wind speed, wind direction and temperature data (each parameter in one data set has 20 data points) were collected, which gives a total of 1000 data points.

5.1.2.2. AERMOD Setup to Simulate the GM Experiment

In this study, the most recent version of AERMOD (version 16216) was used to simulate the concentrations of SF6 near the tracks. The test track was modeled as two rectangular area sources or a series of volume sources. It was assumed that the rate of SF6 emissions from the lanes remained constant and continuous during each experiment. The emission rates were calculated based on the recorded emission rate from each truck and for each day of the experiment *(13)*. The average emission rate was 7.90 ± 0.51 μg m^{-2} s^{-1}.

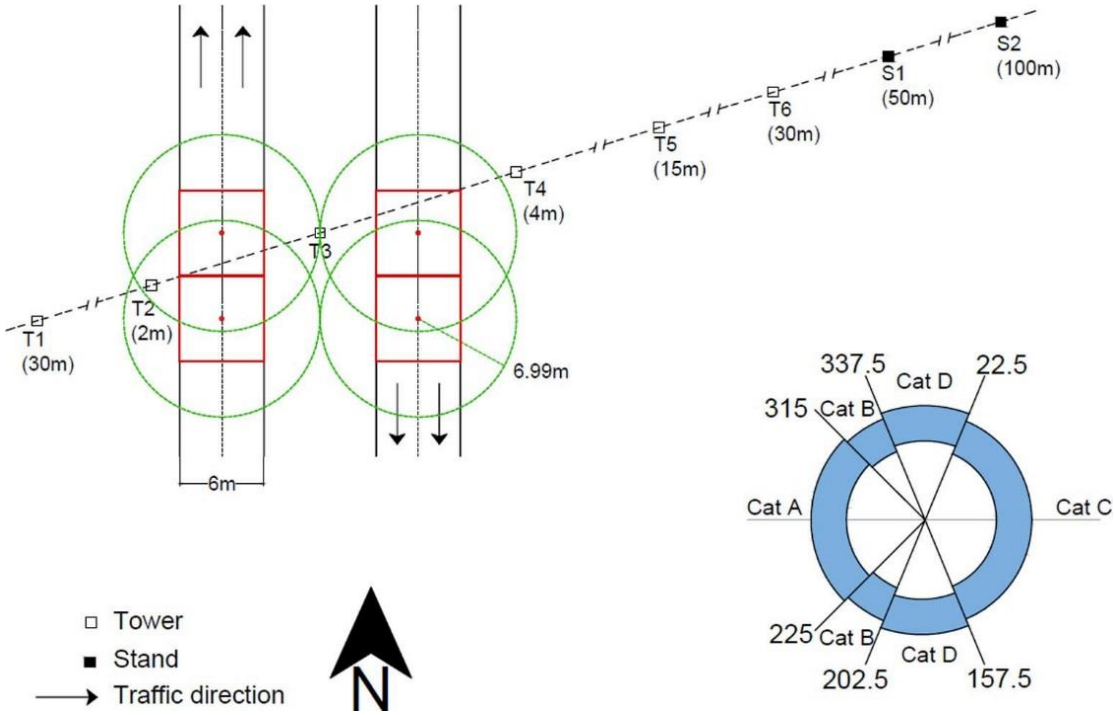

Figure 38- Locations of the tracks, towers and stands where SF6 and local meteorological conditions were measured during the General Motor (GM) Sulfate Dispersion Experiment.

Four volume sources and their exclusion zones (width of volume source + 0.99 m from the center of volume sources) are shown by red and green colors, respectively. Considering the width of volume sources for this study (6 m), T2 is located within the exclusion zone and T3 and T4 are very close to the exclusion zone. The exclusion zone concept is used in regulatory guidance *(67, 189)* to insure that receptors are spaced properly while using the volume source representation to avoid overestimation of concentrations in areas extremely close to the emission sources *(190, 191)*. While is not recommended to place receptors within the exclusion zone for regulatory applications *(67)*, observation and model results from these towers are included for research purpose.

To compare the predicted concentrations with observations, 20 receptors were placed at the exact locations where SF6 concentrations were measured. As the SF6 emissions were released from storage tanks on the trucks *(13)*, a tracer release height of 1.5 m from ground level was considered. The initial vertical dispersion was assumed to be 1.4 m above the dispersion height, based on US EPA guidance for hot-spot analysis *(67)*. On-site wind speed, wind direction and temperature readings based on data from all towers and stands, as well as off-site data obtained from Bishop International Airport Station (AWS: 726370) - the nearest regional weather station - were then processed by AERMET to generate meteorological inputs for AERMOD. Based on recommendations provided by experts in the Michigan Department of Transportation (MIDOT) familiar with the experiment's location, surface albedo, and Bowen ratio were taken as 0.18 and 0.92, respectively, for the October 1975 timeframe. Roughness length as a function of 12 direction categories was also provided by MIDOT. In most directions, it was between 0.023 – 0.047 m. In 180–210 and 240–270 degrees from north, the roughness length was approximately 0.10–0.11 m. The maximum roughness length of 0.228 m occurred in 210–240 degrees from north.

To visualize the AERMOD's predicted vertical distribution of pollutants, a mesh consisting of 20,000 additional receptors was placed on a vertical plane perpendicular to the tracks in the middle of the model domain. The horizontal and vertical distances between the equally spaced receptors were 1 m and 0.1 m, respectively. The receptors were placed from the track's edge to 100 m away to cover both upwind and downwind fields. Note that these receptors were only used to capture the vertical distributions of SF6.

For statistical model performance evaluation, only predictions at those 20 receptor sites where observations were made were ultimately used.

AERMOD simulations were conducted to acquire base case concentrations for each experiment. Moreover, a Monte Carlo simulation technique was applied to evaluate the AERMOD's sensitivity to input wind data. For each experiment, 1500 simulations were conducted by randomly varying wind speed and wind direction from those original values derived by AERMET. In this study, the randomly generated wind speeds and directions were assumed to follow a normal distribution, with a standard deviation of 0.3 m s^{-1} and 30°, respectively, which represent the average daily standard deviation of the two parameters throughout the entire experiment period. As more simulations did not change the mean and standard deviation of the predicted concentrations, it was determined that 1500 simulations were sufficient for the Monte Carlo uncertainty analysis.

To compare model performance for different wind directions, the dataset was classified into 4 categories based on mean wind directions: Category A (225° to 315° from north), category B (315° to 337.5° and 202.5° to 225°), category C (22.5° to 157.5°) and category D (337.5° to 22.5° and 157.5° to 202.5°) (see Figure 38). Considering the prevailing westerly wind in Milford, Category A represents perpendicular wind to the roadway, while category B and D represent oblique and parallel wind to the roadway, respectively. Category C specifies wind direction opposite to the prevailing wind. It generally contains more records with low wind speed.

Table 17- List of Base case and sensitivty runs

Case #	Emission [a]	Options [b]	ADJ_U* [c]	Purpose
1	Volume	Default	No	Base case
2–1	Volume	LW-1	Yes	Evaluate the effect of LW options
2–2	Volume	LW-2	Yes	
2–3	Volume	LW-3	Yes	
3	Area	Default	Yes	Evaluate the effect of emission
4–1	Volume	Default	Yes	Evaluate the effect of ADJ_U*
4–2	Volume	LW-3	No	

a) Based on the EPA guidance, pollutants emitted from vehicular sources can be modeled as either area or volume sources in AERMOD. In practice, the area source option is usually preferred, given the relative ease of defining the dimensions and parameters of emission sources. However, the differences in the capability of AERMOD in predicting near-road pollutant concentrations with different emission representations have not been well tested, given that the current version of AERMOD does not yet include a meander component for area source emissions and does not treatment plume rise.

b) The AERMOD model also applies a minimal standard deviation of the crosswind velocity fluctuation (σv) to increase lateral dispersion in very light winds under stable conditions. By default, the minimal σv is taken as 0.2 m/s. Three additional user-selectable low wind (LW) options are included in the current version of AERMOD, each with different choices for the σv values and treatment of the meander component *(183)*. In summary, LW-1 disables the horizontal meander component and increase minimal σv to 0.5 m/s; LW-2 keeps the horizontal meander component and slightly increases minimal σv to 0.3 m/s; LW-3 also eliminate upwind dispersion but uses the minimal σv to 0.3 m/s as in LW-2. In addition, LW-3 introduces an additional "effective" lateral spread (σy) to account for the enhanced horizontal dispersion in other directions due to meander. The fact that two lanes of vehicles are passing each other in different directions at 80 km/hr could lead to unique turbulence characteristics that the model does not know about. This unique turbulence provides additional justification for the additional minimum turbulence level in the low wind options.

c) The surface friction velocity (u*) is essential in determining many other parameters in the planetary boundary layer (PBL) and thus affects the calculation of pollutant dispersion. However, it was discovered that u* could be underestimated in AERMET under low wind stable conditions, which could lead to an under-estimation of mixing-height and horizontal and lateral turbulence levels and, thus, an overestimation of pollutant concentrations under stable conditions *(51)*. It was determined that the meander weight could also be underestimated due to the under-estimation of u*, which could also lead to overestimation of pollutant concentrations under low wind conditions *(51)*. To rectify this, recent versions of the AERMET model was amended to include a correction for u* (ADJ_U*), which is based on the modified equation for u* suggested by Qian and Venkatram (2011).

In this study, base case simulations were conducted using the default volume-source option, while meteorological data was processed using the default options of AERMET without the ADJ_U* option (footnote of Table 17). In three sensitivity simulations, three different low wind (LW) options were tested. In these LW option simulations, the AERMET option ADJ_U* was used to process the meteorological data. Two additional sensitivity simulations were conducted to investigate the effect of ADJ_U* on the predicted concentrations. In another sensitivity simulation, AERMOD simulations were conducted by representing vehicle emissions from roadways as area sources, and the ADJ_U* option is enabled for meteorology processing. The results from these sensitivity simulations were compared with those from the base case. Table 17 summarizes the simulations conducted in this study. A brief description of the different emission and low wind options as well as ADJ_U* is included as footnotes of Table 17. Other factors that could affected the model performance, such as the initial vertical dispersion, will be investigated in a follow-up study.

5.1.2.3. Model Performance Measures

The predicted concentrations from dispersion modeling were compared with the concentrations observed on-site, both quantitatively and qualitatively. Quantitative evaluations of model performance were conducted using the statistical measures described below. Moreover, scatter plots were used for qualitative visual evaluation to recognize any systematic patterns in modeled estimation versus observed concentrations. The quantitative measures of comparison include the normalized mean square error (NMSE),

the correlation coefficient (R), the fractional bias (FB), and the fraction of predicted values within a factor of two of observed values (FAC2). The definitions of the above-mentioned measures are shown in Equations 15 to 18:

$$NMSE = \frac{\overline{(C_O - C_P)^2}}{\overline{C_O}\,\overline{C_P}} \qquad \text{Equation (15)}$$

$$R = \frac{\overline{(C_O - \overline{C_O})(C_P - \overline{C_P})}}{\sigma_{C_O}\sigma_{C_P}} \qquad \text{Equation (16)}$$

$$FB = 2\frac{(\overline{C_O} - \overline{C_P})}{(\overline{C_O} + \overline{C_P})} \qquad \text{Equation (17)}$$

$FAC2$ = fraction of points within $0.5 \leq \frac{C_P}{C_O} \leq 2.0$ Equation (18)

In the above equations, C indicates concentrations, while subscripts O and P denote observed and predicted concentrations, respectively. The overbar represents arithmetic mean and sigma (σ) represents standard deviation. NMSE measures the mean scatter of the model relative to the observations and provides an estimation of deviations between model predictions and observations. R is the linear correlation coefficient between model results and observations. This would equal one when observations and predictions are positively correlated perfectly, and it varies between −1 and + 1. FB represents the normalized value of model bias and therefore indicates if the model results are systematically biased. Ideally equal to zero, FB varies between −2 and +2.

5.1.3. Results and Discussion

5.1.3.1. Overall Model Performance

Paired comparisons of observations and AERMOD predictions using volume sources with default options and meteorological inputs with default AERMET options for each of the four wind-direction categories, is shown in Figure 39. The data points in categories A- C are further divided into upwind and downwind, as displayed in the respective left and right columns. For categories A and B, towers T1 and T2 are considered as upwind sites and the rest of the towers and stands are considered as downwind sites. For category C, towers T4-T6 and stands S1 and S2 are considered as upwind sites and towers T1-T3 are considered as downwind sites. Just one panel was used for wind category D since it represents wind direction parallel to the road.

The default volume source option can predict downwind concentrations under both low and high wind speed conditions at all three elevations in general. However, it over predicts the upwind concentrations for all cases, regardless of wind direction and speed. All the low wind cases occur when the wind is from east to west (category C) and the upwind concentrations are generally over predicted. There are also significant over predictions in category D, although it is hard to clearly define upwind or downwind locations for category D, due to uncertainty in the wind directions. Moreover, AERMOD using volume sources seems to be biased in dealing with cases above the ground level (9.5 m) as the modeled concentrations are clustered around 1 μg m^{-3} while the observations show variations span as much as two orders of magnitude. As no background

concentrations were specified in the simulations, this suggests that vertical dispersion might be overestimated using volume source to represent vehicle emissions.

5.1.3.2. Vertical Distribution and Uncertainty Analysis

Vertical distributions of the predicted concentrations based on volume sources with default options for four representative cases (perpendicular, oblique, opposite and parallel wind directions) with corresponding measured wind speed and directions are shown in Figure 40. AERMOD can generate smooth concentration fields in the vertical cross-section in all wind directions regardless of wind speed. Overestimation is evident at upwind monitors (e.g. T1 and T2 for wind categories A and B) as shown in the "Monte Carlo Simulation Column" (right panel) of Figure 40.

The polar plots demonstrate that there is a vertical gradient of wind, with slower wind speeds closer to the surface. Wind directions also display large variations, especially for the measurements at the towers in the exclusion zone located either very close to the tracks' edge or in the middle of the two tracks (see Figure 38). These changes clearly show the impact of vehicle flow on wind speed and direction. Since the base case runs are conducted using average wind speed and direction, it is both desirable and necessary to evaluate the uncertainty in the predicted concentrations caused by corresponding uncertainty in both wind speed and direction.

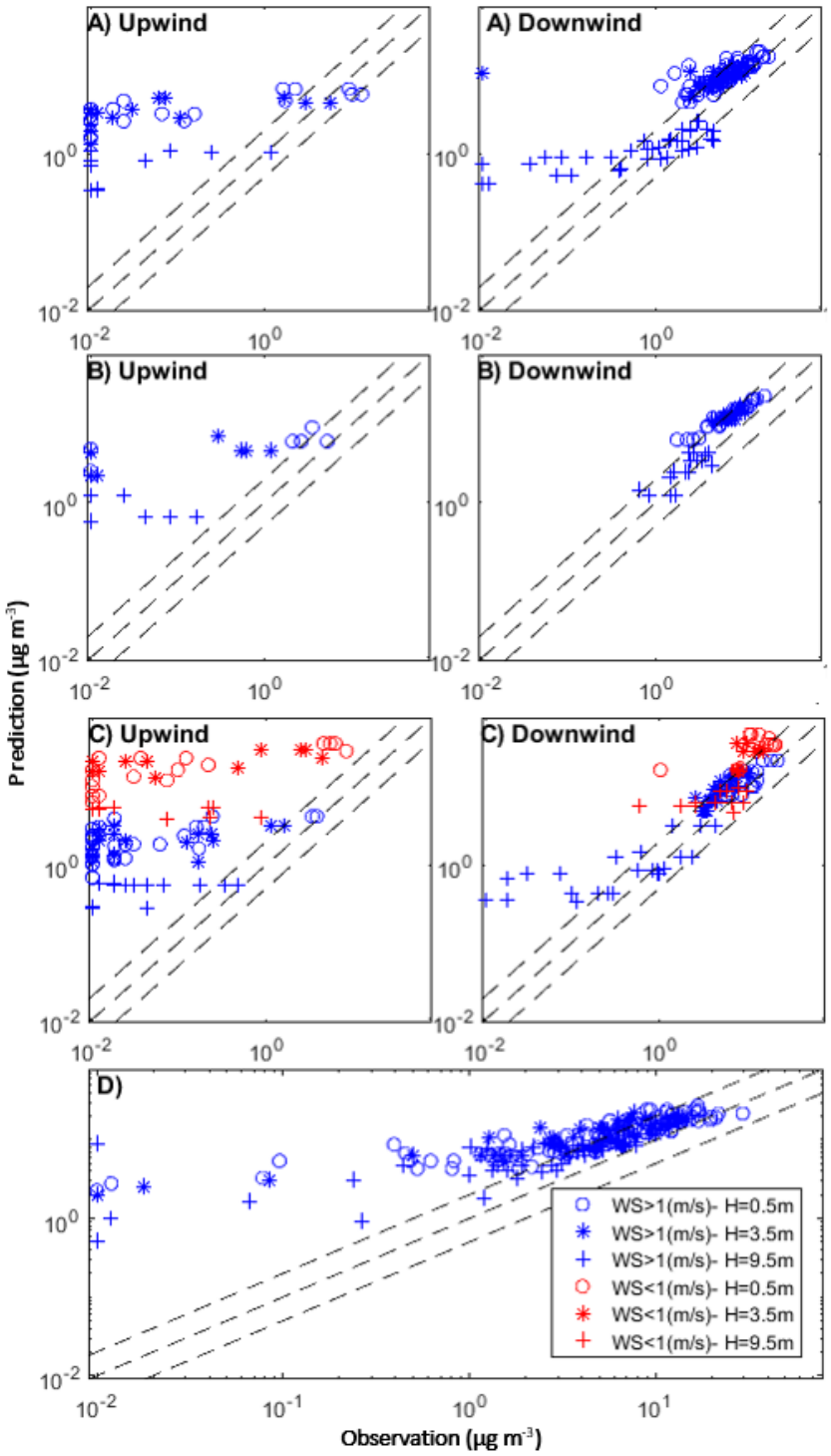

Figure 39- Predicted (using volume sources with default option) and observed concentrations of SF6 (µg m^{-3}) for all experiments grouped by wind-direction categories (A–D).

The scatter plots in cases 1, 2, and 3 (Figure 40) also show that there is a higher level of uncertainty when predicting upwind concentrations and the concentrations at the height of 9.5 m within the exclusion zone, as indicated by the longer error bars. In contrast, lower prediction variations can be observed in case 4, where wind directions are parallel to the road (and thus without clear upwind/ downwind trends). Moreover, the uncertainty caused by wind speed and wind direction is lower for the high concentration data points, which are usually near the surface and close to the roadway in downwind directions.

5.1.3.3. Performance measures of different low wind options

Statistical model performance analysis of the base case model, as well as from the three sensitivity simulations for different low wind options are summarized in Figure 41. By replacing the default setup with different low wind options, considerable changes in model performance can be observed. As displayed in panel A, the correlations between predictions and observations are improved when low wind options are used. The overall correlation coefficients are 0.73, 0.82, 0.75, and 0.80 for the base case model, and models using LW-1, LW-2, and LW-3, respectively. Higher NMSE values at 9.5 m suggest weaker performance of the model at heights compared with the one at the ground level, which is significantly improved by using the LW-3 option. The overall NMSE values (1.22, 0.89, 0.82, and 0.45 for the base case, LW-1, LW-2, and LW-3, respectively) also indicate that better performance could be obtained with low wind options and the best performance could be achieved using the LW-3 option.

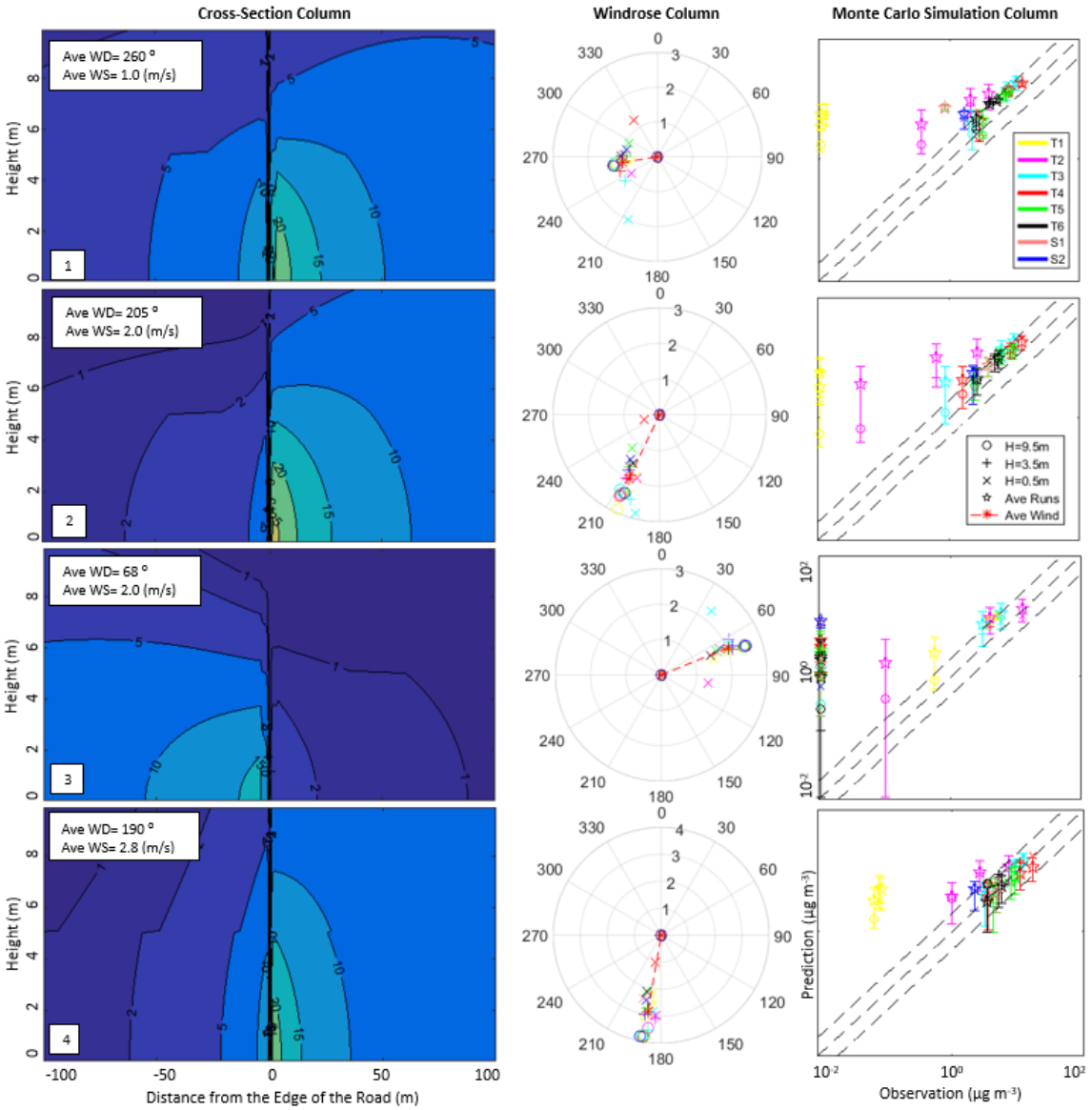

Figure 40- Cross-section of the concentration fields in the perpendicular direction of the road

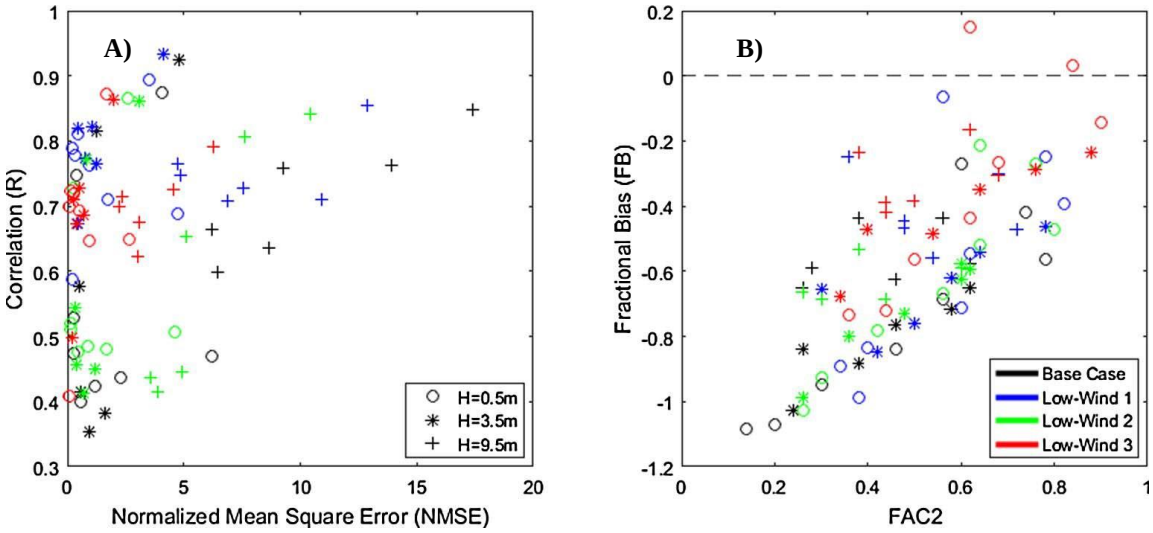

Figure 41- Performance measures for the base case and sensitivity cases with different low wind options at different heights

FB and FAC2 values are shown in panel B. Negative FB values suggest that the overall predicted concentrations are higher than those observed at nearly all locations. As the data shows, the default and LW-2 options have the same performance, with FAC2 < 0.6 and FB < −0.6 for most points. LW-1 performs better in terms of FB (−0.7 < FB) and LW-3 provides more scattered points around the FB = 0 line. When considering FAC2, both the default and LW-2 options show weaker performance than the LW-1 and LW-3 options. Considering all statistical measures in Figure 41, LW-3 shows the best performance among all the options tested.

Considering the relatively better performance of LW-3 based on the statistical measures, model results for individual cases were further investigated. Paired comparisons of AERMOD predictions versus observations for each of the four wind-direction categories, is shown in Figure 42. Comparing Figure 42 and 41 reveals considerable improvement in the predicted upwind concentrations using LW-3 for both high- and low

wind cases, as it shows prediction closer to the 1:1 line compared with base case simulation. The improvement is more evident in predicting low concentrations (< 1 µg m^{-3}) as LW-3 predicts them to be less than 2 µg m−3 while base case simulation over-predicts them to be between 2 and 50 µg m^{-3}.

Figure 43 shows the vertical distribution and the scatter plot as well as Monte Carlo simulation results for four sets of the model results using LW-3 for the same setting as the one in Figure 40 for the base case simulation. In this figure, the cross-section of field concentrations shows lower modeled concentrations at upwind. Based on what was shown and concluded from Figure 41 and Figure 42, the cross-sections provided in Figure 43 are closer to the reality. Figure 43 also shows shorter error bars indicating lower standard deviation and more points between the factor-of-two line and closer to 1:1 line than those of Figure 40, which suggests a better performance and more stability of model when LW-3 is used.

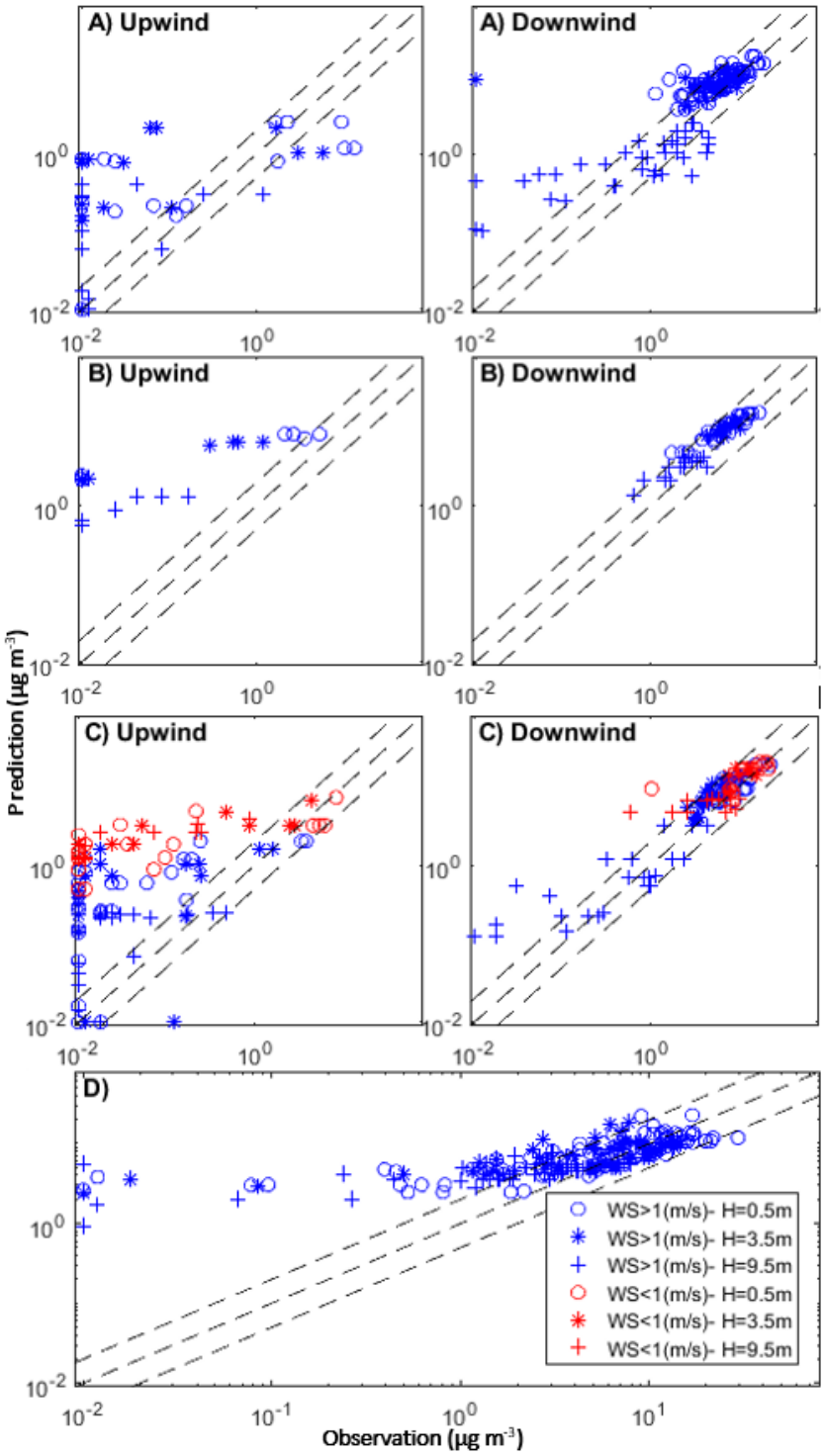

Figure 42- Predicted (using volume sources and low wind option 3) and observed concentrations of SF6 (µg m^{-3}) for all experiments grouped by wind-direction categories (A–D), and 1:1, 1:2 and 2:1 lines.

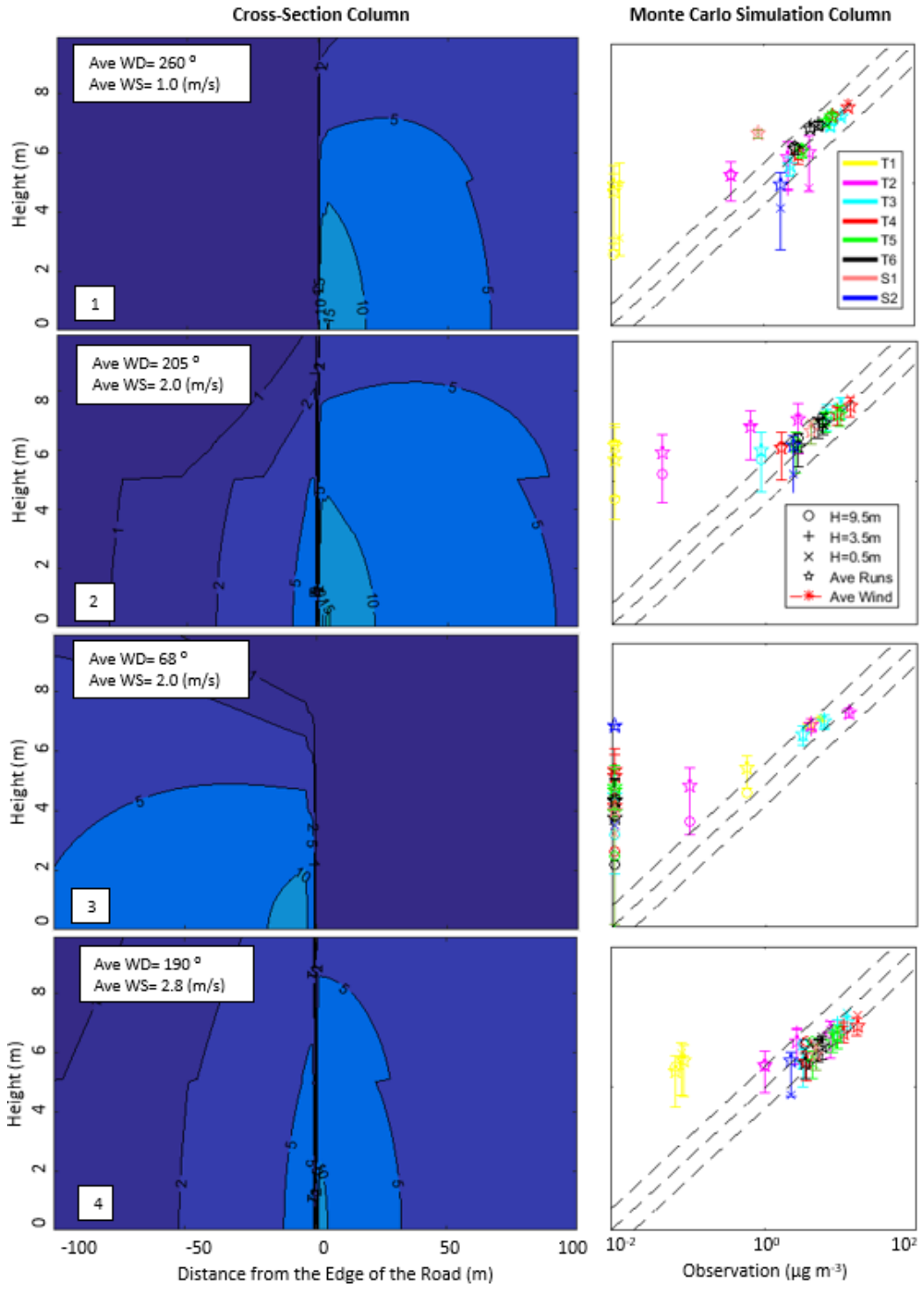

Figure 43- Predicted vertical distributions (left column) and uncertainty of the predicted concentrations by AERMOD volume and low wind option 3 at the receptors on the towers and stands (right column) for four selected cases.

5.1.3.4. Model performance with and without ADJ_U∗ option

To investigate the effect of using ADJ_U* option in running AERMET on AERMOD performance, model results using AERMET outputs obtained with and without ADJ_U* option were compared for the base case and LW-3. Since using ADJ_U* decreases vertical gradient for low wind cases, it is anticipated to obtain results with changes in predicted concentration at lower wind speed cases. The results show slight changes for low wind speed cases but did not show considerable changes for wind speed cases greater than 1 m/s (high wind speed cases). AERMOD using ADJ_U* option leads to smaller difference between predicted concentrations at ground level and 9.5 m height, compared with the model without ADJ_U* option. Figure 44 shows the comparisons of predicted SF6 concentrations at low wind speed cases (wind speed < 1 m/s) using meteorological inputs processed with and without ADJ_U∗. Using ADJ_U* does not change the results dramatically compared with the same setting without ADJ_U* for both the base case and the LW-3 case.

5.1.3.5. Model performance using area sources

Comparisons of observations and AERMOD predictions using area sources and default AERMET for each of the four wind direction categories are shown in Figure 45. While the predicted concentrations in the downwind areas show reasonable overall correlations with observations (FB, NMSE, R, and FAC2 are −0.649, 0.800, 0.829 and 0.439, respectively, similar to those obtained for the default volume source simulations but worse than those from the LW-3 case), predicted concentrations in the upwind

direction by the area sources are essentially zero due to lack of the treatment of meander component. The figure reveals that AERMOD is not sufficiently capable of dealing with upwind cases when using area sources, which put emphasis on the importance of taking meandering into consideration in dispersion modeling.

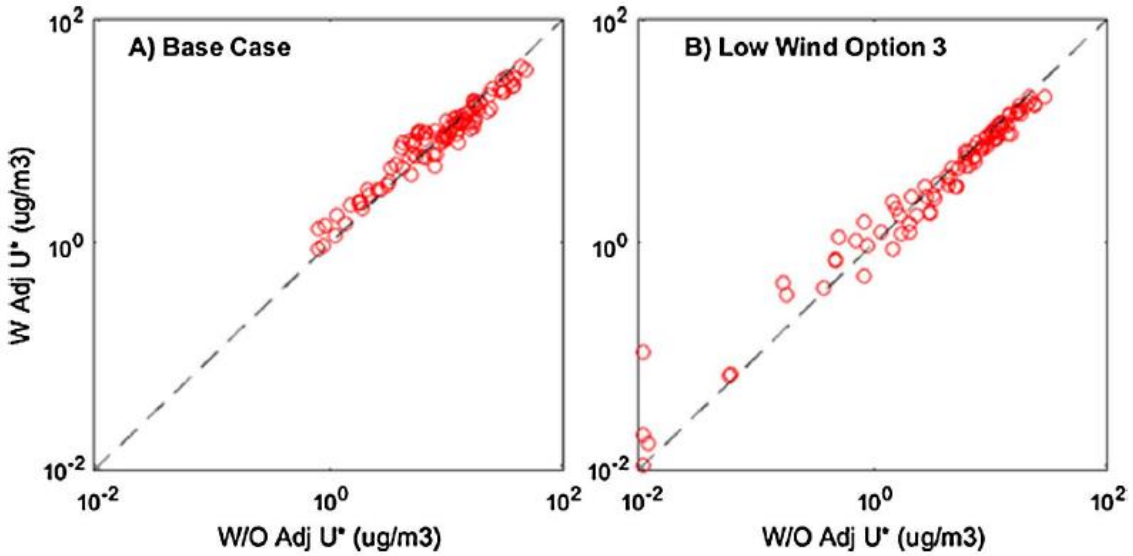

Figure 44- Predicted concentrations for low wind cases (< 1 m/s) using volume sources for Base Case and low wind option 3 with and without ADJ_U*

In addition to the problem in predicting upwind concentrations, in area source representation cannot correctly predict vertical distribution of pollutants under parallel wind condition. Figure 46 shows the effect of using area and volume sources on the predicted vertical distribution of SF6 concentrations for two parallel wind cases using a hypothetical emission rate of 10 µg $m^{-2}s^{-1}$. The winds parallel to the road (0^0 or 180^0) are supposed to generate symmetrical cross-sections of concentration field using different sources. However, this is not the case when area sources are used. As Figure 46 illustrates,

symmetric cross-section concentrations are generated using volume sources in parallel winds but not with area sources.

When the average wind direction is parallel to the road, the predicted vertical concentration fields using area sources show irregular bands of concentrations, or concentration ripples, in higher elevations (above approximately 3 meters and above). Since the AERMOD predictions represent steady- state concentrations, these concentration ripples appear unrealistic. The simulation results shown in Figure 46 are based on stable atmospheric conditions. Another set of simulations are conducted for convective conditions but similar problems show up for areas sources. A closer examination of the model formulation and coding is needed to locate the cause of this problem.

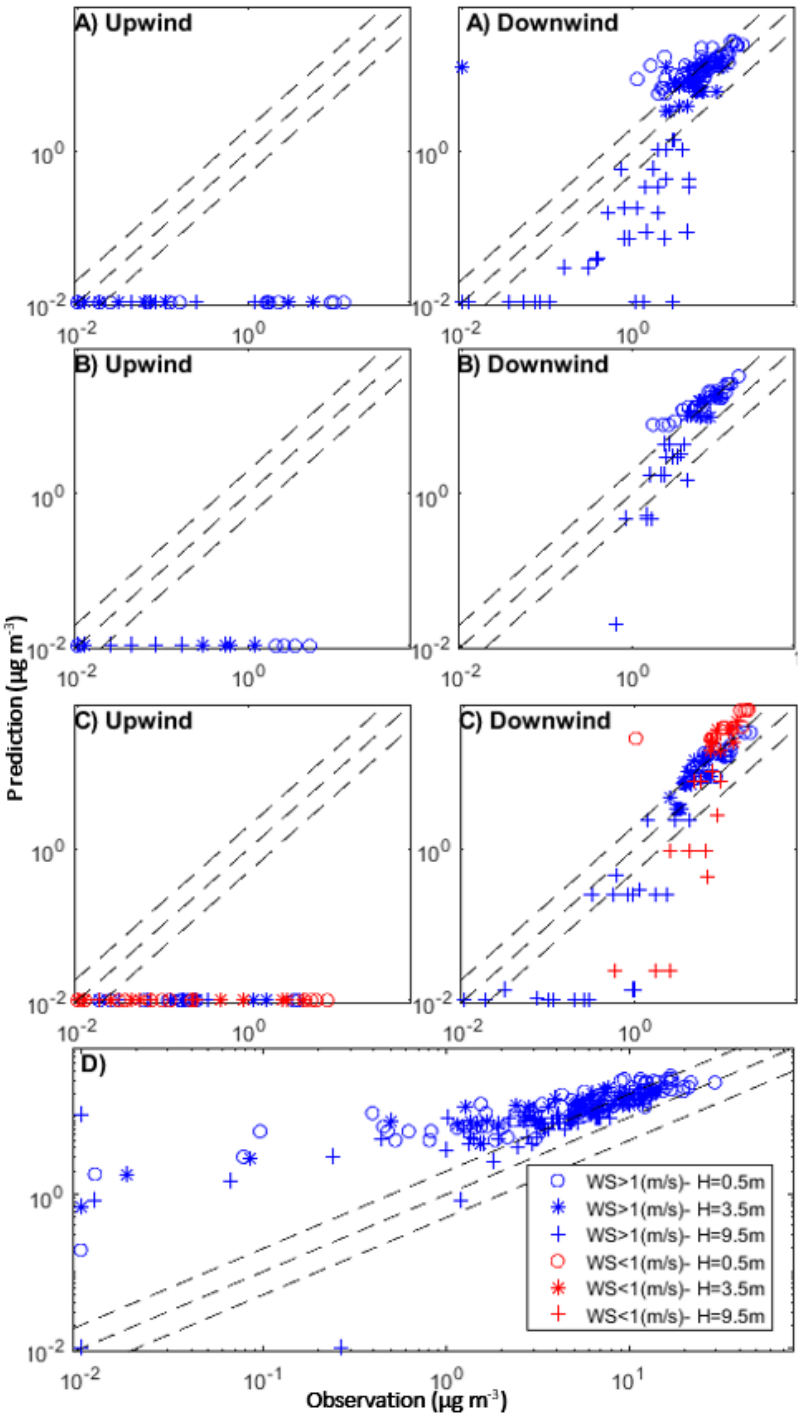

Figure 45- Predicted (using default area source option) and observed concentrations of SF6 (µg m^{-3}) for all experiments grouped by wind direction categories (A–D).

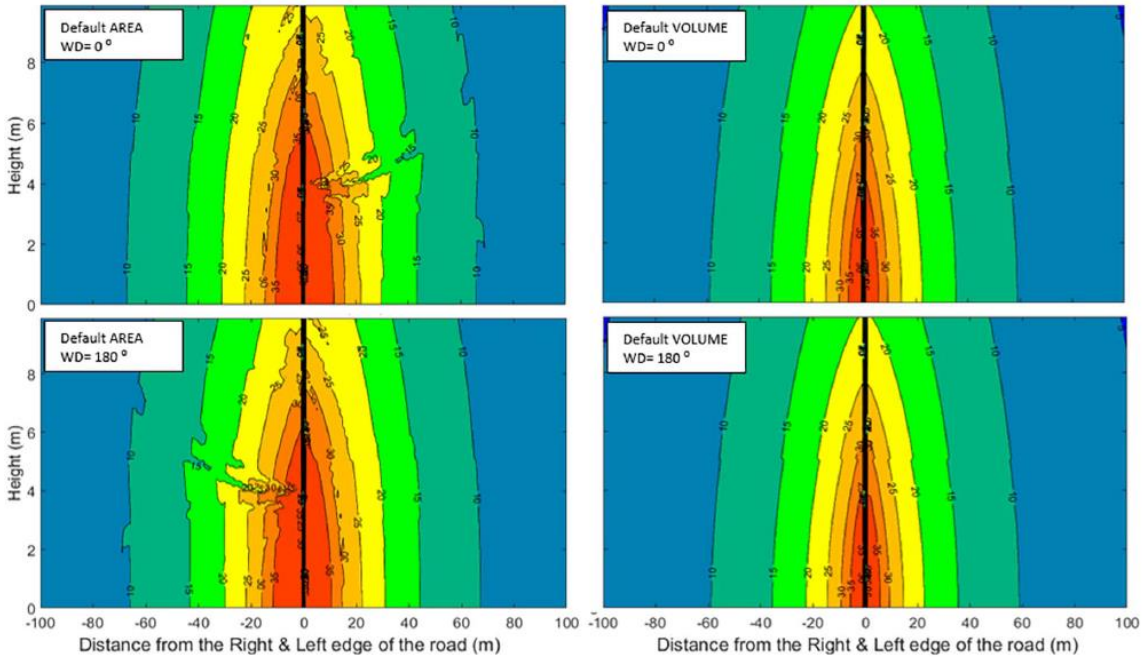

Figure 46- Comparison of predicted vertical cross section of the concentration fields with volume source (right column) and area source (left column) in AERMOD, for parallel wind cases.

5.1.4. Conclusion

The capability of the steady-state dispersion model AERMOD in predicting concentrations of non-reactive tracers near roadways at different evaluations above surface up to 9.5 m was evaluated using the SF6 data collected during the GM Sulfate Dispersion Experiments. In general, AERMOD with area or volume source representations of the emission sources can predict SF6 concentrations at both surface (0.5 m above ground) and higher elevations (3.5 and 9.5 m) at downwind locations. Representing vehicle emissions as volume sources leads to better predictions of the concentrations at both upwind and downwind locations than those with area source emissions. Based on Monte Carlo uncertainty analyses, using volume sources also yielded lower uncertainties in modeled concentrations due to wind speed and direction than those using area sources. A general

overestimation of low concentrations at upwind locations was observed using volume sources regardless of the low wind options tested in this study. However, the model performance under low wind conditions improved by enabling the low wind options in AERMOD. Using volume sources representation and LW-3 yields the best model performance statistically, and improve the general over-estimation problem with default options at upwind. While the volume sources show acceptable performance and stable modeling results within the exclusion zone at 0.5 m and 3.5 m, considerable variation was observed at 9.5 m height. Moreover, vertical concentration fields using area sources show abnormal bands of high concentrations at higher elevations, which might indicate potential problems in the model formulation.

5.1.5. Acknowledgement

The authors would like to thank Dr. Tony Held for providing the GM dataset and related documentation, as well as the original research team that conducted the General Motors Sulfur Dispersion Experiment. The authors would also like to thank Mrs. Yinqing Liu for her technical expertise in determining the modeling procedure, and Michigan Department of Transportation for providing guidance on selecting proper input parameters for AERMOD. The authors would also like to thank the two anonymous reviewers for their constructive comments that help improve the quality of the paper.

6. CONCLUSION

6.1. Summary

The overall objectives of this study are to investigate near-road traffic-related air pollution data and dispersion modeling. Section 2 focuses on near-road $PM_{2.5}$ increment using long-term monitoring data. Section 3 discusses regulatory and research applications of dispersion modeling for transportation air quality analysis. Section 4 explores the sensitivity of dispersion modeling to its three main input sets. Section 5 involves a holistic evaluation of dispersion modeling using a comprehensive tracer study dataset.

In Section 2, $PM_{2.5}$ data collected at a near-road monitoring station were compared with those of other NAAQS monitors during 2016 in Houston, Texas. The near-road $PM_{2.5}$ increment was determined based on EPA guidance for quantitative hot-spot analyses of PM to represent background concentration. The near-road $PM_{2.5}$ increment was statistically significant, even when the monitor was located upwind of the roadway. The traffic contribution to 24-hour $PM_{2.5}$ increment in the near-road environment was estimated to be about 27% of background concentration, which is close to estimates given by previous studies (22%) and is greater than a recent estimate based on a national-scale data analysis (15%), emphasizing the importance of background monitor selection criteria. A multiple linear regression model explains 85% of the variability of 24-hour $PM_{2.5}$ concentrations in the near-road environment and shows improvement in near-road concentration predictions when accounting for wind speed and wind direction.

Section 3 presents an investigation of the application of dispersion modeling for regulatory and research purposes. In the first step, a worst-case scenario (WCS) analysis

was performed for PM hot-spots specific to El Paso, Texas. The WCS analysis consisted of dispersion modeling with all possible combinations of worst-case input parameters that would maximize traffic-related air pollution at a minimum distance from roadways. WCS is based on the premise that if the design value obtained is less than the NAAQS, then one can logically conclude that the WCS does not cause violations of the NAAQS and no future analyses are needed for lesser cases, which was the case for El Paso. In the second step, traffic-related air pollution exposure was investigated using dispersion modeling at the individual level. As such, a methodology was developed for assessing traffic-related emissions exposure by integrating mobility patterns tracked by GPS devices with dynamics of pollutant concentration predicted by regulatory dispersion model. The obtained $PM_{2.5}$ exposure levels exhibit considerable variation between time periods within a day, with higher levels modeled during peak commuting periods and lower levels during midday periods. The results exhibit a significant variation of emissions exposure across time periods and spatial locations, which cannot be captured by simpler metrics such as traffic density and near-road distance. The study evaluated measures of static exposure based on residential location. Results show an increase of 7% in overall exposure levels from static to dynamic assessment.

Section 4 presents a three-step investigation of the sensitivity of traffic-related air pollution dispersion modeling to a variety of input sets. In the first step, the effect of meteorological variables was investigated using parameters like atmospheric stability in various time periods, land use, and modeling options on modeled concentrations. As such, traffic-related concentrations were modeled at different distances from the road with unit

emission rate for various scenarios. Results show that near-road traffic-related concentration decline with distance from the road depends on meteorological conditions and varies by season. Concentrations were measured higher in rural areas when compared to urban land-use conditions due to the retention of heat by urban materials that increase the vertical motion of air, leading to increased pollutant dispersion in urban conditions. Concentrations were predicted higher during nighttime compared to daytime (when emission levels from the source are held equal) because of the stable atmospheric conditions, lower mixing heights, and lower wind speeds, leading to higher concentrations of pollutants at the near-ground level during nighttime periods.

In the second step for Section 4, the sensitivity of traffic-related dispersion modeling to different emission rates was investigated. As such, the $PM_{2.5}$ emission rates from two major sources of exhaust (exhaust, brake, and tire-wear) and resuspended road dust were modeled based on EPA guidelines for two road types (highway and arterial), four time periods of the day (morning peak [6:00 to 9:00 a.m.], midday [9:00 a.m. to 4:00 p.m.], evening peak [4:00 to 7:00 p.m.], and overnight [8:00 p.m. to 6:00 a.m.]), and four seasons. In addition, the increase in traffic-related $PM_{2.5}$ emission and near-road concentrations due to inclusion of resuspended dust in estimations was evaluated and compared in different daily and seasonal time periods for a near-road environment in Tarrant County, Fort Worth, Texas. The estimated increase in traffic-related $PM_{2.5}$ emissions was not shown to be proportional to the increment of estimated near-road traffic-related $PM_{2.5}$ concentrations at the different time periods. Nonlinearity was evident between emission rates and concentrations due to the effect of meteorological variables

and geometry of the network with unevenly scattered traffic-related emission rates (due to different link traffic speeds). Results also show the increase in $PM_{2.5}$ emission rates due to resuspended dust inclusion to be considerably higher than the sum of exhaust, brake, and tire-wear emissions on arterials, as well as show the relative ratio to range between 139% and 208% (between 16% and 19% for highways). The comparison of emission rates shows the importance of the inclusion of resuspended $PM_{2.5}$, particularly when dealing with traffic-related $PM_{2.5}$ in a near-road environment surrounded by arterials.

In the third step shown in Section 4, the sensitivity of near-road traffic-related dispersion modeling to source- and dispersion-related parameters was investigated. Model predictions were obtained for dispersion parameters in different vertical and horizontal distances from the edge of the road and at different wind speeds. Statistical measures were used to perform a quantitative evaluation of the model's predictions using observations obtained from a tracer study and to assess potential improvement of the model's performance due to changes in the regulatory suggested parameters. Results show an increase in release height, initial vertical dispersion coefficient (σ_{zo}), and minimum standard deviation of horizontal concentration distribution ($\sigma_{v,min}$), decreases predicted concentrations at the near-ground level and increases at 9.5 m from ground level located at downwind. Obtained results also show how near-road dispersion modeling under low-speed winds is sensitive to dispersion parameters. Using alternative parameters yielded negligible improvement in quantitative performance measures in different classes of wind speed and wind direction, which may suggest that different input sets can be used to model dispersion under different wind cases.

In Section 5, a holistic evaluation of traffic-related dispersion modeling is presented with different heights from ground level for the first time using General Motors tracer study results. In general, AERMOD with area or volume source representations of the emission sources were shown to predict SF6 concentrations at both surface (0.5 m above ground) and higher elevations (3.5 and 9.5 m) at downwind locations. Representing vehicle emissions as a volume source was shown to lead to better predictions of the concentrations at both upwind and downwind locations than those with area source emissions. Based on Monte Carlo uncertainty analyses, using volume sources also yielded lower uncertainties in modeled concentrations due to wind speed and direction than those using area sources. A general overestimation of low concentrations at upwind locations was observed using volume sources regardless of the low-wind options tested in this study. However, the model performance under low-wind conditions was still improved by enabling the low-wind options in AERMOD. Using volume sources representation and LW-3 yields the best model performance statistically and improves the general overestimation problem with default options at the upwind location.

6.2. Recommendations for Future Research

Section 2 shows how the guideline for defining background air pollution concentration is determinant in traffic-related air pollution estimation. It also places emphasis on the effect of meteorological variables, including wind speed and wind direction, on near-road traffic-related air pollution. In this study, traffic contribution to near-road air pollution was estimated with the most recent near-road $PM_{2.5}$ data, which were available in 24-hour resolution. An identical study with hourly concentrations would

clarify the traffic contribution to and the meteorological variables' effect on near-road air quality.

Section 3 shows the application of traffic-related air pollution dispersion modeling from both regulatory and research points of view. This part of the study indicates that background concentrations are typically much larger than the modeled concentrations, thereby dominating the design value. Additional details in determining background concentrations and the way they are reflected in design value compared with NAAQS might be required for PM hot-spot analysis. From a research point of view, the study on pregnant women showcased a novel application of dispersion modeling for exposure assessment. However, the limited monitoring dataset did not provide a clear image of the effect of mobility on exposure of the target community to air pollution. Using a comprehensive mobility dataset, such as cell phone data in a metropolitan area, can help obtain a better understanding of the effect of mobility on exposure to air pollution from various emission sources including the transportation sector.

Section 4 focuses on the effect of different input sets on dispersion modeling results. Evaluation of the effect of meteorological variables and emission rates using constant and modeled emission rates shows their dramatic effect on near-road traffic-related air quality modeling. However, real-time traffic and site-specific meteorological-variable monitoring data with hourly resolution definitely can help decrease the uncertainty level in analysis. A new tracer study with real-time traffic count and mix also will help obtain a better understanding of the dispersion process, vehicular emission characteristics, and source-specific parametrization.

Section 5 illustrates a comprehensive evaluation of dispersion modeling using tracer study results. Although area and volume representations of vehicular emission sources are treated equally in regulatory guidelines, obtained results show significantly better performance of dispersion modeling using volume representation of emission sources. Hence, another evaluation of regulatory guidelines might be required from this point of view. Moreover, vertical concentration fields using area sources show abnormal bands of high concentrations at higher elevations, which might indicate potential problems in the model formulation.

REFERENCES

1. Sapkota, A., A.P. Chelikowsky, K.E. Nachman, A.J. Cohen, and B. Ritz, *Exposure to particulate matter and adverse birth outcomes: A comprehensive review and meta-analysis.* Air Quality, Atmosphere and Health, 2012. **5**(4): p. 369-381.
2. Khreis, H., C. Kelly, J. Tate, R. Parslow, K. Lucas, and M. Nieuwenhuijsen, *Exposure to traffic-related air pollution and risk of development of childhood asthma: A systematic review and meta-analysis.* 2017(1873-6750 (Electronic)).
3. Bell, M.L., K. Belanger, K. Ebisu, J.F. Gent, H.J. Lee, P. Koutrakis, and B.P. Leaderer, *Prenatal exposure to fine particulate matter and birth weight: variations by particulate constituents and sources.* Epidemiology, 2010. **21**(6): p. 884-91.
4. Qiao, J., W.H. Lu, J. Wang, X.J. Guo, and Q.M. Qu, *Vascular risk factors aggravate the progression of Alzheimer's disease: a 3-year follow-up study of Chinese population.* 2014(1938-2731 (Electronic)).
5. Foraster, M., X. Basagana, I. Aguilera, M. Rivera, D. Agis, L. Bouso, A. Deltell, J. Marrugat, R. Ramos, J. Sunyer, J. Vila, R. Elosua, and N. Kunzli, *Association of long-term exposure to traffic-related air pollution with blood pressure and hypertension in an adult population-based cohort in Spain (the REGICOR study).* Environ Health Perspect., 2014. **122**(4): p. 404-11.
6. Wellenius, G.A., M.A. Burger, B.A. Coull, J. Schwartz, H.H. Suh, P. Koutrakis, G. Schlaug, D.R. Gold, and M.A. Mittleman, *Ambient air pollution and the risk of acute ischemic stroke.* Arch Intern Med, 2012. **172**(3): p. 229-34.
7. Zamora, M.L., J.C. Pulczinski, N. Johnson, R. Garcia-Hernandez, A. Rule, G. Carrillo, J. Zietsman, B. Sandragorsian, S. Vallamsundar, M.H. Askariyeh, and K. Koehler, *Maternal exposure to PM2.5 in south Texas, a pilot study.* Science of The Total Environment, 2018. **628–629**: p. 1497-1507.
8. Kioumourtzoglou, M.-A., J.D. Schwartz, M.G. Weisskopf, S.J. Melly, Y. Wang, F. Dominici, and A. Zanobetti, *Long-term PM(2.5) Exposure and Neurological Hospital Admissions in the Northeastern United States.* Environmental Health Perspectives, 2016. **124**(1): p. 23-29.
9. Girguis, M.S., M.J. Strickland, X. Hu, Y. Liu, S.M. Bartell, and V.M. Vieira, *Maternal Exposure to Traffic-Related Air Pollution and Birth Defects in Massachusetts.* Environmental research, 2016. **146**: p. 1-9.
10. Weinstock, L., N. Watkins, R. Wayland, and R. Baldauf, *EPA's Emerging Near-Road Ambient Monitoring Network: A Progress Report.* EM Magazine. Air & Waste Management Association,, 2013.
11. Rowangould, G.M., *A census of the US near-roadway population: Public health and environmental justice considerations.* Transportation Research Part D: Transport and Environment, 2013. **25**: p. 59-67.
12. U.S. Department of Housing and Urban Development. *AHS 2013 National Summary Tables V1.2*. American Housing Survey (AHS) 2016; Accessed at:

https://www.census.gov/programs-surveys/ahs/data/2013/ahs-2013-summary-tables/national-summary-report-and-tables---ahs-2013.html.
13. Cadle, S.H., D.P. Chock, P.R. Monson, and J.M. Heuss, *General Motors Sulfate Dispersion Experiment: Experimental Procedures and Results.* Journal of the Air Pollution Control Association, 1977. **27**(1): p. 33-38.
14. Finn, D., K.L. Clawson, R.G. Carter, J.D. Rich, R.M. Eckman, S.G. Perry, V. Isakov, and D.K. Heist, *Tracer studies to characterize the effects of roadside noise barriers on near-road pollutant dispersion under varying atmospheric stability conditions☆.* Atmospheric Environment, 2010. **44**(2): p. 204-214.
15. Benson, P.E., *CALINE4 - A Dispersion Model For Predicting Air Pollutant Concentrations Near Roadways*. 1989. FHWA/CA/TL/-84/15. Accessed at: https://www.weblakes.com/products/calroads/resources/docs/CALINE4.pdf
16. Venkatram, A., M. Snyder, V. Isakov, and S. Kimbrough, *Impact of wind direction on near-road pollutant concentrations.* Atmospheric Environment, 2013. **80**: p. 248-258.
17. Baldauf, R., E. Thoma, M. Hays, R. Shores, J. Kinsey, B. Gullett, S. Kimbrough, V. Isakov, T. Long, R. Snow, A. Khlystov, J. Weinstein, F.-L. Chen, R. Seila, D. Olson, I. Gilmour, S.-H. Cho, N. Watkins, P. Rowley, and J. Bang, *Traffic and Meteorological Impacts on Near-Road Air Quality: Summary of Methods and Trends from the Raleigh Near-Road Study.* Journal of the Air & Waste Management Association, 2008. **58**(7): p. 865-878.
18. Zhu, Y., J. Pudota, D. Collins, D. Allen, A. Clements, A. DenBleyker, M. Fraser, Y. Jia, E. McDonald-Buller, and E. Michel, *Air pollutant concentrations near three Texas roadways, Part I: Ultrafine particles.* Atmospheric Environment, 2009. **43**(30): p. 4513-4522.
19. Patton, A.P., C. Milando, J.L. Durant, and P. Kumar, *Assessing the Suitability of Multiple Dispersion and Land Use Regression Models for Urban Traffic-Related Ultrafine Particles.* Environmental Science & Technology, 2017. **51**(1): p. 384-392.
20. Klompmaker, J.O., D.R. Montagne, K. Meliefste, G. Hoek, and B. Brunekreef, *Spatial variation of ultrafine particles and black carbon in two cities: Results from a short-term measurement campaign.* Science of The Total Environment, 2015. **508**: p. 266-275.
21. Kimbrough, S., R.W. Baldauf, G.S.W. Hagler, R.C. Shores, W. Mitchell, D.A. Whitaker, C.W. Croghan, and D.A. Vallero, *Long-term continuous measurement of near-road air pollution in Las Vegas: Seasonal variability in traffic emissions impact on local air quality.* Air Quality, Atmosphere and Health, 2013. **6**(1): p. 295-305.
22. Zhang, Z., A. Khlystov, L.K. Norford, Z. Tan, and R. Balasubramanian, *Characterization of traffic-related ambient fine particulate matter (PM2.5) in an Asian city: Environmental and health implications.* Atmospheric Environment, 2017. **161**: p. 132-143.

23. Ginzburg, H., X. Liu, M. Baker, R. Shreeve, R. Jayanty, D. Campbell, and B. Zielinska, *Monitoring study of the near-road PM2.5 concentrations in Maryland.* 2015(1096-2247 (Print)).
24. Askariyeh, M.H., S. Vallamsundar, and R. Farzaneh, *Investigating the Impact of Meteorological Conditions on Near-Road Pollutant Dispersion between Daytime and Nighttime Periods.* Transportation Research Record, 2018. **2672**(25): p. 99-110.
25. Steffens, J.T., D.K. Heist, S.G. Perry, V. Isakov, R.W. Baldauf, and K.M. Zhang, *Effects of roadway configurations on near-road air quality and the implications on roadway designs.* Atmospheric Environment, 2014. **94**: p. 74-85.
26. Heist, D., Isakov, V., Perry, S., Snyder, M., Venkatram, A., Hood, C., Stocker, J., Carruthers, D., Arunachalam, S., and Owen, R. C., *Estimating near-road pollutant dispersion: A model inter-comparison.* Transportation Research Part D-Transport and Environment, 2013. **25**: p. 93-105.
27. Isakov, V., S. Arunachalam, S. Batterman, S. Bereznicki, J. Burke, K. Dionisio, V. Garcia, D. Heist, S. Perry, M. Snyder, and A. Vette, *Air Quality Modeling in Support of the Near-Road Exposures and Effects of Urban Air Pollutants Study (NEXUS).* International Journal of Environmental Research and Public Health, 2014. **11**(9).
28. Askariyeh, M.H., S.H. Kota, S. Vallamsundar, J. Zietsman, and Q. Ying, *AERMOD for near-road pollutant dispersion: Evaluation of model performance with different emission source representations and low wind options.* Transportation Research Part D: Transport and Environment, 2017. **57**(Supplement C): p. 392-402.
29. Karner, A., D.S. Eisinger, and D.A. Niemeier, *Near-roadway air quality-Synthesizing the findings from real-world data.* Environ. Sci. & Technol., 2010. **44**(14): p. 5334-5344.
30. DeWinter, J.L., S.G. Brown, A.F. Seagram, K. Landsberg, and D.S. Eisinger, *A national-scale review of air pollutant concentrations measured in the U.S. near-road monitoring network during 2014 and 2015.* Atmospheric Environment, 2018. **183**: p. 94-105.
31. Guerreiro, C., S. Larssen, F. de Leeuw, and V. Foltescu, *Air Quality in Europe-2011 Report*. 2011, Denmark, Copenhagen: Technical Report by the European Environment Agency.
32. Keuken, M.P., M. Moerman, M. Voogt, M. Blom, E.P. Weijers, T. Röckmann, and U. Dusek, *Source contributions to PM2.5 and PM10 at an urban background and a street location.* Atmospheric Environment, 2013. **71**: p. 26-35.
33. U.S. EPA, *National Ambient Air Quality Standards for particulate matter; Final Rule. 40 CFR parts 50, 51, 52, 53 and 58*. 2013. p. 3086–3287. EPA-HQ-OAR-2007-0492. Accessed at: https://www.federalregister.gov/documents/2013/01/15/2012-30946/national-ambient-air-quality-standards-for-particulate-matter

34. He, M. and S. Dhaniyala, *A dispersion model for traffic produced turbulence in a two-way traffic scenario.* Environmental Fluid Mechanics, 2011. **11**(6): p. 627-640.
35. Held, T., D.P.Y. Chang, and D.A. Niemeier, *UCD 2001: An improved model to simulate pollutant dispersion from roadways.* Atmospheric Environment, 2003. **37**(38): p. 5325-5336.
36. Benson, P.E., *CALINE 4: A Dispersion Model for Predicting Air Pollutant Concentration Near Roadways*. 1979, California Department of Transportation, Division of New Technology and Research: Sacramento, CA. Accessed at:
37. Claggett, M., *Improvements to CAL3QHCR Model*, in *The 93rd Transportation Research Boad Annual Meeting*. 2014: Washington, D.C.
38. Kota, S., Q. Ying, and Y. Zhang, *TAMNROM-3D. Three-Dimensional Eulerian Model to Simulate Air Quality near Highways.* Transportation Research Record: Journal of the Transportation Research Board, 2010. **2158**(x): p. 61-68.
39. U.S. EPA, *User's Guide for the AMS/EPA Regulatory Model-AERMOD*. 2004. EPA-454/B-03-003. Accessed at: https://www.michigan.gov/documents/deq/deq-aqd-aqe_aermapug_257866_7.pdf
40. U.S. EPA, *User's Guide for the AMS/EPA Regulatory Model (AERMOD)*. 2016, Office of Air Quality Planning and Standards: Research Triangle Park, NC. EPA-454/B-16-011. Accessed at: https://nepis.epa.gov/Exe/ZyPDF.cgi/P100QVCE.PDF?Dockey=P100QVCE.PDF
41. U.S. EPA, *User's Guide for the AMS/EPA Regulatory Model (AERMOD)*. 2018, Office of Air Quality Planning and Standards: Research Triangle Park, NC. EPA-454/B-18-001. Accessed at: https://www3.epa.gov/ttn/scram/models/aermod/aermod_userguide.pdf
42. Benson, P.E., *CALINE3 – A Versatile Dispersion Model for Predicting Air Pollutant Levels Near Highways and Arterial Streets*. 1979, California Department of Transportation. Accessed at:
43. Carruthers, D.J., R.J. Holroyd, J.C.R. Hunt, W.S. Weng, A.G. Robins, D.D. Apsley, D.J. Thompson, and F.B. Smith, *UK-ADMS: A new approach to modelling dispersion in the earth's atmospheric boundary layer.* Journal of Wind Engineering and Industrial Aerodynamics, 1994. **52**: p. 139-153.
44. CERS, *ADMS 5 User Guide Atmospheric Dispersion Modeling System*. 2015. Accessed at: http://www.cerc.co.uk/environmental-software/assets/data/doc_userguides/CERC_ADMS_5_1_User_Guide.pdf
45. Snyder, M.G. and D.K. Heist, *User's Guide for R-LINE Model Version 1.2 A Research LINE source model for near-surface releases*. 2013. p. 1-33. Accessed at: https://www.cmascenter.org/r-line/documentation/1.2/RLINE_UserGuide_11-13-2013.pdf
46. U.S. EPA, *Revisions to the Guidelines on Air Quality Models*. 2015. p. 1-49. 9781136696862. Accessed at: https://www3.epa.gov/ttn/scram/11thmodconf/EPA-HQ-OAR-2015-0310-0001.pdf

47. Chen, H., Bai, S., Eisinger, D., Niemeier, D., Claggett, M. *Predicting Near-Road PM2.5 Concentrations: Comparative Assessment of CALINE4, CAL3QHC, and AERMOD*. in *Transportation Research Board*. 2009. Washington, D.C.
48. Claggett, M. and S. Bai, *Comparing predictions from the CAL3QHCR AERMOD models for highway applications*, in *Transportation-Related Environmental Analysis, Ecology, and Air Quality Summer Conference*. 2012: Little Rock, Arkansas.
49. Claggett, M., *Comparing Predictions from the CAL3QHCR and AERMOD Models for Highway Applications.* Transportation Research Record: Journal of the Transportation Research Board, 2014. **2428**(2): p. 18-26.
50. Schewe, G., *Using AERMOD in PM2.5 and PM10 Conformity Hot-Spot Analysis*, in *Transportation Planning, Land Use, and Air Quality*. 2011: San Antonio, Texas.
51. Qian, W. and A. Venkatram, *Performance of Steady-State Dispersion Models Under Low Wind-Speed Conditions.* Boundary-Layer Meteorology, 2011. **138**(3): p. 475-491.
52. Hanna, S.R. and B. Chowdhury, *Minimum turbulence assumptions and u* and L estimation for dispersion models during low-wind stable conditions.* Journal of the Air & Waste Management Association, 2014. **64**(3): p. 309-321.
53. Stull, R.B., *An introduction to boundary layer meteorology*. Atmospheric and Oceanographic Sciences Library. 1988: Springer Netherlands.
54. Berkowicz, R., M. Ketzel, G. Vachon, P. Louka, J.M. Rosant, P.G. Mestayer, and J.F. Sini, *Examination of Traffic Pollution Distribution in a Street Canyon Using the Nantes'99 Experimental Data and Comparison with Model Results.* Water, Air and Soil Pollution: Focus, 2002. **2**(5): p. 311-324.
55. Di Sabatino, S., P. Kastner-Klein, R. Berkowicz, R.E. Britter, and E. Fedorovich, *The Modelling of Turbulence from Traffic in Urban Dispersion Models — Part I: Theoretical Considerations.* Environmental Fluid Mechanics, 2003. **3**(2): p. 129-143.
56. Kastner-Klein, P., E. Fedorovich, M. Ketzel, R. Berkowicz, and R. Britter, *The Modelling of Turbulence from Traffic in Urban Dispersion Models — Part II: Evaluation Against Laboratory and Full-Scale Concentration Measurements in Street Canyons.* Environmental Fluid Mechanics, 2003. **3**(2): p. 145-172.
57. Britter, R.E., *Flow and Dispersion in Urban Areas* Annu. Rev. Fluid Mech, 2003. **35**: p. 469–96.
58. Mazzeo, N. and L. Venegas, *Evaluation of turbulence from traffic using experimental data obtained in a street canyon.* Int J Environ Pollut, 2005. **25**: p. 164–176.
59. Solazzo, E., S. Vardoulakis, and X. Cai, *Evaluation of traffic-producing turbulence schemes within Operational Street Pollution Models using roadside measurements.* Atmospheric Environment, 2007. **41**(26): p. 5357-5370.
60. Vachon, G., P. Louka, J.M. Rosant, P.G. Mestayer, and J.F. Sini, *Measurements of Traffic-Induced Turbulence within a Street Canyon during the Nantes'99 Experiment.* Water, Air and Soil Pollution: Focus, 2002. **2**(5): p. 127-140.

61. Vardoulakis, S., B.E.A. Fisher, K. Pericleous, and N. Gonzalez-Flesca, *Modelling air quality in street canyons: a review.* Atmospheric Environment, 2003. **37**(2): p. 155-182.
62. U.S. EPA, *AERMOD Model Formulation and Evaluation*. 2016: Research Triangle Park, North Carolina. Accessed at: https://www3.epa.gov/ttn/scram/models/aermod/aermod_mfed.pdf
63. U.S. EPA, *Integrated Science Assessment for Particulate Matter: Final Report*. 2009, National Center for Environmental Assessment, Office of Research and Development: Research Triangle Park, NC. EPA/600/R–08/139F. Accessed at: http://www.epa.gov/ttn/naaqs/standards/pm/s_pm_2007_isa.html.
64. U.S. EPA, *Near-road NO2 Monitoring Technical Assistance Document*. 2012, Office of Air Quality Planning and Standards: Research Triangle Park, NC. EPA-454/B-12-002. Accessed at: https://www3.epa.gov/ttnamti1/files/nearroad/NearRoadTAD.pdf
65. Askariyeh, M., S. Vallamsundar, J. Zietsman, and T. Ramani, *Assessment of Traffic-Related Air Pollution: Case Study of Pregnant Women in South Texas.* International Journal of Environmental Research and Public Health, 2019. **16**(13).
66. Sofowote, U.M., R.M. Healy, Y. Su, J. Debosz, M. Noble, A. Munoz, C.H. Jeong, J.M. Wang, N. Hilker, G.J. Evans, and P.K. Hopke, *Understanding the PM2.5 imbalance between a far and near-road location: Results of high temporal frequency source apportionment and parameterization of black carbon.* Atmospheric Environment, 2018. **173**: p. 277-288.
67. U.S. EPA, *Transportation Conformity Guidance for Quantitative Hot-Spot Analyses in PM2.5 and PM10 Nonattainment and Maintenance Areas*. 2015, Office of Transportation and Air Quality. EPA-420-B-15-084. Accessed at: https://www3.epa.gov/ttn/naaqs/aqmguide/collection/cp2/20101201_otaq_epa-420_b-10-040_transport_conform_hot-spot_analysis_appx.pdf
68. TCEQ. *Air Quality Data: Yearly Summary Report*. 2016; Accessed at: https://www.tceq.texas.gov/cgi-bin/compliance/monops/yearly_summary.pl.
69. Quintana, P., B. Samimi, M. Kleinman, L. Liu, K. Soto, G. Warner, C. Bufalino, J. Valencia, D. Francis, M. Hovell, and R. Delfino, *Evaluation of a real-time passive personal particle monitor in fixed site residential indoor and ambient measurements.* Journal of Exposure Science & Environmental Epidemiology, 2000(1053-4245 (Print)).
70. Ramachandran, G., J. Adgate, N. Hill, K. Sexton, G. Pratt, and D. Bock, *Comparison of short-term variations (15-minute averages) in outdoor and indoor PM2.5 concentrations.* Journal of the Air & Waste Management Association, 2011(1096-2247 (Print)).
71. Schweizer, D., R. Cisneros, and G. Shaw, *A comparative analysis of temporary and permanent beta attenuation monitors: The importance of understanding data and equipment limitations when creating PM2.5 air quality health advisories.* Atmospheric Pollution Research, 2016. **7**(5): p. 865-875.

72. Shin, S.E., C.H. Jung, and Y.P. Kim, *Analysis of the Measurement Difference for the PM10 Concentrations between Beta-ray Absorption and Gravimetric Methods at Gosan* Aerosol and Air Quality Research, 2011. **11**: p. 846–853.
73. Zhu, Y., T.J. Smith, M.E. Davis, J.I. Levy, R. Herrick, and H. Jiang, *Comparing Gravimetric and Real-Time Sampling of PM(2.5) Concentrations Inside Truck Cabins.* Journal of Occupational and Environmental Hygiene, 2011. **8**(11): p. 662-672.
74. U.S. EPA, *3-Year Quality Assurance Report for Calendar Years 2011, 2012, and 2013 PM2.5 Ambient Air Monitoring Program*. 2015, Office of Air Quality Planning and Standards: RTP, NC. Accessed at: https://www3.epa.gov/ttnamti1/files/ambient/pm25/qa/20112013pm25qareport.pdf
75. Brown, G.S., B. Penfold, A. Mukherjee, K. Landsberg, and S.D. Eisinger, *Conditions Leading to Elevated PM2.5 at Near-Road Monitoring Sites: Case Studies in Denver and Indianapolis.* International Journal of Environmental Research and Public Health, 2019. **16**(9).
76. Houston-Galveston Area Council, *Houston-Galveston-Brazoria (HGB) PM2.5 Advance Path Forward Update*. 2015. Accessed at: https://www.epa.gov/sites/production/files/2016-02/documents/houstonupdate2015.pdf
77. SAS Institute Inc. *JMP Statistical Software*. JMP Statistical Discovery 2017; Accessed at: www.jmp.com/.
78. Shapiro, S.S. and M.B. Wilk, *An Analysis of Variance Test for Normality (Complete Samples).* Biometrika, 1965. **52**(3/4): p. 591-611.
79. Chakravarti, I., R. Laha, and J. Roy, *Handbook of Methods of Applied Statistics. Volume I: Techniques of Computation Descriptive Methods, and Statistical Inference.* 1967: John Wiley and Sons.
80. Kitchen, C.M.R., *Nonparametric vs parametric tests of location in biomedical research.* American journal of ophthalmology, 2009. **147**(4): p. 571-572.
81. Venkatram, A., V. Isakov, E. Thoma, and R. Baldauf, *Analysis of air quality data near roadways using a dispersion model.* Atmospheric Environment, 2007. **41**(40): p. 9481-9497.
82. Almeida, S.M., C.A. Pio, M.C. Freitas, M.A. Reis, and M.A. Trancoso, *Source apportionment of fine and coarse particulate matter in a sub-urban area at the Western European Coast.* Atmospheric Environment, 2005. **39**(17): p. 3127-3138.
83. U.S. EPA/SAFETEA-LU, *LIMITATIONS ON CERTAIN FEDERAL ASSISTANCE*, in *United States Code*. 2003. 42USC7506. Accessed at: https://www.gpo.gov/fdsys/pkg/USCODE-2015-title42/pdf/USCODE-2015-title42-chap85-subchapI-partD-subpart1-sec7506.pdf
84. Code of Federal Register, *Title 40CFR Part 93.101*. 1996. Accessed at: https://www.gpo.gov/fdsys/pkg/CFR-1996-title40-vol9/pdf/CFR-1996-title40-vol9-sec93-101.pdf

85. Noel, G.J. and R. Wayson, *MOVES2010a Regional Level Sensitivity Analysis*. 2012, Volpe National Transportation Systems Center. DOT-VNTSC-FHWA-12-05. Accessed at: https://ntl.bts.gov/lib/46000/46500/46598/DOT-VNTSC-FHWA-12-05.pdf
86. Choi, D., M. Beardsley, D. Brzezinski, J. Koupal, and J. Warila. *MOVES Sensitivity Analysis: The Impacts of Temperature and Humidity on Emissions* 2011; Accessed at: https://www3.epa.gov/ttnchie1/conference/ei19/session6/choi.pdf.
87. Eastern Research Group, *Study of MOVES Inputs for the National Emissions Inventory*. 2014, Prepared for Coordinating Research Council Project A-84. Accessed at:
88. NCHRP, *Input Guidelines for Motor Vehicle Emissions Simulator Model-Volume 1-3: Practitioners Handbook: Project Level Inputs*. 2014: Transportation Research Board of the National Academies. Accessed at: http://www.trb.org/Main/Blurbs/172040.aspx
89. U.S. EPA, *Transportation Conformity Guidance for Quantitative Hot-Spot Analyses in PM2.5 and PM10 Nonattainment and Maintenance Areas*. 2010, Office of Transportation and Air Quality. EPA-420-B-10-040. Accessed at: https://www3.epa.gov/ttn/naaqs/aqmguide/collection/cp2/20101201_otaq_epa-420_b-10-040_transport_conform_hot-spot_analysis_appx.pdf
90. Glaze, M. and R. Wayson, *MOVES Sensitivity Analysis Update*. 2012, Transportation Research Board Summer Meeting: Little Rock, AR. Accessed at:
91. INRIX. *INRIX*. 2017; Accessed at: http://inrix.com/.
92. Texas Department of Transportation (TxDOT). *I-10 Connect Project*. El Paso District 2017; Accessed at: http://www.txdot.gov/inside-txdot/projects/studies/el-paso/i10-connect.html.
93. TCEQ, *Air Dispersion Modeling Team Initiative to Update Meteorological Data*. 2013. Accessed at: https://www.tceq.texas.gov/assets/public/permitting/air/Modeling/aermod/BackgroundInformation/aermet.pdf
94. HEI, *Traffic-Related Air Pollution: A Critical Review of the Literature on Emissions, Exposure, and Health Effects*, in *Special Report 17*. 2010, Health Effects Institute Panel on the Health Effects of Traffic-Related Air Pollution: Boston, MA. Accessed at: https://www.healtheffects.org/publication/traffic-related-air-pollution-critical-review-literature-emissions-exposure-and-health
95. Harrison, R.M., R. Tilling, M.S.C. Romero, S. Harrad, and K. Jarvis, *A study of trace metals and polycyclic aromatic hydrocarbons in the roadside environment.* Atmos. Environ., 2003. **37**: p. 2391-2391.
96. Reponen, T., S.A. Grinshpun, S. Trakumas, D. Martuzevicius, Z.M. Wang, G. LeMasters, J.E. Lockey, and P. Biswas, *Concentration gradient patterns of aerosol particles near Interstate highways in the Greater Cincinnati airshed.* J. Environ. Monit., 2003. **5**: p. 557-557.
97. Pirjola, L., P. Paasonen, D. Pfeiffer, T. Hussein, K. Hämeri, T. Koskentalo, A. Virtanen, T. Rönkkö, J. Keskinen, T.A. Pakkanen, and R.E. Hillamo, *Dispersion*

of particles and trace gases nearby a city highway: Mobile laboratory measurements in Finland. Atmospheric Environment, 2006. **40**(5): p. 867-879.
98. Peters, A., S. von Klot, M. Heier, I. Trentinaglia, A. Hormann, H.E. Wichmann, and H. Lowel, *Exposure to traffic and the onset of myocardial infarction.* New Engl. J. Med., 2004. **351**: p. 1861-1861.
99. Riediker, M., R. Williams, R. Devlin, T. Griggs, and P. Bromberg, *Exposure to particulate matter, volatile organic compounds, and other air pollutants inside patrol cars.* Environ Sci Technol, 2003. **37**(0013-936X (Print)): p. 2084-93.
100. Schwartz, J., A. Litonjua, H. Suh, M. Verrier, A. Zanobetti, M. Syring, B. Nearing, R. Verrier, P. Stone, G. MacCallum, F.E. Speizer, and D.R. Gold, *Traffic related pollution and heart rate variability in a panel of elderly subjects.* Thorax, 2005. **60**(6): p. 455.
101. Mukherjee, A. and M. Agrawal, *World air particulate matter: sources, distribution and health effects.* Environmental Chemistry Letters, 2017. **15**(2): p. 283-309.
102. Zhang, L., X. Chen, X. Xue, M. Sun, B. Han, C. Li, J. Ma, H. Yu, Z. Sun, L. Zhao, B. Zhao, Y. Liu, J. Chen, P. Wang, Z. Bai, and N. Tang, *Long-term exposure to high particulate matter pollution and cardiovascular mortality: A 12-year cohort study in four cities in northern China.* Environment International, 2014. **62**: p. 41-47.
103. Diaz-Robles, L., J. Fu, and G. Reed, *Emission Scenarios and the Health Risks Posed by Priority Mobile Air Toxics in an Urban to Regional Area: An Application in Nashville, Tennessee* Aerosol and Air Quality Research, 2013. **13** (3): p. 795-803.
104. van den Hooven, E.H., F. Pierik, Y. de Kluizenaar, S.P. Willemsen, Hofman A, v.R. Sw, Z. Py, M. Jp, S. E, H. Miedema, and V.W. Jaddoe, *Air pollution exposure during pregnancy, ultrasound measures of fetal growth, and adverse birth outcomes: a prospective cohort study.* Environ. Health Perspect., 2012(1552-9924 (Electronic)).
105. Aguilera, I., R. Garcia-Esteban, C. Iniguez, M.J. Nieuwenhuijsen, A. Rodriguez, M. Paez, F. Ballester, and J. Sunyer, *Prenatal exposure to traffic-related air pollution and ultrasound measures of fetal growth in the INMA Sabadell cohort.* Environmental health perspectives, 2010. **118**(5): p. 705-711.
106. Slama, R., V. Morgenstern, J. Cyrys, A. Zutavern, O. Herbarth, H.-E. Wichmann, and J. Heinrich, *Traffic-related atmospheric pollutants levels during pregnancy and offspring's term birth weight: a study relying on a land-use regression exposure model.* Environmental health perspectives, 2007. **115**(9): p. 1283-1292.
107. Kaur, S., M.J. Nieuwenhuijsen, and R.N. Colvile, *Fine particulate matter and carbon monoxide exposure concentrations in urban street transport microenvironments.* Atmospheric Environment, 2007. **41**(23): p. 4781-4810.
108. Sarnat, S.E., M. Klein, J.A. Sarnat, W.D. Flanders, L.A. Waller, J.A. Mulholland, A.G. Russell, and P.E. Tolbert, *An examination of exposure measurement error from air pollutant spatial variability in time-series studies.* Journal of exposure science & environmental epidemiology, 2010. **20**(2): p. 135-146.

109. Wang, S., J. Hao, M.S. Ho, J. Li, and Y. Lu, *Intake fractions of industrial air pollutants in China: estimation and application.* The Science of the total environment, 2006. **354**(2-3): p. 127-141.
110. Zhou, Y., J.I. Levy, J.S. Evans, and J.K. Hammitt, *The influence of geographic location on population exposure to emissions from power plants throughout China.* Environment International, 2006. **32**(3): p. 365-373.
111. Shah, P.S. and T. Balkhair, *Air pollution and birth outcomes: a systematic review.* Environment international, 2011. **37**(2): p. 498-516.
112. Dons, E., C. Beckx, T. Arentze, G. Wets, and L. Panis, *Using an Activity-Based Framework to Determine Effects of a Policy Measure on Population Exposure to Nitrogen Dioxide.* Transportation Research Record: Journal of the Transportation Research Board, 2011. **2233**: p. 72-79.
113. Hatzopoulou, M., J.Y. Hao, and E.J. Miller, *Simulating the impacts of household travel on greenhouse gas emissions, urban air quality, and population exposure.* Transportation, 2011. **38**(6): p. 871-887.
114. Lefebvre, W., B. Degrawe, C. Beckx, M. Vanhulsel, B. Kochan, T. Bellemans, D. Janssens, G. Wets, S. Janssen, I. de Vlieger, L.I. Panis, and S. Dhondt, *Presentation and evaluation of an integrated model chain to respond to traffic- and health-related policy questions.* Environmental Modelling & Software, 2013. **40**: p. 160-170.
115. Jedrychowski, W.A., F.P. Perera, A. Pac, R. Jacek, R.M. Whyatt, J.D. Spengler, T.S. Dumyahn, and E. Sochacka-Tatara, *Variability of total exposure to PM2.5 related to indoor and outdoor pollution sources Krakow study in pregnant women.* The Science of the total environment, 2006. **366**(1): p. 47-54.
116. Nethery, E., M. Brauer, and P. Janssen, *Time-activity patterns of pregnant women and changes during the course of pregnancy.* Journal of exposure science & environmental epidemiology, 2009. **19**(3): p. 317-324.
117. Valero, N., I. Aguilera, S. Llop, A. Esplugues, A. de Nazelle, F. Ballester, and J. Sunyer, *Concentrations and determinants of outdoor, indoor and personal nitrogen dioxide in pregnant women from two Spanish birth cohorts.* Environment international, 2009. **35**(8): p. 1196-1201.
118. Choi, H., F. Perera, A. Pac, L. Wang, E. Flak, E. Mroz, R. Jacek, T. Chai-Onn, W. Jedrychowski, E. Masters, D. Camann, and J. Spengler, *Estimating individual-level exposure to airborne polycyclic aromatic hydrocarbons throughout the gestational period based on personal, indoor, and outdoor monitoring.* Environmental health perspectives, 2008. **116**(11): p. 1509-1518.
119. Klepeis, N.E., W.C. Nelson, W.R. Ott, J.P. Robinson, A.M. Tsang, P. Switzer, J.V. Behar, S.C. Hern, and W.H. Engelmann, *The National Human Activity Pattern Survey (NHAPS): a resource for assessing exposure to environmental pollutants.* Journal of exposure analysis and environmental epidemiology, 2001. **11**(3): p. 231-252.
120. Wu, J., C. Jiang, G. Jaimes, S. Bartell, A. Dang, D. Baker, and R.J. Delfino, *Travel patterns during pregnancy: comparison between Global Positioning*

System (GPS) tracking and questionnaire data. Environmental health : a global access science source, 2013. **12**(1): p. 86-86.
121. Turner, D.B., *Workbook of Atmospheric Dispersion Estimates: An Introduction to Dispersion Modeling*. 2nd Edition ed. 1994, Boca Raton: Lewis Publishers.
122. U.S. Geological Survey (USGS). *Land Use Database*. 2017; Accessed at: https://landcover.usgs.gov/.
123. Daakir, M., M. Pierrot-Deseilligny, P. Bosser, F. Pichard, C. Thom, Y. Rabot, and O. Martin, *Lightweight UAV with on-board photogrammetry and single-frequency GPS positioning for metrology applications.* ISPRS Journal of Photogrammetry and Remote Sensing, 2017. **127**: p. 115-126.
124. Duan, N., *Models for human exposure to air pollution.* Environ Int, 1982. **8**: p. 305-309.
125. Ott, W.R., *Concepts of human exposure to air pollution.* Environ Int, 1982. **7**: p. 179-196.
126. Klepeis, N., *Modeling human exposure to air pollution*, in *HumanExposure Analysis*, W. Ott, L. Wallace, and A. Steinemann, Editors. 2006, CRC Press: BocaRaton. p. 1-18.
127. Marshall, J.D., W.J. Riley, T.E. McKone, and W.W. Nazaroff, *Intake fraction of primary pollutants: motor vehicle emissions in the South Coast Air Basin.* Atmospheric Environment, 2003. **37**(24): p. 3455-3468.
128. Vallamsundar, S., J. Lin, K. Konduri, X. Zhou, and R.M. Pendyala, *A comprehensive modeling framework for transportation-induced population exposure assessment.* Transportation Research Part D: Transport and Environment, 2016. **46**: p. 94-113.
129. Bloch, M., J. DeParle, M. Ericson, and R. Gebeloff, *Food Stamp Usage Across the Country*, in *The New York Times*. 2009.
130. TCEQ, *2014 On-Road Mobile Source Annual, Summer Weekday and Winter Workday Emissions Inventories*. 2015. Accessed at:
131. Cimorelli, A.J., S.G. Perry, A. Venkatram, J.C. Weil, R.J. Paine, R.B. Wilson, R.F. Lee, W.D. Peters, and R.W. Brode, *AERMOD: A Dispersion Model for Industrial Source Applications. Part I: General Model Formulation and Boundary Layer Characterization.* Journal of Applied Meteorology, 2005. **44**(5): p. 682-693.
132. Zhu, Y., W.C. Hinds, S. Kim, and C. Sioutas, *Concentration and size distribution of ultrafine particles near a major highway.* J. Air Waste Manage. Assoc., 2002. **52**: p. 1032-1032.
133. Hitchins, J., L. Morawska, R. Wolff, and D. Gilbert, *Concentrations of submicrometre particles from vehicle emissions near a major road.* Atmospheric environment, 2000. **34**(1): p. 51-59.
134. Shepard, F.D. and B.H. Cottrell Jr, *Benefits and safety impact of night work-zone activities*. 1986.
135. Sullivan, E.C., *Accident rates during nighttime construction*. 1989. Accessed at:
136. Hall, J.W. and V.M. Lorenz, *Characteristics of construction-zone accidents.* Transportation Research Record, 1989(1230).

137. Colbert, D., *Productivity and safety implications of night-time construction operations.* Independent Research Study Rep, 2003.
138. Zhu, Y., T. Kuhn, P. Mayo, and W. Hinds, *Comparison of Daytime and Nighttime Concentration Profiles and Size Distributions of Ultrafine Particles near a Major Highway.* Environmental Science & Technology, 2006. **40**(8): p. 2531-2536.
139. Li, L., J. Qian, C.-Q. Ou, Y.-X. Zhou, C. Guo, and Y. Guo, *Spatial and temporal analysis of Air Pollution Index and its timescale-dependent relationship with meteorological factors in Guangzhou, China, 2001–2011.* Environmental Pollution, 2014. **190**: p. 75-81.
140. Zhao, S., Y. Yu, D. Yin, J. He, N. Liu, J. Qu, and J. Xiao, *Annual and diurnal variations of gaseous and particulate pollutants in 31 provincial capital cities based on in situ air quality monitoring data from China National Environmental Monitoring Center.* Environment International, 2016. **86**: p. 92-106.
141. Baldauf, R., E. Thoma, M. Hays, R. Shores, J. Kinsey, B. Gullett, S. Kimbrough, V. Isakov, T. Long, R. Snow, A. Khlystov, J. Weinstein, F.-L. Chen, R. Seila, D. Olson, I. Gilmour, S.-H. Cho, N. Watkins, P. Rowley, and J. Bang, *Traffic and meteorological impacts on near-road air quality: summary of methods and trends from the Raleigh Near-Road Study.* J. Air & Waste Manage. Assoc, 2008. **58**(865– 878).
142. TxDOT, *Standard Specifications for Construction and Maintenance of Highways, Streets, and Bridges*. 2014. Accessed at: ftp://ftp.dot.state.tx.us/pub/txdot-info/des/spec-book-1114.pdf
143. U.S. EPA. *Heat Island Effect*. 2016; Accessed at: https://www.epa.gov/heat-islands.
144. U.S. EPA. *Regional, State and Local Modelers Workshop*. 2007. Virginia Beach, VA.
145. U.S. EPA, *Addendum user's guide for the AMS/EPA regulatory model - AERMOD*. 2015. p. 1-189. 978-1-249-25120-0. Accessed at: https://www3.epa.gov/ttn/scram/dispersion_prefrec.htm#aermod
146. Lawson, S.J., I.E. Galbally, J.C. Powell, M.D. Keywood, S.B. Molloy, M. Cheng, and P.W. Selleck, *The effect of proximity to major roads on indoor air quality in typical Australian dwellings.* Atmospheric Environment, 2011. **45**(13): p. 2252-2259.
147. Barros, N., T. Fontes, M.P. Silva, and M.C. Manso, *How wide should be the adjacent area to an urban motorway to prevent potential health impacts from traffic emissions?* Transportation Research Part A: Policy and Practice, 2013. **50**: p. 113-128.
148. Cohen, J., R. Cook, C.R. Bailey, and E. Carr, *Relationship between motor vehicle emissions of hazardous pollutants, roadway proximity, and ambient concentrations in Portland, Oregon.* Environmental Modelling & Software, 2005. **20**(1): p. 7-12.

149. Janssen, N., P. van Vliet, F. Aarts, H. Harssema, and B. Brunekreef, *Assessment of exposure to traffic related air pollution of children attending schools near motorways.* Atmospheric Environment, 2001. **35**(22): p. 3875-3884.
150. Federal Register, *Appendix W to Part 51—Guideline on Air Quality Models*. 2005. p. 68229–68261. Accessed at: http://www.epa.gov/scram001/guidance/guide/appw_05.pdf
151. Golder, D., *Relations among stability parameters in the surface layer.* Boundary-Layer Meteorology, 1972. **3**(1): p. 47-58.
152. Seinfeld, J.H. and S.N. Pandis, *Atmospheric chemistry and physics : from air pollution to climate change*. 2nd ed. ed. 2006, Hoboken, N.J. :: J. Wiley.
153. Hu, S., S. Fruin, K. Kozawa, S. Mara, S.E. Paulson, and A.M. Winer, *A wide area of air pollutant impact downwind of a freeway during pre-sunrise hours.* Atmos. Environ., 2009. **43**: p. 2541-2541.
154. Khreis, H., K.M. Warsow, E. Verlinghieri, A. Guzman, L. Pellecuer, A. Ferreira, I. Jones, E. Heinen, D. Rojas-Rueda, N. Mueller, P. Schepers, K. Lucas, and M. Nieuwenhuijsen, *The health impacts of traffic-related exposures in urban areas: Understanding real effects, underlying driving forces and co-producing future directions.* Journal of Transport & Health, 2016. **3**(3): p. 249-267.
155. Weinmayr, G., E. Romeo, M. De Sario, S. Weiland, and F. Forastiere, *Short-term effects of PM10 and NO2 on respiratory health among children with asthma or asthma-like symptoms: a systematic review and meta-analysis.* Environ Health Perspect., 2010(1552-9924 (Electronic)).
156. U.S. EPA. *NAAQS Table*. Criteria Air Pollutants 2017; Accessed at: https://www.epa.gov/criteria-air-pollutants/naaqs-table.
157. Brugge, D., J. Durant, and C. Rioux, *Near-highway pollutants in motor vehicle exhaust: A review of epidemiologic evidence of cardiac and pulmonary health risks.* Environ. Health, 2007. **6**: p. 23-23.
158. U.S. EPA, *MOVES2014a User Guide*. 2015, Office of Transportation and Air Quality Accessed at: https://nepis.epa.gov/Exe/ZyPDF.cgi?Dockey=P100NNCY.txt
159. Amato, F., O. Favez, M. Pandolfi, A. Alastuey, X. Querol, S. Moukhtar, B. Bruge, S. Verlhac, J.A.G. Orza, N. Bonnaire, T. Le Priol, J.F. Petit, and J. Sciare, *Traffic induced particle resuspension in Paris: Emission factors and source contributions.* Atmospheric Environment, 2016. **129**: p. 114-124.
160. Thorpe, A. and R.M. Harrison, *Sources and properties of non-exhaust particulate matter from road traffic: A review.* Science of The Total Environment, 2008. **400**(1): p. 270-282.
161. Abu-Allaban, M., J.A. Gillies, A.W. Gertler, R. Clayton, and D. Proffitt, *Tailpipe, resuspended road dust, and brake-wear emission factors from on-road vehicles.* Atmospheric Environment, 2003. **37**(37): p. 5283-5293.
162. Kundu, S. and E.A. Stone, *Composition and sources of fine particulate matter across urban and rural sites in the Midwestern United States.* Environmental science. Processes & impacts, 2014. **16**(6): p. 1360-1370.

163. ADOT, *Air Quality Regional Conformity Analysis: Nogales PM2.5-PM10 Nonattainment Areas*. 2017. Arizona Department of Transportation (ADOT) Project No. 189 SC 000 H8045 01L. Accessed at: https://www.azdot.gov/docs/default-source/environmental-planning-library/h8045_nogales_finalairqualityconformityanalysis.pdf?sfvrsn=2
164. U.S. EPA, *Using MOVES2014 in Project-Level Carbon Monoxide Analyses*. 2015. Accessed at: https://nepis.epa.gov/Exe/ZyPdf.cgi?Dockey=P100M2FB.pdf
165. U.S. EPA, *AP-42: Section 13.2.1 Paved Roads* Accessed at: https://www3.epa.gov/ttnchie1/ap42/ch13/final/c13s0201.pdf
166. Code of Federal Register, *Title 40CFR Part 58, Appendix D, Section 4.3.2*. 2017. Accessed at: https://www.ecfr.gov/cgi-bin/retrieveECFR?gp=&r=PART&n=40y6.0.1.1.6
167. U.S. EPA. *Ambient Monitoring Technology Information Center (AMTIC)*. 2019; Accessed at: https://www3.epa.gov/ttnamti1/nearroad.html.
168. Texas A&M Transportation Institute, *Update of On-Road Inventory Development Methodologies for MOVES2014*. 2014. Accessed at: ftp://amdaftp.tceq.texas.gov/pub/EI/onroad/mvs14_utilities/MOVES2014_Utilities_Report_Final_December_2014.pdf
169. Texas A&M Transportation Institute, *Methodologies for Conversion of Data Sets for MOVES Model Compatibility*. 2013. Accessed at:
170. CoCoRaHS. *Community Collaborative Rain, Hail and Snow Network: Daily Precipitation Reports*. 2017; Accessed at: https://www.cocorahs.org/ViewData/ListDailyPrecipReports.aspx.
171. U.S. EPA, *User's Guide for the AERMOD Meteorological Preprocessor (AERMET)*. 2016. EPA-454/B-16-010. Accessed at: https://www3.epa.gov/ttn/scram/7thconf/aermod/aermet_userguide.pdf
172. TCEQ. *Meteorological Data for Air Dispersion Modeling*. 2017; Accessed at: https://www.tceq.texas.gov/permitting/air/nav/datasets.html.
173. NOAA. *Surface Air Database*. 2018; Accessed at: ftp://ftp.ncdc.noaa.gov/pub/data/noaa.
174. NOAA. *NOAA/ESRL Radiosonde Database*. 2018; Accessed at: https://ruc.noaa.gov/raobs/.
175. Harrison, R.M., P.L. Leung, L. Somervaille, R. Smith, and E. Gilman, *Analysis of incidence of childhood cancer in the West Midlands of the United Kingdom in relation to proximity to main roads and petrol stations.* Occupational and environmental medicine, 1999. **56**(11).
176. Wilhelm, M. and B. Ritz, *Residential proximity to traffic and adverse birth outcomes in Los Angeles county, California, 1994-1996.* Environmental health perspectives, 2003. **111**(2): p. 207-16.
177. Heinrich, J., R. Topp, U. Gehring, and W. Thefeld, *Traffic at residential address, respiratory health, and atopy in adults: the National German Health Survey 1998.* Environmental Research, 2005. **98**(2): p. 240-249.
178. McConnell, R., K. Berhane, L. Yao, M. Jerrett, F. Lurmann, F. Gilliland, N. Künzli, J. Gauderman, E. Avol, D. Thomas, and J. Peters, *Traffic, Susceptibility,*

and Childhood Asthma. Environmental Health Perspectives, 2006. **114**(5): p. 766-772.
179. Jerrett, M., R.T. Burnett, R. Ma, C.A. Pope, D. Krewski, K.B. Newbold, G. Thurston, Y. Shi, N. Finkelstein, E.E. Calle, and M.J. Thun, *Spatial Analysis of Air Pollution and Mortality in Los Angeles.* Epidemiology, 2005. **16**(6): p. 727-736.
180. Finkelstein, M.M., M. Jerrett, and M.R. Sears, *Traffic Air Pollution and Mortality Rate Advancement Periods.* American Journal of Epidemiology, 2004. **160**(0002-9262 (Print)).
181. Cimorellia, A.J., S.G. Perryb, A. Venkatramc, J.C. Weild, R.J. Painee, R.B. Wilsonf, R.F. Leeg, W.D. Petersh, and R.W. Brode, *AERMOD : A Dispersion Model for Industrial Source Applications . Part I : General Model Formulation and Boundary Layer Characterization.* Journal of Applied Meteorology, 2005. **44**: p. 682-693.
182. Eckman, R.M., *Re-examination of empirically derived formulas for horizontal diffusion from surface sources.* Atmospheric Environment, 1994. **28**(2): p. 265-272.
183. Paine, R., O. Samani, M. Kaplan, E. Knipping, and N. Kumar, *Evaluation of low wind modeling approaches for two tall-stack databases.* J Air Waste Manag Assoc, 2015. **65**(11): p. 1341-53.
184. Askariyeh, M.H., S.H. Kota, S. Vallamsundar, J. Zietsman, and Q. Ying, *Evaluation of AERMOD for Near-Road Pollutant Dispersion Using Data from the General Motors Sulfur Dispersion Experiment*, in *Transportation Research Board 96th Annual MeetingTransportation Research Board*. 2017, Transportation Research Board: Washington, DC.
185. U.S. EPA, *Transportation Conformity Guidance for Quantitative Hot-spot Analyses in PM 2.5 and PM 10 Nonattainment and Maintenance Areas*. 2015. Accessed at: https://nepis.epa.gov/Exe/ZyPDF.cgi?Dockey=P100NMXM.pdf
186. Chock, D.P., *General motors sulfate dispersion experiment—An overview of the wind, temperature, and concentration fields.* Atmospheric Environment (1967), 1977. **11**(6): p. 553-559.
187. Wilson, W.E., L.L. Spider, T.G. Ellestad, P.J. Lamothe, T.G. Dzubay, R.K. Stevens, E.S. Macias, R.A. Fletcher, J.D. Husar, R.B. Husar, K.T. Whitby, D.B. Kittelson, and B.K. Cantrell, *General Motors Sulfate Dispersion Experiment: Summary of EPA Measurements.* Journal of the Air Pollution Control Association, 1977. **27**(1): p. 46-51.
188. Chock, D.P., *General Motors Sulfate Dispersion Experiment: Assessment of the EPA HIWAY Model.* Journal of the Air Pollution Control Association, 1977. **27**(1): p. 39-45.
189. Code of Federal Register, *40 CFR Part 51*. 2015. 206. Accessed at: https://www.gpo.gov/fdsys/pkg/FR-2015-07-29/pdf/2015-18075.pdf
190. Yizheng Wu, D.N., *Strategy of AERMOD Configuration for Transportation Conformity Hot-Spot Analyses*, in *The 95th Transportation Research Board*. 2016: Washington D.C., January, 2016.

191. De Nevers, N., *Air Pollution Control Engineering*. 2000, Boston, MA: McGraw-Hill.